RENEWABLE ENERGY POWERED ORGANIC RANKINE CYCLE

(KITAR ORGANIK RANKINE DENGAN KUASA TENAGA BOLEH DIPERBAHARUI)

SANJAYAN VELAUTHAM

RESEARCH VOTE NO:
75125

Jabatan Termo-Bendalir
Fakulti Kejuruteraan Mekanikal
Universiti Teknologi Malaysia

2006

ACKNOWLEDGEMENT

ABSTRACT

This project studies the feasibility of an Organic Rankine Cycle (ORC) driven by solar thermal energy for sustainable power generation for small and medium sized commercial usage. An experimental study on a solar parabolic trough collector (PTC) for the use in the Organic Rankine Cycle, (ORC) is also focused here. ORC is principally a conventional Rankine Cycle that uses organic compound as the working fluid instead of water and it is particularly suitable for low temperature applications. Appropriate organic compound includes refrigerants and azeotropes. The ORC and the solar collector are sized according to the solar flux distribution in Malaysia. The location of study is Kota Kinabalu, highest yearly average of solar radiation, and Chuping, longest yearly average solar duration in the country for year 2003. The power generation system consists of two cycles, the solar thermal cycle that harness solar energy and the power cycle, which is the ORC that generates electricity. The solar thermal cycle circulates heat transfer fluid (HTF) in the cycle and harness thermal energy from the sun and transfers it to the organic compound in the ORC via a heat exchanger. The parabolic trough collector in this study is 1 meter in length and it consists of a curved mirror that concentrates sunlight on a tube with a heat transfer fluid (HTF) inside that runs parallel in the focal line of the mirror. The HTF selected in this analysis is water which is done during the experimental study also Therminol 55 and Therminol VP3 for the parametric study which is currently used for commercial thermal applications. For this research, 2 organic compounds were analyzed, R123 and Isobutene. These two compounds are optimized for selection. The results produced from the experimental study on the parabolic trough collector, (PTC), showing the variation of absorber temperatures and the value of power generated in terms of the solar collector designed is presented.

ABSTRAK

Projek ini menyelidik kebolehkerjaan bagi satu Kitar Organik Rankine (ORC) dipandu oleh tenaga haba suria untuk penjanaan tenaga yang mampan untuk penggunaan komersial kecil dan sederhana.Projek ini juga menumpu kepada kajian ujikaji ke atas satu pemungut solar parabolik bagi kegunaan pada Kitar Organik Rankine (ORC) untuk tujuan penjanaan tenaga. ORC secara prinsipnya adalah Kitar Rankine konvensional yang menggunakan kompound organik menggantikan air sebagai cecair kerja dan ia sangat sesuai untuk aplikasi pada suhu rendah. Kompound organik yang sesuai merangkumi agen penyejuk dan azeotrope. ORC dan penyerap suria adalah disaizkan mengikut pembahagian fluk suria di Malaysia. Lokasi kajian adalah di Kota Kinabalu, purata sinaran suria yang tertinggi, dan Chuping, jangka masa sinaran matahari terpanjang untuk Negara ini pada tahun 2003. Sistem penjanaan tenaga mengandungi 2 kitar, kitar haba suria yang menyerap tenaga suria dan kitar tenaga yang berfungsi untuk menjana elektik. Kitar haba suria mengalirkan cecair pindah haba (HTF) di dalam kitar dan menyerap tenaga haba dari matahari dan memindahkannya ke kompound organik melalui penukar haba. Ukuran panjang pemungut solar parabolik dalam ujikaji ini adalah 1 meter dan ia mengandungi suatu cermin lengkuk yang akan menumpu sinaran matahari ke atas tiub pemungut haba yang mengandungi aliran cecair pemindah haba (HTF) berkedudukan selari denan titik tumpu cermin lengkuk tersebut.HTF yang dipilih untuk analisis ini yang dijalankan secar ujikaji adalah air dan secara parametrik ialah Therminol 55 dan Therminol VP3, yang sedang digunakan secara komersial untuk aplikasi haba. Untuk kajian ini, 2 kompound organik dianalisis, R123 dan Isobutana. Kedua-duanya akan dioptimasikan untuk pilihan. Keputusan nilai-nilai suhu pada tiub pemungut haba dan jumlah tenaga yang terjana hasil dari ujikaji yang dijalankan ke atas pemungut solar parabolik ini akan dipersembahkan.

TABLE OF CONTENTS

LIST OF FIGURES

NO OF FIGURE   **TITLE**   **PAGE**

NO OF FIGURE   **TITLE**   **PAGE**

LIST OF APPENDICES

INTRODUCTION

Importance of Energy

Energy is defined as the ability to perform work by means of physical or chemical resources. Energy and work have the same unit, which is Joule according to SI Unit, both are scalar unit. A scalar unit is measured in quantitative value only. Energy exists in all matters but work is produced by the energy in the matter. The study of energy is called thermodynamic. The focus of study in thermodynamic is to convert energy sources into work which is a more useful form for human consumption.

Energy comes in various forms; some examples are kinetic energy, potential energy, thermal energy and chemical energy. According to conservation of energy principle, energy cannot be created or destroyed but energy can only be converted from one form to another. Due to this reason, energy seldom comes in one form and all the energy forms are related to each other. For example, in a falling object, it has both kinetic energy and potential energy. Potential energy exist due to the elevation of the object in the gravitational field, while kinetic energy is the resultant of the motion of the object in relative to the a reference point. To define energy in an easier way, all matters including the smallest atoms have energy in them.

The first and most important energy source is the sun and it is the source of light and energy for all the living on this planet. Using radiation from the sun, the plants do a chemical process named photosynthesis, to provide food and oxygen for animals and human. As time progress, humans found fire and uses wood as fuel for the fire. Other types of energy sources that assisted the early human evolution is wind and hydraulic – water from river. Fire is use to cook, as a light source and heat source for industry like pottery. While wind is mainly used for exploration as it is use

for sail boats, though it also utilized in agriculture. Hydraulic is very important with the invention of water wheel for agricultural sector as it requires water to irrigate farms to grow food.

In the early Industrialization Period in Europe, the depletion of wood cause the change of energy source to coal. Coal is widely used to power train, steam boat and manufacturing industry especially in the steel industry. At the same time, oil was found and made into kerosene for domestic use to provide light for people in the night. Gasoline was found at the same time as oil but was not widely used until the invention of car. In 1882, Thomas Alva Edison constructed the first power plant to generate electricity [1]. At that time electricity was solely used for lighting purpose only.

Today in this modern era, the usage of electricity was intensified to a stage where electricity is the nerve of progress of the world. Most gadgets, machineries or appliances operate on electricity, from the domestic use all the way to big industries. The consumption of energy in the world in 2002 is growing at 1.5 % percent at 404.98×10^{15} Btu [2]. This increment of the energy consumption was mainly due to the increase of human population.

1.1 Energy Scenario in Malaysia

In Malaysia, we had several main electric utility companies in charge of providing electricity to the country. The major electric utility company is Tenaga Nasional Berhad (TNB) which takes on the power production, transmission and distribution in Peninsular Malaysia, while in Sabah, it is by Sabah Electricity Sendirian Berhad (SESB) and Sarawak by Sarawak Electricity Supply Company (Sesco).

There are also several independent power producers (IPPs) producing power for the country. These IPPs are only in charge of generating electricity but the transmission and distribution falls into the responsibilities of the three main electric utility companies. These three utility companies will buy electricity from the IPPs and distribute and sell them to customers. The buying of electricity between the

utility companies and IPPs involve an agreement called the Power Purchase Agreement (PPA).

Currently, thermal power plants of these companies are operating either on Brayton Cycle; Rankine Cycle or combined cycles to produce power. All these plants are fossil fuel thermal power plants. According to TNB [3], there are a total of 19 thermal plants in the whole of Peninsular Malaysia, including power plants by the IPPs. While there are 10 hydro power plants which are owned by TNB. Total installed capacity of all the power plants in Peninsular Malaysia is 16 987.5 MW as at 31st August 2003, of which 6,834.0 MW are by IPPs. As for Sabah, the total installed capacity is 758MW for year 2003 [3]. While in Sarawak for year 2000, the total installed capacity is 846 MW [4].

1.1.1   Current Electricity Usage in Malaysia

Malaysia is considered as a developing country and consumes quite a large amount of electricity to fuel its development. According to the 8th Malaysia Plan (RMK8), the electricity coverage in Peninsular Malaysia is at 100 % therefore no improvement is needed. While for Sabah, in year 2000 the electricity coverage is at 79 % and will be increased to 85 % by the year 2005. In year 2000, Sarawak electricity coverage is at 80 % and in year 2005 should be at 90 %. The total investment for the electricity supply industry from 1995 to 2000 is at RM 41.11 billion. The electric tariff for domestic use in Peninsular now is at 23.5 sen per kWh, Sabah at 24.4 sen per kWh and Sarawak at 27.1 sen per kWh [4].

In year 2003, the total amount of electricity consumed is 68,254.3 GWh . According to the latest unaudited report by TNB the first half of 2004, the company had sold 35,223.9 GWh of electricity which is a 6 % growth when compared to the first half of 2003. From the Figure 1.1 given by TNB, it indicates the maximum demand for year 2003 is at 11,329 MW [3]. These values given by TNB include the electricity consumption in Sabah. As for Sarawak, 2,537 GWh of electric was used in year 2000 [4].
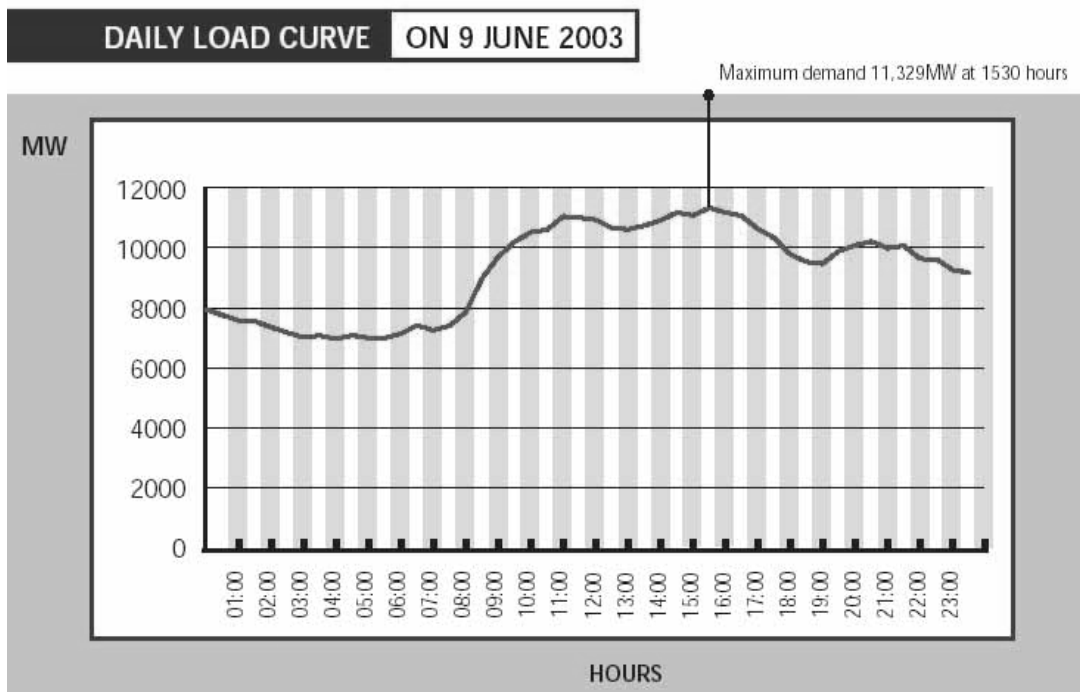
Figure 1.1: Load Curve for 9th June 2003 [3]

1.1.2 Future Prospect of Energy Generation in Malaysia

In the 8th Malaysian Plan (RMK8), Malaysia's 5 years plan from 2001 to year 2005, the focus of the Plan is to develop a fifth fuel for Malaysia's energy needs. Currently four fuels that is being used, in descending order according to percentage, natural gas (78.7 %), coal (7.9 %), fuel oil and diesel oil (5.3 %). According to RMK8, the government of Malaysia hopes to build a sustainable development in this sector especially in minimization environmental effect and increase efficiency. In the duration of the Plan, it is expected that the consumption of electricity will increase at 7.3 % per year [4].

In the effort to diversify the fuel mix, the petroleum based fuel will be reduced to 67% by the year 2005. Therefore, the fifth fuel which is renewable energy will be encouraged to be used to fill up the gap. In RMK8, renewable energy sources are being encouraged are solar, biomass, biogas, wind and mini-hydro. There are incentives are being considered for renewable energy related research and

commercialization of research findings as well as financial and fiscal incentives will be given [4].

A recent study identified the renewable energy resource potential in the country, in ringgit value, as shown in Table 1.1:

Table 1.1: Variety of renewable energy sources and its potential value [4]

Renewable Energy Resource	Energy Value in RM Million(Annual)
Forest residues	11,984
Palm oil biomass	6,379
Solar thermal	3,023
Mill residues	836
Hydro	506
Solar PV	378
Municipal waste	190
Rice husk	77
Landfill gas	4

1.2 Conventional Methods of Power Generation

Energy harnessing or power generation is about the conversion of energy from one source into another. Currently, the most widely used form of secondary energy is the electricity. Being a secondary energy source, electricity is different from coal, oil or petroleum which is a primary energy. Secondary energy source refers to an energy that is converted from primary energy source. Electricity is important because it an easier form of energy that can be easily generated and distributed. Therefore, currently all the power generation sector in the world, converts primary energy source into electricity. There are numerous methods of converting primary energy source into electricity. One of the most widely used methods is thermal power plant.

1.2.1 Thermal Power Plant

Thermal power plant refers to the use of thermal energy converted into electricity. Most of the thermal power plant utilizes thermal energy from the burning of fossil fuel, for example coal, natural gas and distilled fuel. Fossil fuels are preferred because of the high quality heat generated from the burning of these fuels. Three typical thermal power plants are steam power plant, gas power plant and binary cycle which combines both steam and gas turbine. Most thermal power plant existing today utilizes fossil fuel to generate heat energy for the working fluids.

1.2.1.1 Steam Power Plant

In a steam power plant, it uses steam as the working fluid to absorb the heat from the burning of fossil fuel like coal, distilled fuel and also natural gas. Figure 1.2 depicts the schematic diagram of the basic components and configurations in a typical Rankine Steam Cycle or Rankine Cycle. While, Figure 1.3 illustrates T-s diagram of an ideal Rankine Steam Cycle. The numbers found on the T-s diagram corresponds to the points found in Figure 1.2. In a Rankine Cycle, there are 4 components, turbine which is connected to generator, condenser, pump and boiler.

Work is produced by the isentropic expansion of the superheated steam in turbine - from state 1 to state 2 in Figure 1.3. After the expansion at state 2, the steam will be in saturated liquid-vapour phase with high dryness fraction. From state 2, working fluid is condensed by heat sink in the condenser and exit at state 3. In condenser, heat is released by the system to the environment. Pressure of working fluid is increased by the pump to boiler pressure.

Compressed liquid at state 4 is heated at constant pressure in the boiler. The heat transfer from the combustion of fossil fuel to the working fluid will increase its' temperature. The increase will initiate the phase change from compressed liquid to saturated liquid-vapour and finally to superheated vapour at state 1. If all the 4 processes explained are ideal then it is called the ideal Rankine Cycle. Ideal process

refs to reversible and adiabatic process or isentropic process. The thermal efficiency for a typical commercial Rankine Cycle power plant is at around 34%.
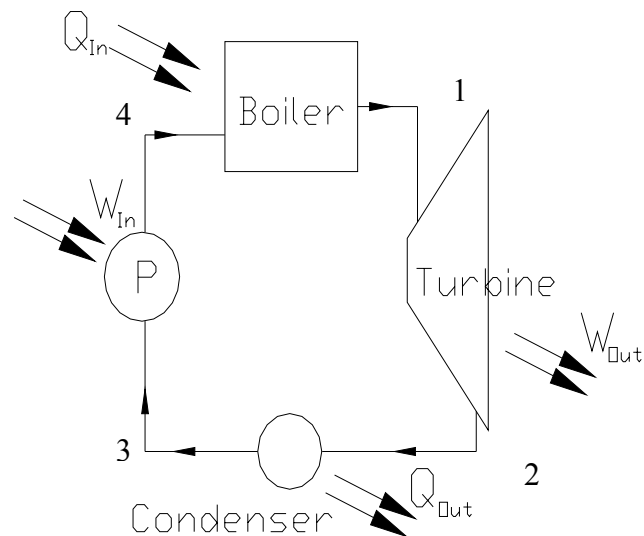
Figure 1.2: Steam Thermal Power Plant
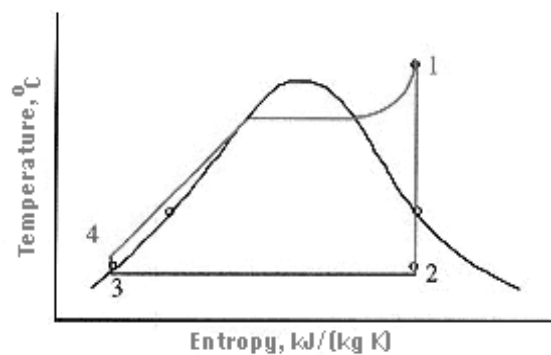
Figure 1.3: T-s Diagram of Rankine Steam Cycle

1.2.1.2 Gas Power Plant

In gas power plant, instead of using steam it uses combusted air. Referring to Figure 1.4, which is an ideal gas power plant; air is drawn from the atmosphere at state 1 and compressed isentropically to a higher pressure by a compressor. At state 2, the compressed air is mixed with fuel and combusted at a constant pressure in the combustion chamber. The combusted air exits to state 3 at high temperature around 1300 °C.

The combusted air with a high temperature and pressure will expand in the turbine. Same as in the steam power plant, the expansion of the combusted air will turn the turbine shaft to produce work. The expansion of the combusted air will reduce its pressure and temperature. Thus, electricity is generated by a generator which is coupled to the turbine. At stage 4 or the exit of the turbine, the combusted air is released into the atmosphere for an open cycle plant but for a closed cycle, the air will be recirculated into the whole processes again after heat rejection to atmosphere through a condenser.

Normally an open cycle is used for gas power plant because air in atmosphere is free. The basic layout of an open-cycle gas turbine is as Figure 1.4. As for Figure 1.5, it indicates the ideal processes of gas turbine cycle which is called the ideal Brayton Cycle. The T-s diagram shows a closed cycle, for an open cycle, the line from point 4 to point 1 is not drawn. For Brayton Cycle, the thermal efficiency is at 35% for turbine inlet temperature of 1300˚C.
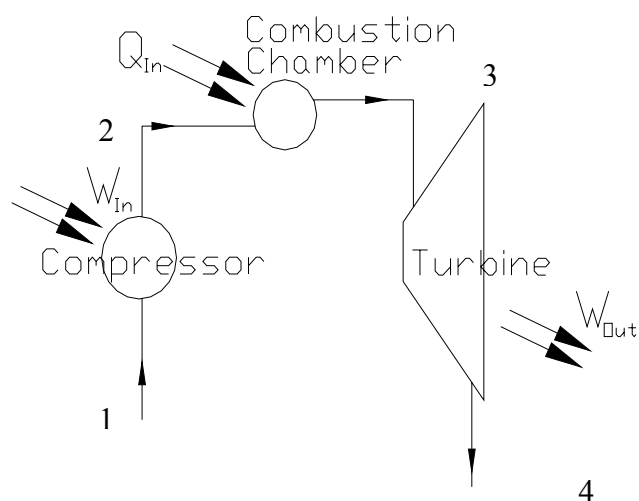
Figure 1.4: Gas Turbine Thermal Plant
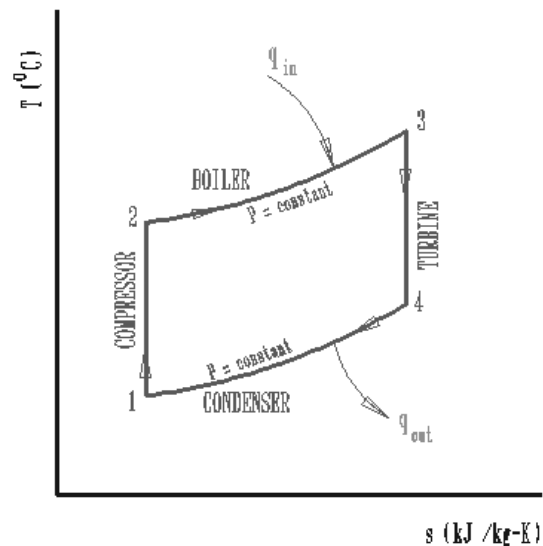
Figure 1.5: T-s Diagram of a Closed Brayton Cycle.

1.2.1.3 Binary Cycle

Binary cycle or combined cycle is a combination of two power cycles and usually it is the combination of gas power cycle and steam power cycle. These two power cycles are coupled in series because such configuration gives a higher thermal efficiency compared to the parallel coupling.

In a binary cycle, gas power cycle or Brayton Cycle is used as the topping cycle while the bottoming cycle is the Rankine Cycle. Brayton Cycle is placed as the topping cycle because the exhaust gas temperature is very high and can be used at the heat recovery steam generator (HRSG). This HRSG function as a boiler for conventional Rankine Cycle. Through this HRSG the exhaust gas transfers heat to superheat the steam in the Rankine Cycle which sits at the bottom of the cycle as shown in Figure 1.6. All the other processes involved for both cycles are the same as explained in the previous sections. The typical thermal efficiency for this binary cycle is at around 55%.
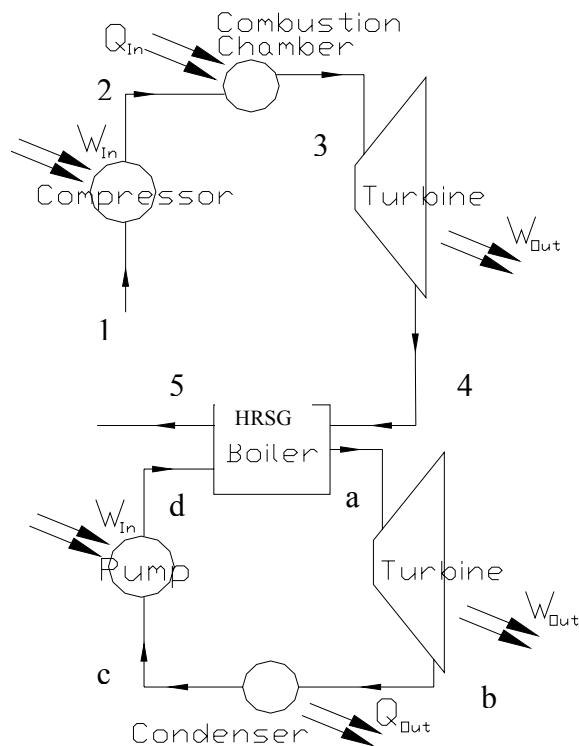
Figure 1.6: Schematic Diagram of Binary Cycle

1.3   Objective

In this study, it is desired to determine the feasibility of solar energy as a potential heat source for an Organic Rankine Cycle within Malaysia context. The focus of this study is on the thermodynamic aspect rather than the economics of the system.

In this study there are two cycles involved, solar thermal cycle and power cycle. Power cycle refers to the Organic Rankine Cycle that converts thermal energy to electricity. While, the solar thermal cycle role is to harness solar radiation into thermal energy for the power cycle. Two important parameters in this solar thermal cycle are the heat transfer fluid outlet temperature and the absorber temperature.

There are a few objectives to be achieved from this study. The first objective is to check on the solar thermal cycle that is to find the maximum outlet temperature of heat transfer fluid from the thermal cycle. The solar thermal collector that will be used for this purpose is the parabolic trough collector.

The second objective of this study is to evaluate the effects of the heat transfer from the received radiation. The heat transfer effect is very important on the solar thermal cycle since the working fluid will affect the heat input required and output temperature of the cycle. Thus the cycle efficiency will be affected. The aim is to try to optimize the performance of the system by trying different types of methods in order to maximize the outlet temperature of the system.

The final objective of this study is to find the best organic compounds to be used as working fluid for Organic Rankine Cycle. The choice of working fluid is very important for an Organic Rankine Cycle since the working fluid will affect the heat input required and work output of the cycle.

1.4   Scope

In order to fulfil the objectives proposed, a few boundary conditions have to be set as guidelines for this study. Study of solar thermal energy for power generation in Malaysia is still in its introductory stage, therefore to do an experimental study on the solar driven ORC or power cycle will take up large amount of resources in term of money and time. Hence, a parametric study will be done on the ORC instead. This parametric study will serve as a preliminary study and reference for experiments in the future. However an experimental study will be done on the solar thermal cycle.

The parametric study on the ORC is conducted using computer software. Selection of the software for programming will not be limited as there is a wide variety of software that can be used in the market. The computer software used might be combinations of software. The choice of the software will depend on the availability and ease of use.

Although there are many types of solar thermal collectors found in the market, only the parabolic trough collector will be studied here. The experimental study will be done on the parabolic collector test rig. This experimental study is conducted manually. The scopes outlined for this dissertation is to study the solar radiation by measurable parameters and also parametric study to optimise heat transfer to the solar parabolic trough collector.

The selection of organic fluid for the system will be done from the ready-made blends in the market. As a result, decision of the type of compound will be limited to the blends of organic compound found in the market. No custom made blending will be done in the study. This is due to the fact that custom made blend requires experimentation and a detail study of the appropriate equations of state.

CHAPTER II

LITERATURE REVIEW

Renewable Energy

Traditional thermal power plant, as explain in previous chapter, uses fossil fuel that is mined from a non-renewable source. A non-renewable source refers to the possibility of depletion of the source. By relying on non-renewable source, the world is in the danger of running out of primary energy sources. According to report, fossil fuel especially the petroleum can only last till 2009 more while natural gas will only last longer till year 2055 [5]. Besides that, fossil fuel price fluctuates considerably with the economy and politics of the world and at the time of study it had reached USD 53.83 a barrel [6]. Therefore a renewable energy concept is formulated to overcome the problems of this fossil fuel based power generation system.

In this search for renewable sources, energy sources which are sustainable and clean are researched to replace fossil fuel. Over the years, numerous renewable energy source to generate power are discovered, for example using wind, waves or water to run turbine; solar which is using sunlight to generate electricity; and also biomass which is the burning of rubbish or agriculture by-product as heat source. Even though these energy sources can be converted to electricity but it is still in its infancy stage. These technology developed to harness these energy are still very costly.

Currently, solar energy is considered one of a highly potential renewable energy sources in Malaysia. Such claim arises from the fact that solar energy can be directly converted to electricity using solar cells like photovoltaic cell or photoelectric cell. Though these solar cells can turn sunlight into electricity but it is very expensive and the amount of electricity it produces is little compared to its cost. Besides, the life cycle of the solar cells is short. The solar cells will degrade with the amount of sunlight it converts to electricity and it can last for 30 years [7].

Seeing the great potential of harnessing sunlight but constrained by the limitation of the solar cell, another alternative to harness sunlight are looked into. The other way to harness sunlight is by using the sunlight as a heat source itself and it is also called solar thermal. One of the example of using solar as thermal energy is the solar water heater. Solar water heater is widely used in Malaysia for domestic and industry application.

2.1 Power Cycle

2.1.1 Selection of Power Cycle

As mentioned in Chapter 1, there are two types of power cycle widely used in the industry, Brayton Cycle and Rankine Cycle. Though there are two power cycles available but in this study only Rankine Cycle will be considered. The reason for such a decision is based on the turbine inlet temperature (TIT). TIT for conventional Rankine Cycle is just 550 – 600 °C while a gas turbine the TIT is 1300°C. The temperature is quite impossible for solar thermal source alone to achieve such a TIT.

According to Fisher *et al.* [8], TIT that can be achieved is just 800 °C using solar tower and it is only achieved when the solar radiation is at its peak. The solar tower needs a lot of direct radiation from the sun therefore it will be good in places like desert where direct radiation are more readily available. Therefore only Rankine Cycle will be considered in this study.

2.1.2 Problem in Conventional Rankine Cycle

Though Rankine Cycle is selected as the power cycle but there are a number of problems which exist in conventional Rankine Cycle. One of the main problem is water needs to be superheated in the Rankine Cycle. The superheating is necessary to ensure the quality of saturated water after the expansion in the turbine is dry. The quality of saturated water after the turbine should not go below 0.88. When the quality is lower, percentage of vapour will be higher and erosion in turbine blade will be at a higher rate. The efficiency of a Rankine Cycle can be found using the mean temperature of the system.

Hence to solve the problem of high moisture content and low efficiency, normally a steam thermal plant has reheat. Reheating increases the efficiency by increasing the mean temperature and also will give low moisture content in the turbine. But more than two reheats are not recommended as it increases the complexity and cost of the plant.

Another problem for steam thermal plant is the need to create a vacuum in the condenser. The temperature of a condenser is set by the temperature of the cooling fluid. For Malaysia, the temperature of the cooling fluid or water from sea is at 24 °C. As a result, the temperature of the condenser will be set at either 24 °C where the pressure for the water at condenser will be at 0.03 bar. These pressure is much lower compared to the atmospheric pressure, 1 bar, so the condenser will need to be at vacuum pressure. It is expensive and difficult to maintain the vacuum in condenser as it is big.

2.1.3 Organic Rankine Cycle

Seeing the problem with conventional Rankine cycle, Organic Rankine Cycle (ORC) is considered a better alternative for this study. An Organic Rankine Cycle is a cycle where organic compound like refrigerant replace water as the working fluid with. This organic compound requires lower heat source as compared to water

because the organic compound has lower specific vaporization heat and these organic compound do not need to be superheated like water.

Having a low specific vaporization heat will amount to lower heat source needed to heat the fluid to vapour form. Due to the negative gradient of the saturated vapour line in the T-s diagram, water needs to be superheated to lower the moisture content in the turbine. But for organic compound superheating is not needed because its' saturated vapour line has a positive gradient in the T-s diagram, therefore, even after expansion it will still be in the vapour region [9].

2.1.4   Characteristics of an Ideal Working Fluid

In choosing a working fluid for the Rankine Cycle, there are a few characteristics that determine whether the fluid is a good working fluid for Rankine Cycle or otherwise. These characteristics are meant to obtain the best thermal efficiency for the Rankine Cycle. Firstly the fluid needs to have a high critical temperature so that maximum temperature, which limited by the metallurgical limit, of the Rankine Cycle is relatively low. And at this saturation pressure, it should have a large enthalpy of vaporization. Secondly, the saturation pressure for the fluid at the condenser should be higher than the atmospheric pressure. This is to avoid having a vacuum in the condenser [9].

Another factor is the specific heat of the fluid should be small so that little heat transfer is required to heat the liquid to boiling point. Next is the saturated vapour line of T-s diagram should be steep. This is important to ensure the moisture content of fluid when it is in the turbine is always low. The freezing temperature of the fluid should be below the room temperature. If the freezing temperature is higher than the room temperature, the fluid will solidify while flowing through the pipe [9].

Next factors include the fluid should be chemically stable and will not contaminate the materials of construction at any temperature. The fluid should be non-toxic, non-corrosive, not excessively viscous and low in the cost. This feature of

the fluid is to make the fluid is economically feasible and environmentally friendly and harmless to the materials and the people [9].

2.1.5 Literature of Organic Rankine Cycle

According to Larjola [10], the most common refrigerants for ORC are R11, R113, R114, Toluene (C_7H_8) and Fluorinol. After testing a few refrigerants, it is found that for high speed ORC applications, toluene is the most suitable for high temperature process while isobutane (C_4H_{10}) is the most suitable for low temperature system [10]. Hung *et al* tested a few refrigerants like benzene, ammonia, R11, R12, R134a and R113 for ORC and found that benzene gives the highest system efficiency at the temperature between 500 °C and 560 °C [11].

Working ORC includes Coolidge Solar Thermal Electric Power Plant in America. The plant uses toluene as the working fluid for the ORC [12]. Kalina cycle is also an example of ORC that uses mixture of water and ammonia as working fluid [13]. A few literatures suggest and use HCFC123 or R123 (1,1–dichloro–2,2,2–trifluoroethane) as the working fluid for their ORC in their research on improving the current power generation system [14, 15, 16, 17, 18, 19]. Gary J. Zyhowski [20] in the seminar at the 21st IIR International Congress for Refrigerant in Washington recommended the use of R245fa (1,1,1,3,3–pentafluoropropane) as the organic compound in the ORC.

DiPippo [21] did a review on the operating ORCs in geothermal power generation. In the same literature, it is found that Otake geothermal pilot plant in Japan uses isobutane as the working fluid and the plant efficiency is 12.9 %. Another plant in Japan the Nigorikawa pilot plant uses R114 and has an efficiency of 9.81%. Brady binary cycle uses n-pentane and operates with 8.1% efficiency.

2.2   Solar Availability in Malaysia

There are 2 types of solar radiations received from the sun, they are direct or beam radiation and diffuse radiation. Beam radiation is the solar radiation received without being scattered by the atmosphere. Diffuse radiation is the radiation that is received after its direction has been changed by scattering by clouds in the sky. Total solar radiation is the sum of beam and diffuse radiation on a surface or it is also called as global radiation [22].

These measurements of solar radiation are done by solarimeter or pyranometer and also pyrheliometer or actinometer. These two instrument measures the total radiation from the sun. A solarimeter can measure diffuse radiation by shading the beam radiation using shade ring. These instruments give the value of solar radiation in J/m^2 which is the irradiation. Irradiance is the rate of radiant energy is incident on a surface, per unit area. Irradiation is the incident energy per unit area on a surface, found by integration of irradiance over a specified time which is normally an hour or day [22].

Being in the tropic region, the weather in Malaysia is hot and humid all year round. Therefore, in Malaysia the climate is hot and humid which means that there are abundant of solar radiation all year long. But it is difficult to find a cloudless sky for the whole day even during severe drought in Malaysia. This means that the value of direct radiation is small because the existence of cloud will scatter the solar radiation into diffuse radiation. On an average day, Malaysia receives about 6 hours of sunshine with Alor Setar can get a maximum 8.7 hours of sunshine, monthly average. Kuching only receives an average of 3.7 hours of sunlight in extreme case [23].

Metrological Malaysia Department uses the solarimeter and only measure the total solar radiation. The lowest monthly mean solar radiation in Malaysia is 9.6 MJ/m^2 a day occurs during November to January, during the monsoon season. While the highest monthly mean is 23.3 MJ/m^2 from February to March [23]. Figure 2.1 shows the average total daily solar radiation distribution in Malaysia. The legend

gives the values in MJ/m^2. From the same figure, it is seen that solar radiation in the northern part of Peninsular Malaysia and Sabah is very high.
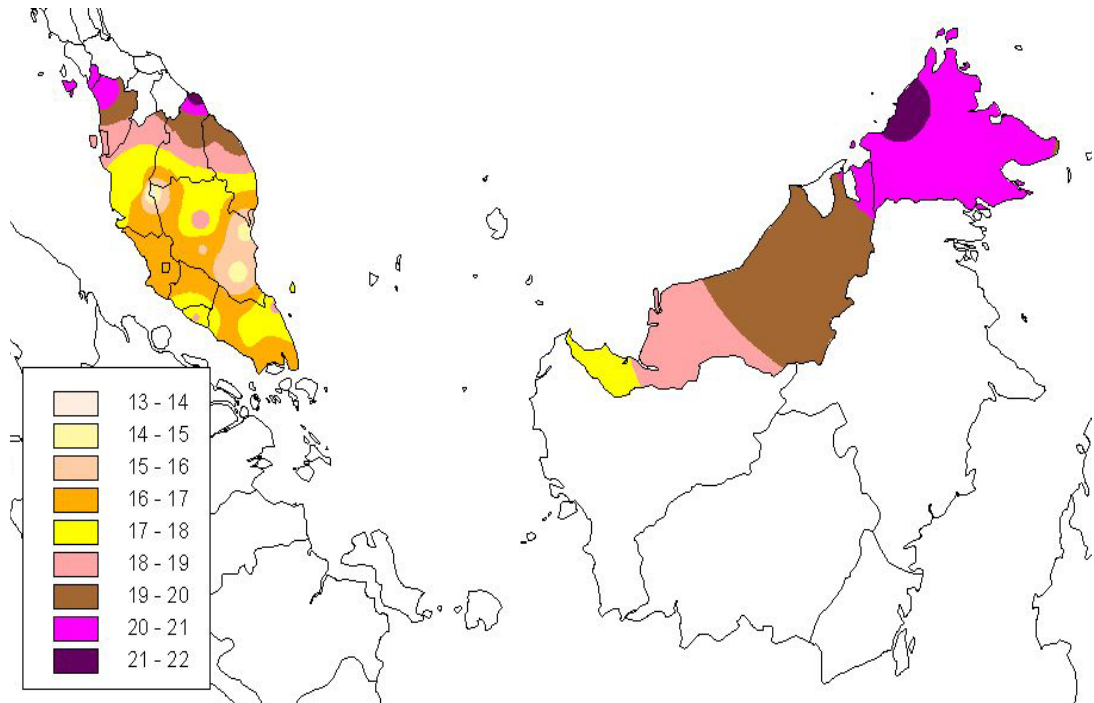
Figure 2.1: Solar Radiation Distribution in Malaysia [23]

2.3 Solar Collector

Currently there are three methods to harness solar energy into electricity. Basically the solar collectors can be categorized into 3 types, the first is the photovoltaic cell, concentrating solar collector, non-concentrated collector. The first photovoltaic or PV converts solar energy into electricity while the other 2 types convert solar energy into thermal energy or heat source.

2.3.1 Photovoltaic

This collector is considered a direct converter as it converts the sunlight directly into electricity. This photovoltaic is made up of semiconductors like the diodes and transistors and the semiconductors used in the PV is called solar cell. The solar cells are often made up of multicrystalline silicon. But there are also other ways

of manufacturing the silicon to make the solar cell. Others include amorphous silicon, monocrystalline silicon and crystalline silicon. The efficiency of the solar cell in the lab can reach up to 30 % but in the commercial the best efficiency is at 18 %. The conversion of sunlight to electricity uses a process called the photovoltaic effect [24].

2.3.2 Concentrated Solar Collector

The characteristic of a concentrated collector is that the collector uses mirror to reflect the sunlight to a focal point where there is absorber that collects the thermal heat. A concentrated solar collector can only reflect beam radiation. There are two types of concentrated solar collector used, one of it is point focus collector and another is line focus collector. In Malaysia, these types of collector are not available.

An example of a line focus is the parabolic trough and this collector focuses the solar radiation to the focal line where a tube is placed. Working fluids or heat transfer fluids is flowing in the tube to collect the heat. This is the most commercialized concentrated collector and it is used in the Solar Electric Generation System (SEGS) in California. Figure 2.2 shows the parabolic trough.
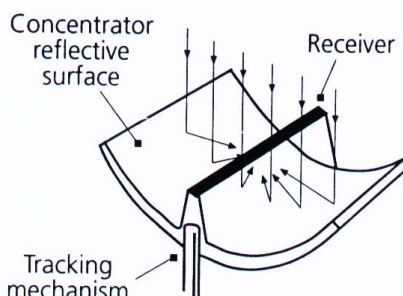
Figure 2.2: Parabolic Trough Solar Collector [25]

Basically point focus collector uses mirrors to concentrates solar radiation to the point of focus of the collector. Example of point focus collector is heliostat or central receiver and parabolic dish. The layout of the central receiver system is an array of field of mirrors or heliostats on the ground focus the radiation to a central receiver placed in a tower. These heliostats have a control system to track the sunlight in order for it to focus the sunlight to the receiver. This type of collector

gives a better concentration compared to the parabolic trough. Figure 2.3 depicts the layout and the working of the collector.
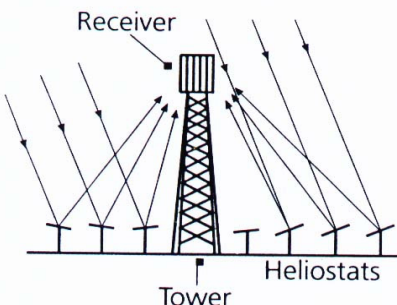
Figure 2.3: Central Receiver Solar Collector [25]

Parabolic dish is also another type of concentrated collector and this collector looks exactly like a normal satellite dish. Among all the concentrated collectors, this collector concentration factor is the highest. Due to small size it has application in relatively small capacity engine and it is highly potential in the small stand-alone remote application. Figure 2.4 shows the diagram and mechanism of the dish and Table 2.1 shows the comparisons of all the concentrated collectors.
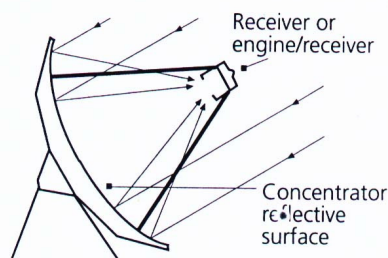
Figure 2.4: Parabolic Dish Solar Collector [25]

Table 2.1: Comparison between the three concentrated solar collectors [25]

Collector	Solar Concentration (× suns)	Operating Temp. (Hot side)	Thermodynamic Cycle Efficiency
Parabolic Trough	100	300 – 500 °C	Low
Central Receiver	1000	500 – 1000 °C	Moderate
Parabolic Dish	3000	800 – 1200 °C	High

2.3.3 Non-concentrated Solar Collector

Flat plate collector and evacuated tube collector are non-concentrated solar collector. A non-concentrated one collects total radiation of the sunlight without concentrating the radiation. Although non-concentrated can collect both the diffuse and beam radiation but the concentrated collector is much better in term of fluid temperature.

In Malaysia, flat plate collector is widely used and sold in the country. Flat plate collector is normally used domestically as solar water heater. There are two ways of collecting the solar radiation, one is the glazed and another is unglazed. The glazing refers to the type of cover plate used in the flat plate. Evacuated tube collector also used widely in Malaysia. The difference between a flat plate and evacuated tube is the type of tube used in the collector. The tube of the later is vacuumed. Figure 2.5 shows an example of a flat plate collector.
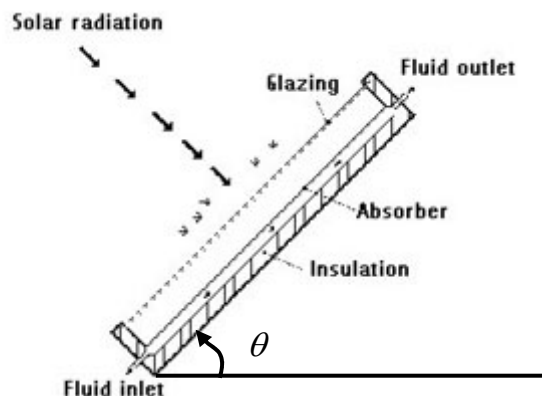
Figure 2.5: Glazing Flat Plate Collector [25]

For a higher fluid temperature, evacuated tubes are used. These evacuated tubes give a better efficiency and better heat collection because in the between the 2 tubes, the outer tube and the inner tube, it is vacuum. Therefore the heat loss through conduction and convection is prevented. Better efficiency and heat collection will result to higher fluid outlet temperature. The diagram of an evacuated tube collector is the same as the flat plate collector.

In order to eliminate the use of pump in flat plate a system called the thermosyphon or thermobouyancy is used. This system relies on the natural convection where the hot or warmer fluid will rise while the cooler fluid will go flow

to the bottom due to density difference. This system uses the same concept as a boiler in a steam plant. Thermosyphon is a natural convection that allows hot liquid rises. For liquid, density decreases as the temperature increases, therefore the hot liquid will become lighter and ascends [26].

For thermosyphon system solar collector, there is a tank on top of the solar collector. Cooler fluid that enters the tank will flow down to the collector where tubes of the collector are connected to the tank. As the water is heated by the radiation, the temperature of the water will increase to a stage it will flow upwards to the tank. In the tank, the hot fluid will ascend to the top of the tank. The hot water will exit the tank through another tube on top of the tank. Figure 2.6 depicts the process of thermosyphoning.
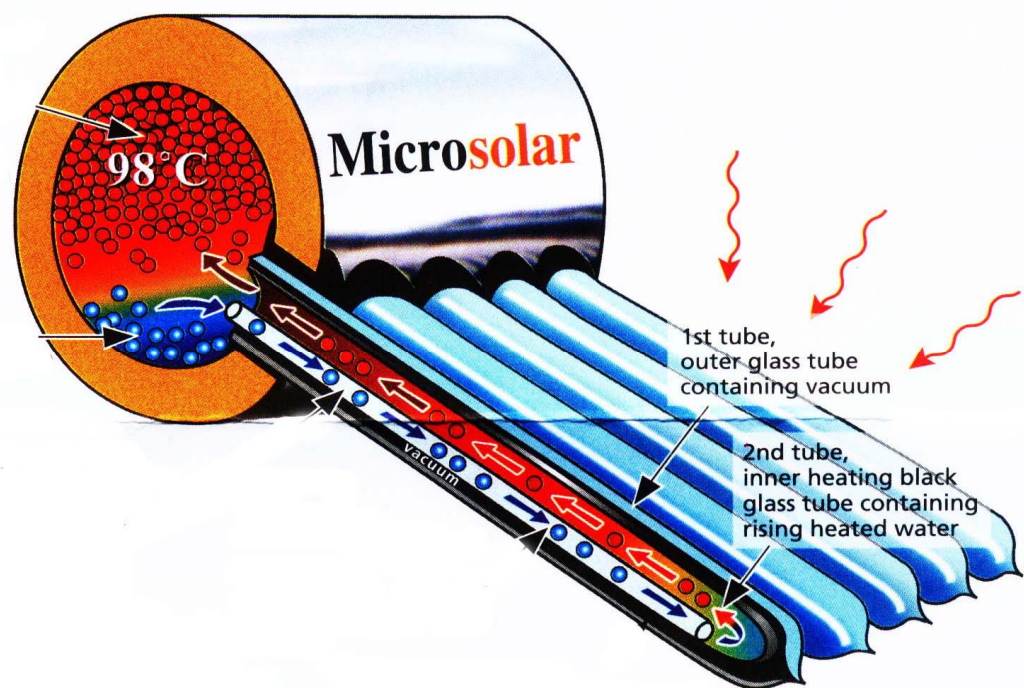
Figure 2.6: Thermosyphon System Collector [27]

2.4   Solar Electric Generation System (SEGS)

After an extensive literature review, it is found in United State America there are 9 working solar thermal power plants that are operational which is connected to the grid system. In the power plant, solar parabolic trough, either LS-1, LS-2 or LS-3 are used to collect the solar radiation [7]. The schematic diagram of the plant is as Figure 2.7. The power plant is a steam power plant with modification of the boiler, instead of using coal-fired or oil-fired, it uses heat transfer fluid, either Therminol VP1 or Therminol VP3, to transfer the thermal heat from the sun through the collector to the water in the steam turbine loop. Therminol VP1 consists of Diphenyl ether 73.5% and Biphenyl 26.5%, while Therminol VP3 is a blend of 90% of Cyclohexylbenzene and 10% of Bicyclohexyl [28].

In this SEGS, the plant is considered fossil fuel assisted because it has a boiler on a stand-by basis. The boiler functions as a backup when the temperature of the heat transfer fluid is insufficient to superheat the water. Due to the restriction of the regulation for a renewable energy power plant in USA, the amount heat supplied by fossil fuel-fired boiler must not be more than 25% of the total heat supplied to the system. The total capacity for all the 9 plants is 354 MWe. These power plants were built by the Luz Industries and now are owned by Solel Solar System Ltd. These plants are located in different parts of California [7].
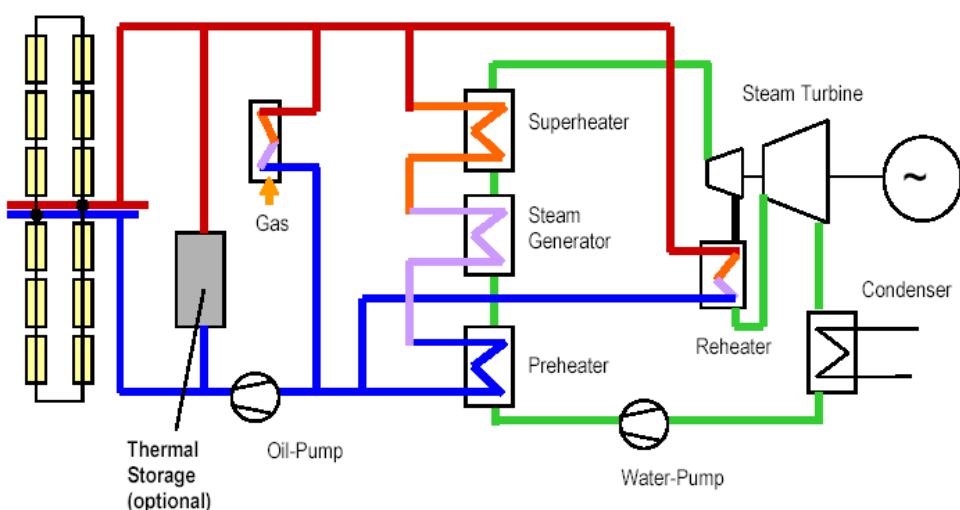
Figure 2.7: Schematic Diagram of a SEGS Plant in America. [29]

CHAPTER III

MATHEMATICAL FORMULATION

Working Model

The first step in this study is to develop an idea of the working model. Figure 3.1 shows the schematic diagram of the proposed working model. In this model, there will be 2 cycles, the first or number 1 is the solar thermal cycle and number 2 is the power cycle. The solar thermal cycle has a solar collector, a pump, and a heat exchanger. This cycle collects the solar radiation using collector and converts it into thermal energy by heat transfer fluid or HTF. The heat transfer fluid will exchange heat to the organic fluid in the power cycle via a heat exchanger. The pump circulates the fluid in the cycle.
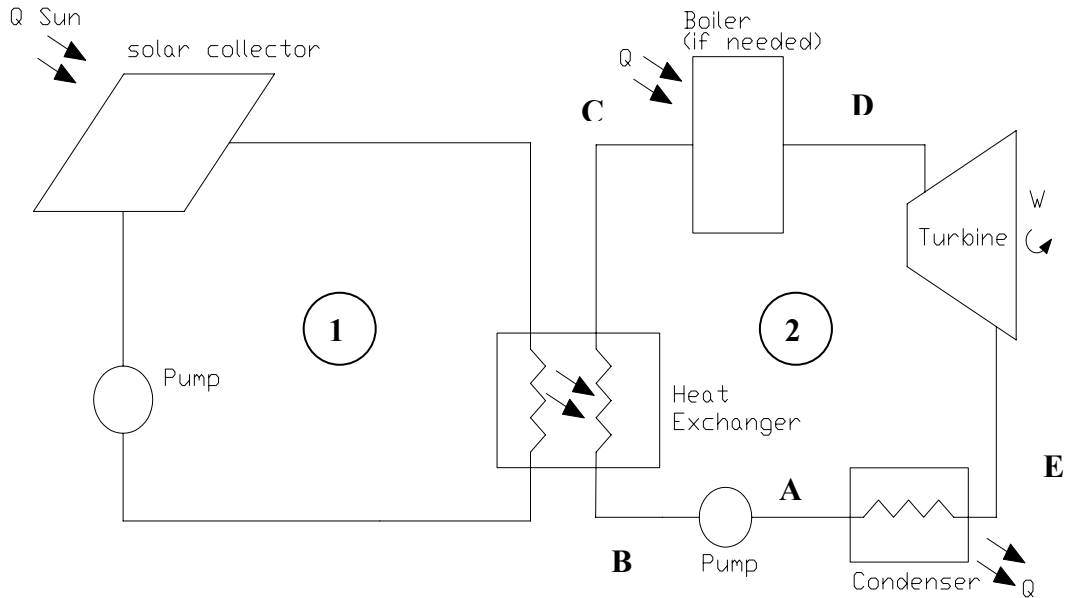
Figure 3.1: Model of the Proposed System
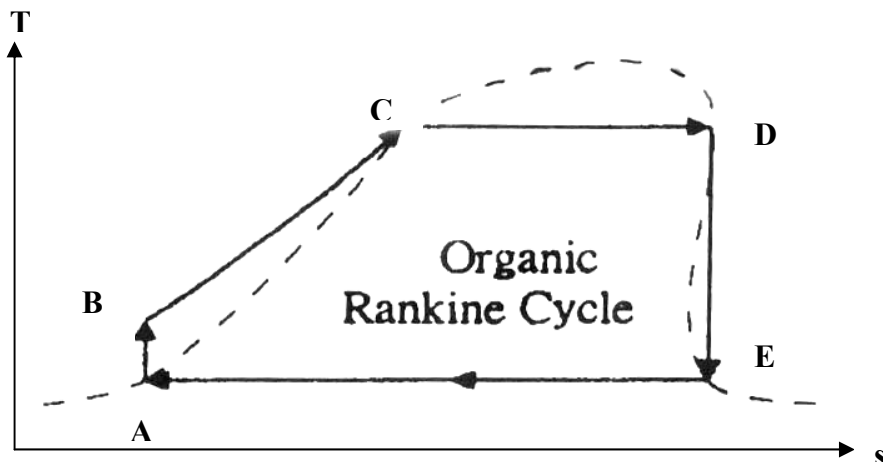
Figure 3.2: T-s Diagram of Proposed ORC [19].

The power cycle or the Organic Rankine Cycle converts thermal energy into the kinetic energy. Cycle 2 in Figure 3.1 shows the schematic of the proposed ORC, while Figure 3.2 shows the T-s diagram of the ORC processes. In this cycle, the pump will increase the organic fluid pressure which is in compressed liquid phase from state A to state B. The compressed liquid at state B leaves the pump and enters heat exchanger. Before the fluid enters the turbine, it should be at the saturated vapour line, point D, or in the superheated vapour region, beyond point D.

But in the heat exchanger, the amount of heat transferred from HTF to organic fluid is subjected to the solar radiation received. Point C in Figure 3.2 denotes the organic fluid is in after it is heated in the heat exchanger. Although in T-s diagram, point C is at the saturated liquid line but in actual point C could be anywhere in between point B and D. Point C is equivalent to point D if boiler is not used or required.

In order to make sure the fluid is in vapour phase, point D, when it enters the turbine, the stand-by boiler is placed after the heat exchanger. The vapour of the organic fluid will expand in the turbine and exits at point E. The expansion in the turbine will turn the turbine and produce work. After expansion, the fluid will be condensate from point E to point A in condenser the release the excessive thermal energy. In the initial stage, boiler option will not be considered as it is assumed the heat exchanger able to heat working fluid to point D or gaseous phase. The boiler is

fossil fuel fired and it will increase the system reliability especially when solar radiation is low.

3.1 Solar Radiation

Location of the plant is important as sun is the fuel source for this power plant and different location receives different amount of solar radiation. It is crucial to find the most suitable site that has the highest total daily radiation and the longest sunshine hour. Two locations will be chosen for this study, they are Kota Kinabalu and Chuping. Kota Kinabalu has the highest average solar radiation in Malaysia, while Chuping has the longest sunshine hour in Malaysia.

In the Malaysia Metrological Department, the sunshine duration was only recorded till year 1999 but the solar radiation data was given for year 2003. Therefore, we will assume that the sunshine duration for year 1999 is the same as the year 2003.

The solar radiation data is provided by the Malaysia Metrological Department is at the hourly rate using the unit of MJm^{-2}. But for our study, we will require the unit in $kWhm^{-2}$. Conversion factor:

$$MJ/m^2 = \frac{1}{3.6} kWh/m^2 \qquad (3.1)$$

In this study, the suitability of 2 different solar collectors, solar trough collector and flat plate collector, will be investigated. Since solar radiation data provided by Malaysia Metrological Department only in the form of total solar radiation, therefore estimated beam and diffuse radiation are calculated. This breakdown is important for the study of solar trough collector which is a concentrated collector. The solar radiation from the Malaysia Metrological Department is an hourly data. Ratio of diffusion radiation over total radiation is, [22]:

$$I_d \over I = \begin{cases} 1.0 - 0.249k_T & k_T < 0.35 \quad (i) \\ 1.557 - 1.84k_T & 0.35 < k_T < 0.75 \ (ii) \\ 0.177k_T & k_T > 0.75 \quad (iii) \end{cases}$$

(3.2)

where I_d = Diffuse radiation

I = Total radiation from solar radiation data

k_T = hourly clearness index

Here, k_T can be found, $k_T = \dfrac{I}{I_0}$

(3.3)

where I_0 = extraterrestrial radiation on a horizontal surface for an hour period

I_0 can be calculated by Equation (3.4) below,

$$I_0 = \frac{12 \times 3600}{\pi} G_{SC} \left(1 + 0.336 \cos \frac{360n}{365} \right) \left[\cos\phi \cos\delta (\sin\omega_2 - \sin\omega_1) + \frac{\pi(\omega_2 - \omega_1)}{180} \sin\phi \sin\delta \right]$$

where G_{SC} = Solar constant

n = day of year (from Table 3.1)

ϕ = Latitude (North positive)

δ = Declination, angular position of the sun at solar noon (North positive)

ω = Hour angle, angular displacement of the sun east or west of local meridian (East positive)

Declination [22],

$$\delta = 23.45 \sin\left(360 \frac{284 + n}{365} \right)$$

(3.5)

Hour angle [30],

$$\varpi = \pm (1/4)h_{min}$$

(3.6)

where h_{min} = time in minutes before local solar noon

Solar time [22],

SH = Standard time + $4(L_{st} - L_{loc})$ + E

(3.7)

where L_{st} = standard meridian for the local time zone

L_{loc} = longitude of the location in question

E is defined as Equation (3.8) below:

$$E = 229.2(0.000075 + 0.001868 \cos B - 0.03207 \sin B - 0.014615 \cos 2B - 0.04089 \sin 2B)$$

where $B = (n - 1)\dfrac{360}{365}$ (3.9)

n = number of days in a year

Table 3.1: Recommended Average Days for Months and Values of n by Months [31]

Month	n for ith Day of Month	For the Average Day of the Month		
		Date	n, Day of Year	δ, Declination
January	i	17	17	−20.9
February	$31 + i$	16	47	−13.0
March	$59 + i$	16	75	−2.4
April	$90 + i$	15	105	9.4
May	$120 + i$	15	135	18.8
June	$151 + i$	11	162	23.1
July	$181 + i$	17	198	21.2
August	$212 + i$	16	228	13.5
September	$243 + i$	15	258	2.2
October	$273 + i$	15	288	−9.6
November	$304 + i$	14	318	−18.9
December	$334 + i$	10	344	−23.0

Total Radiation, $I = I_d + I_b$ (3.10)

where I_b = Beam Radiation

3.2 Solar Thermal Cycle

In this solar thermal cycle, there are few main components that require attention, namely, parabolic mirror, heat transfer fluid and also the heat exchanger. In this cycle, the working fluid will always be maintained in a single phase, which is in liquid phase. This is to ensure a consistent flow rate in the cycle. A phase change, from liquid to gas, will also gives problem to the pump, pipe size and also the heat exchanger.

3.2.1   Parabolic Collector
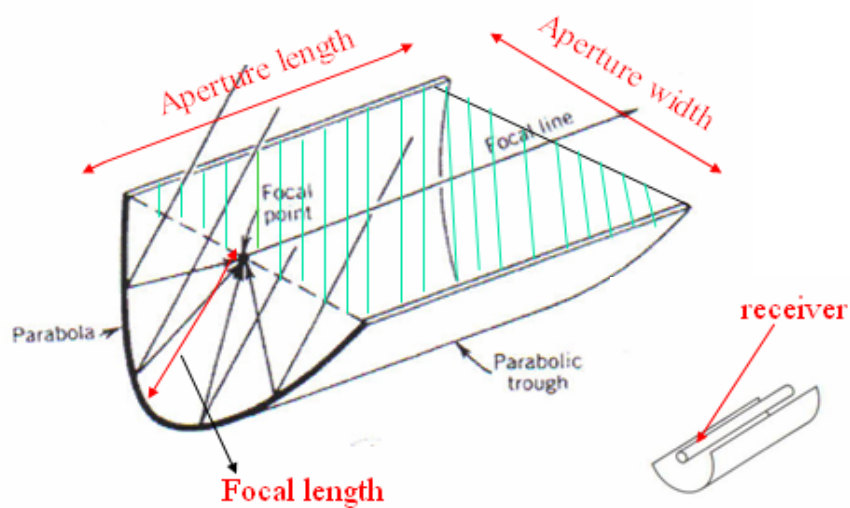
Figure 3.3: Details of Parabolic Trough Collector

In analyzing the solar parabolic collector, it is important to identify each and every part of the collector and the terms used on the solar collector. Figure 3.3 briefly describes the solar parabolic collector. In the concept and design of the parabolic collector, the first definition is strictly geometric as ratio of aperture area to receiver area.

The ratio of these two areas defines the concentration ratio of the parabolic trough as:

$$C = \frac{A_A}{A_R}$$

(3.11)

Where A_A = aperture area

A_R = receiver area

C = concentration ratio

Another important aspect in analyzing the solar collector is its efficiency. Therefore the following subtopics will derive the equation of efficiency for the parabolic collector. The efficiency is important to find the outlet temperature of the fluid. Basically the thermal efficiency of any solar thermal collector is:

$$\eta_{th} = \frac{Q_{collect}}{Q_{sun}}$$ (3.12)

where $Q_{collect}$ = amount of solar thermal energy collected

Q_{sun} = amount of solar radiation from the sun.

3.2.2 Solar Trough

In this subtopic, the discussion of the governing equation of the solar trough collector is based on the workshop presented by Riffelmann during the 6th International Summer School Solar Energy 2000 [34].
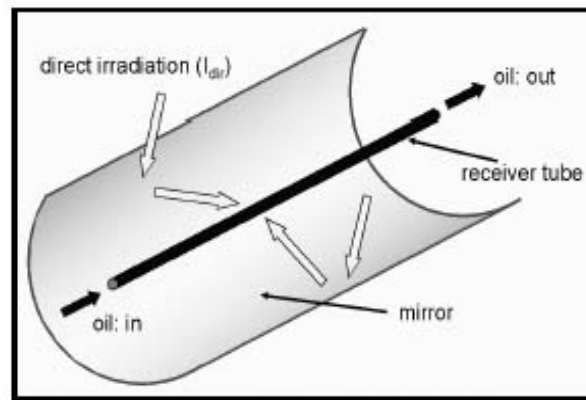
Figure 3.4: Collector system [34].
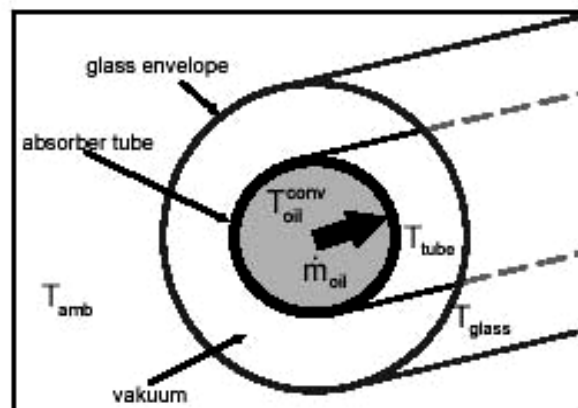
Figure 3.5: Receiver System [34]

There are a few assumption made for the calculation of the collector efficiency, short length, steady state condition and the solar radiation is perpendicular

to the aperture. Figures 3.4 and 3.5 illustrate the collector system which is the solar trough thermal collector and the receiver of the system, the vacuum tube receiver. In Figure 3.5, T_{amb} refers to the ambient temperature, T_{glass} is the temperature of the glass envelope, T_{tube} is the absorber tube temperature and T_{oil} refers to the temperature of the HTF or oil. The collector efficiency is given by:

$$\eta_{collector} = \frac{\dot{Q}_{used}}{I_b \times A_{Ap}} \tag{3.13}$$

where $\dot{Q}_{used}$ = useful energy gained by HTF

I_b = beam component of solar radiation

A_{Ap} = aperture area of the solar trough
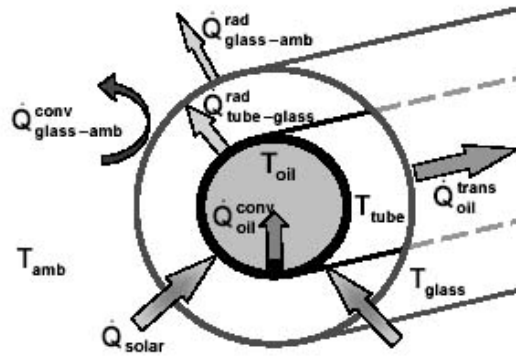
Figure 3.6: Energy Flow of the Receiver System [34]

From Figure 3.6, the energy balance around the receiver tube leads to:

$$\dot{Q}_{solar} = \dot{Q}_{used} + \dot{Q}_{losses} \tag{3.14}$$

where $\dot{Q}_{solar}$ = solar radiation absorbed by the black tube,

$\dot{Q}_{used}$ = energy gained by the HTF or oil

$\dot{Q}_{losses}$ = thermal losses of the hot absorber to the ambient.

$\dot{Q}_{solar}$ is dependent on the beam irradiance I_b, aperture area of the mirror A_{ap} and the optical efficiency $\eta_{optical}$:

$$\dot{Q}_{solar} = \eta_{optical} \times I_b \times A_{ap} \tag{3.15}$$

The optical efficiency contains complex about reflectivity, absorption, transmission and spillage of the mirror, the glass envelope and the absorber tube. For LS-3, the

newest solar trough used in SEGS Power Plant, the optical efficiency is 0.73. The thermal efficiency, ratio of useful energy to the absorbed energy is:

$$\eta_{thermal} = \frac{\dot{Q}_{used}}{\dot{Q}_{solar}} \qquad (3.16)$$

Therefore, collector efficiency is:

$$\eta_{collector} = \eta_{optical} \times \eta_{thermal} \qquad (3.17)$$

The energy gained by the HTF is in temperature increase and is calculated by:

$$\dot{Q}_{used} = \dot{m}c_p \left(T_{HTF,out} - T_{HTF,in}\right) \qquad (3.18)$$

with mass flow as $\dot{m}$ and heat capacity of HTF is c_p.

First, the heat is transferred to the absorber tube wall by conducting and then enters the HTF by convection. The first heat resistance is neglected because it is smaller compared to the second heat loss, therefore:

$$\dot{Q}_{used} = \dot{Q}_{HTF}^{conv} = \alpha_{tube} \times A_{tube} \left(T_{tube} - T_{HTFaverage}\right) \qquad (3.19)$$

where α_{tube} = heat transfer coefficient

$$T_{HTFaverage} = \frac{\left(T_{oil,out} - T_{out,in}\right)}{2} \qquad (3.20)$$

The rest of the incoming solar energy is lost from the absorber tube by radiation to the glass envelope. This equation is a function of the Stefan-Boltzmann constant σ, the emissivity if the glass envelope ε_{glass} and the tube surface ε_{tube}, the area of both glass A_{glass} and tube A_{tube} and of the temperatures of the tube respectively the glass to the power of four. The special geometry – one tube surrounded by another one – is defined using the following equation:

$$\dot{Q}_{lossed} = \dot{Q}_{tube-glass} = \sigma \left[\frac{T_{tube}^4 - T_{glass}^4}{\frac{1}{\varepsilon_{tube}} \times \frac{A_{tube}}{A_{glass}} \left(\frac{1}{\varepsilon_{glass}} - 1\right)} \right] \qquad (3.21)$$

This energy heats up the glass envelope and – for the assumption of steady state conditions – is completely lost to the ambient by radiation and convection:

$$\dot{Q}_{lossed} = \dot{Q}_{glass}^{rad} + \dot{Q}_{glass}^{conv} \qquad (3.22)$$

In this case the equation for radiation losses gets simpler:

$$\dot{Q}_{glass}^{rad} = \varepsilon_{glass} \times \sigma \times A_{glass}\left(T_{glass}^4 - T_{amb}^4\right) \tag{3.23}$$

This convection energy flux $\dot{Q}_{glass}^{conv}$ is a function of the glass surface A_{glass} and of the temperature difference between the glass and the ambient air. It includes also the heat transfer coefficient α_{tube} that is influenced by the geometry, the surface abilities, the properties of air and mainly wind speed:

$$\dot{Q}_{glass}^{conv} = \alpha_{glass} \times A_{glass} \times\left(T_{glass} - T_{amb}\right) \tag{3.24}$$

This equation can be solved for different boundary conditions.

Solar trough collector cannot be found in the Malaysian market. Therefore in this study, LS-3 solar trough collector will be chosen as it is being used for the existing SEGS IX Power Plant. This plant utilises the solar trough collector by Solel Solar Systems Ltd. that has the commercial name of LS-3. The collector efficiency is 68% [30]. Table 3.2 indicates the commercially available solar trough with their specifications. Most of these solar trough found in the tables is the result of the research on the SEGS Plants.

Table 3.2: Commercially Available Solar Trough and Their Specifications [7].

Collector	Acurex 3001	M.A.N. M480	Luz LS-1	Luz LS-2		Luz LS-3
Year Developed	1981	1984	1984	1985	1988	1989
Area (m^2)	34	80	128	235		545
Aperture (m)	1.8	2.4	2.5	5		5.7
Length (m)	20	38	50	48		99
Receiver Diameter (m)	0.051	0.058	0.042	0.07		0.07
Concentration Ratio	36:1	41:1	61:1	71:1		82:1
Optical Efficiency	0.77	0.77	0.734	0.737	0.764	0.8
Receiver Absorptivity	0.96	0.96	0.94	0.94	0.99	0.96
Mirror Reflectivity	0.93	0.93	0.94	0.94	0.94	0.94
Receiver Emittance	0.27	0.17	0.3	0.24	0.19	0.19
@ Temperature (°C/°F)			300/572	300/572	350/662	350/662
Operating Temperature (°C)	295/563	307/585	307/585	349/660	390/734	390/734

3.2.3   Heat Transfer Fluid

Two heat transfer fluids (HTF) will be considered in this research, one of the HTF chosen is due to the previous working model in the SEGS plant [35] and another is recommended by the HTF manufacturer [28]. The chosen HTF are Therminol VP3 (90% Cyclohexylbenzene and 10% Bicyclohexyl) and Therminol 55 (C14-30-alkylaromatic derivatives). All these HTF are manufactured by Solutia Inc [28]. The calculations involving these compounds are based on the thermodynamic properties table provided by the company.

From the thermodynamic tables, the data will be curve fitted using least square regression to get an equation. The equation obtained is the representation of the thermodynamic table and will be used for the programming of the parametric study. Least square regression for polynomial curve involve the assumption that dependent variable y can written in the general form,

$$y = a_0 + a_1 x + a_2 x^2 + ... + a_m x^m$$

where a_i are the model parameter. The least square regression involves the minimization of the sum of squares errors.

3.2.4   Heat Exchanger

Heat collected from the solar collector is transfer to the power cycle through heat exchanger. Heat from HTF to be transferred is given by:

$$Q_{hot} = \dot{m} c \Delta T \qquad (3.25)$$

where $\dot{m}$ =mass flow rate of HTF

ΔT = temperature drop in HTF ($T_{out} - T_{in}$)

c = specific heat of HTF

The heat exchanger is assumed to be simple cross-flow heat exchanger with 100% effectiveness – heat from hot fluid is totally absorbed by the cool fluid. A cross-flow heat exchanger is depicted in the Figure 3.7. Fluid B is the hot fluid while

Fluid A is cool fluid. The temperature of Fluid A at outlet, T2 is higher than T1, temperature at inlet. Outlet temperature of Fluid B, T4 is lower than temperature at inlet, T3. But T2 will be lower than T4.
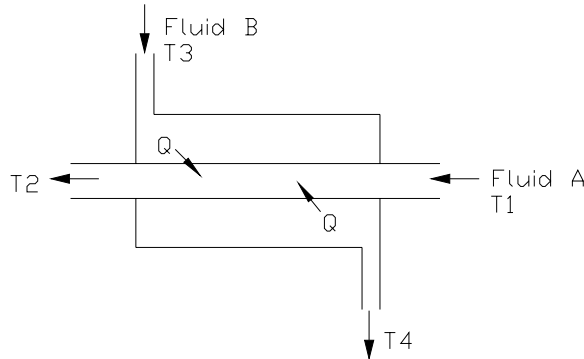
Figure 3.7: Cross-Flow Heat Exchanger

The equation of the heat exchanger, heat loss in the hot fluid is equals to the heat gain in cool fluid:

$$Q_{hot} = Q_{cool} \tag{3.26}$$

3.3   Organic Rankine Cycle

In the Organic Rankine Cycle (ORC) there are 4 main components in the cycle. These components are turbine, condenser, pump and heat exchanger or boiler. In this cycle, all the processes will be assumed to be ideal process, adiabatic and reversible. The calculation involved in subtopics below will refer to Figure 3.2.

3.3.3   Organic Compound (Refrigerant)

In this study, only two types of ready made blends will be investigated. The selection of the organic compound is based from literature review. Selected blends from literature are R123 (1,1–dichloro–2,2,2–trifluoroethane) and isobutane. R123 and isobutane are selected because these organic compounds are tested and found to be a good working fluid for an ORC [10, 14, 15, 16, 17, 18, 19]. The thermodynamic table for R123 uses table developed from modified Benedict-Webb-Rubin (MBWR) equation of state done by B.A. Younglove and M.O. McLinden [36]. Isobutane

thermodynamic table is also developed from MBWR equation of state and it is computed and tabulated by B.A. Younglove and J.F. Ely [37]. For programming purposes, the tabulated data are plotted and least square method is used to fit the graph to obtain an equation to represent these data.

3.3.4   Turbine (Figure 3.2, state D-E)

The isentropic expansion of the vapour in the turbine will provide mechanical work. The expansion of the vapour will lower the pressure and the temperature of the vapour at the turbine outlet or point E. Turbine work ouput, W_t is found from First Thermodynamic Law:

$$W_t = \dot{m} \times \eta_t \times (h_D - h_E) \tag{3.27}$$

where η_t = isentropic efficiency of turbine = 1

$\quad h$ = specific enthalpy

3.3.5   Condenser (Figure 3.2, state E-A)

In the condenser the vapour or saturated vapour will goes through a constant pressure phase change to saturated liquid, transferring all the latent heat to cooling fluid, usually sea water or water from river. The pressure of this condenser is restricted by the temperature of the cooling fluid. Pressure and temperature is dependent on each other in the saturated liquid-vapour phase. The heat released through condenser, Q_{out} is derived from formula below:

$$Q_{out} = \dot{m}(h_E - h_A) \tag{3.28}$$

3.3.6 Pump (Figure 3.2, state A-B)

The pump is required in the system to circulate the fluid in the cycle. The saturated liquid leaving the condenser at the lower pressure is return to the high pressure here. This pump is assumed to be isentropic compression. The work for this pump, W_p, is calculated by the following equation:

$$W_p = \dot{m}\frac{(P_B - P_A)v}{\eta_p} \tag{3.29}$$

where $\dot{m}$ is the flow rate of the fluid; v is the volume of the saturated liquid of the inlet; and η_p is the isentropic efficiency of the pump, equals to 1. The specific enthalpy of the pump outlet is given by:

$$h_B = h_A + \frac{W_p}{\dot{m}} \tag{3.30}$$

where h_A = specific enthalpy at the inlet of the pump.

3.3.7 Boiler or Heat Exchanger (Figure 3.2, state B-D)

In the proposed system, though both heat exchanger and boiler are two different components but the governing equation for both is the same. The high pressure compressed liquid will be heated at constant pressure to saturated vapour or superheated vapour state. The outlet condition of the working fluid is given by the following equation:

$$h_D = h_E + \frac{Q_{in}}{\dot{m}} \tag{3.31}$$

3.3.8 Cycle Efficiency

In the study of ORC, the performance of the system is evaluated by the thermal efficiency of the system. The thermal efficiency η_{th} is given by:

$$\eta_{th} = \frac{W_t - W_p}{Q_{in}} \times 100 \tag{3.32}$$

In the actual system, there are losses involved. Losses incur in the turbine and condenser processes due to pressure drop and also pressure increase in the boiler. These losses are neglected and the system is assumed to be in steady state, no heat loss and no pressure drop. The system is ideal.

CHAPTER IV

METHODOLOGY

Introduction

There are a number of programs that can be used to do the parametric study, for example, Mathcad, Mathlab, Fortran, Visual Basic and Borland C++. Considering the mathematical formulations involved, the choice of programs that will be used will be MATHLAB and Microsoft Excel. These programs are chosen mainly because of the programs are flexible, user-friendly and also easily available in the market.

4.1 Main Flowchart

This main flowchart, Figure 4.1, will show the chronological order of the methodology applied in the parametric study. The relationships of all the sub-programming are also shown in this flowchart. This subsection will briefly explain the steps and the details of the steps will be explained in the following subsections. The first step is optimization of the ORC with R123 and isobutane. Through the ORC program, the selection of the organic compound will be done. Values from the cycle are used in the next programming involving HTF. Solar component program will involve the breakdown of diffuse and direct radiation. The result from the program is used for calculation involving solar trough. The unit of the solar data will be converted through solar conversion program. This is to create a consistent unit with the ORC heat rate. With value from ORC and the solar radiation data, collector area for each collector will be calculated and finally selection of the collector will be done.

41
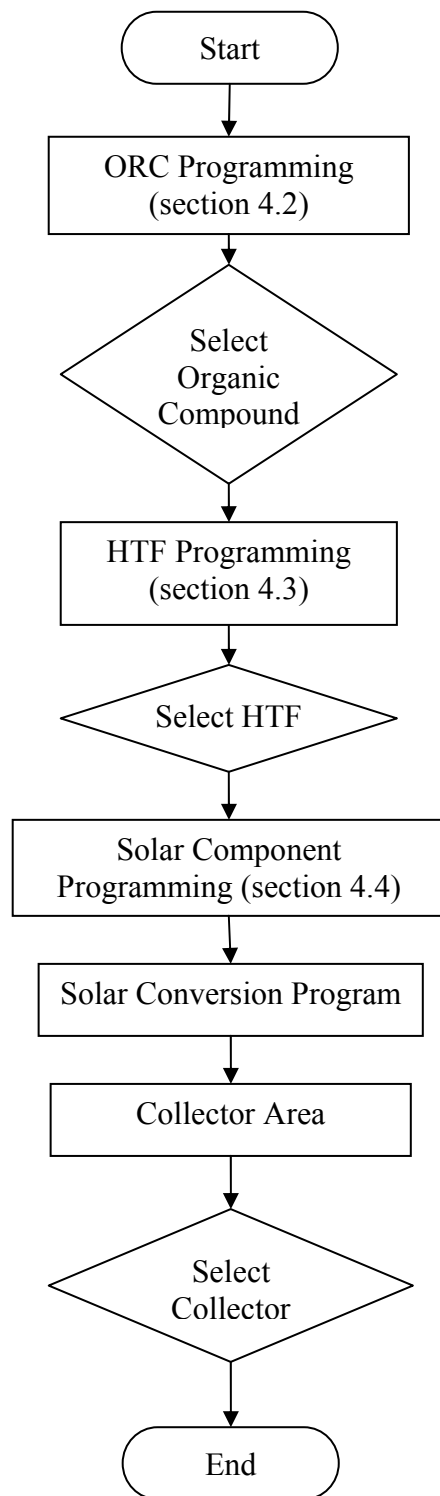
Figure 4.1: Main Flow Chart

4.2 Organic Rankine Cycle Program

The objective of the program is to find the optimized pressure for the organic compound to provide the highest work output. The optimization will be done of the organic fluids, isobutane and R-123. The optimization of the ORC is done along the saturated vapour line only as this will bring the ORC closer to the Carnot Cycle. The approach involved in the optimization program is shown in Figure 4.2.

Referring to the Figure 4.2, first step to the program is to obtain the equation of state for the organic compound. The programming to obtain the equation will be further elucidated in the subsection later on. The temperature for the condenser is fixed at 24˚C for isobutane and 27˚C for R123. From the fixed temperature, the pressure is determined. Next, the program will increase the turbine inlet pressure and from the pressure, turbine inlet temperature (TIT) is obtained as the turbine inlet is always fixed along the saturated vapour line.

Turbine inlet enthalpy and entropy will be calculated from the known pressure and temperature. Isentropic expansion in turbine, therefore the turbine outlet entropy is equals the turbine inlet. With the known entropy and condenser pressure, the enthalpy at turbine outlet is obtained. The difference of enthalpy between the turbine inlet and turbine outlet is obtained. Assuming the pump work is small and negligible, therefore the heat input is equivalent to the enthalpy difference at saturated liquid line at condenser and turbine inlet.

Efficiency is calculated by the knowing the heat input and work output of the cycle. This programming will continue until the turbine inlet pressure reaches the critical temperature of the organic fluid.
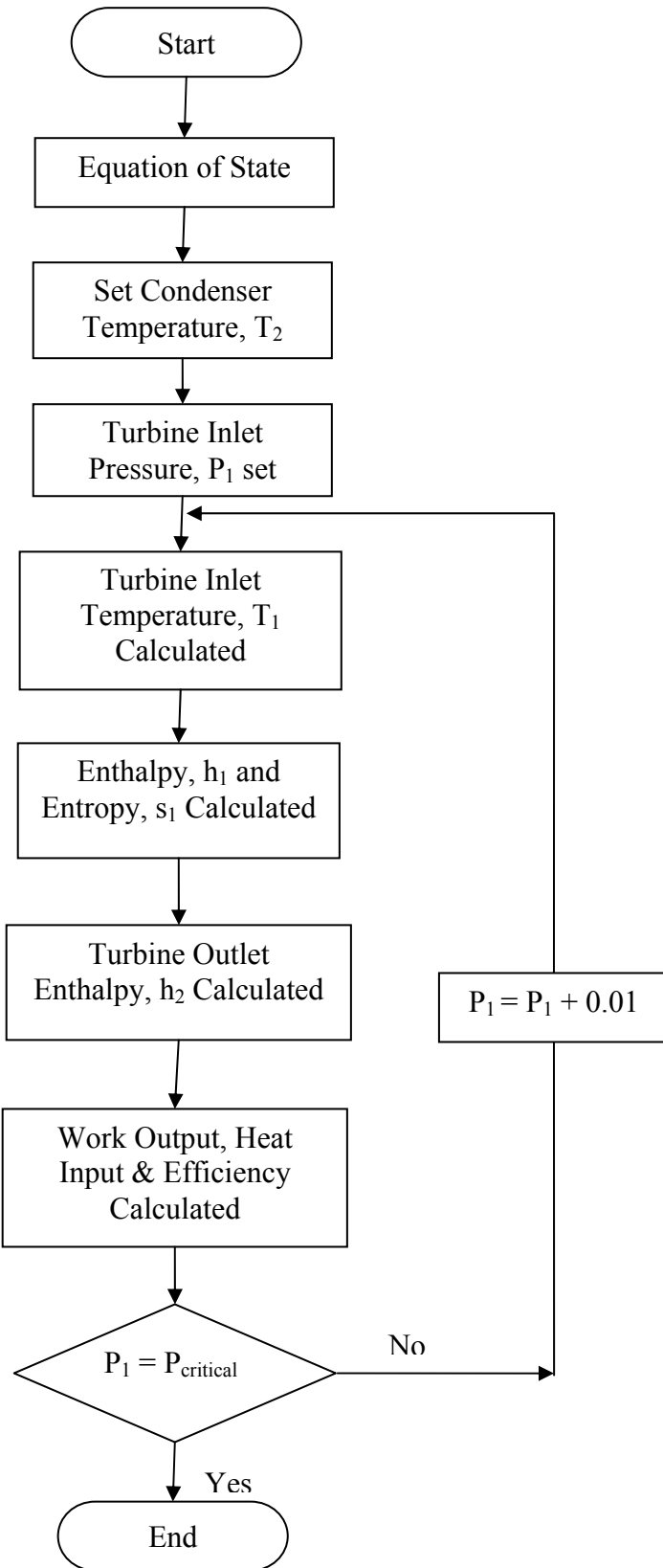
Figure 4.2: Flow Chart for ORC Programming

4.2.1 Equation of state

For HTF and organic compound (OC), all the available thermodynamic properties data are tabulated by the manufacturer. In this study, the parametric study is done with the use of computer programming; therefore, the tabulated data will be required in equation form. In order to get the equation of state for the OC and HTF, we will use least square regression method to curve fit the tabulated data.

The first step to find the equation of state is to insert the tabulated data in the Microsoft Excel. Then the data will be plotted and by using the built-in program in the software, the equation will be shown. The built-in program uses least square regression to find the equation. Figure 4.3 below shows the flow chart for the method of obtaining the equation of state. The least square method by using Microsoft Excel will be plotted to a polynomial that suite all the points the best.
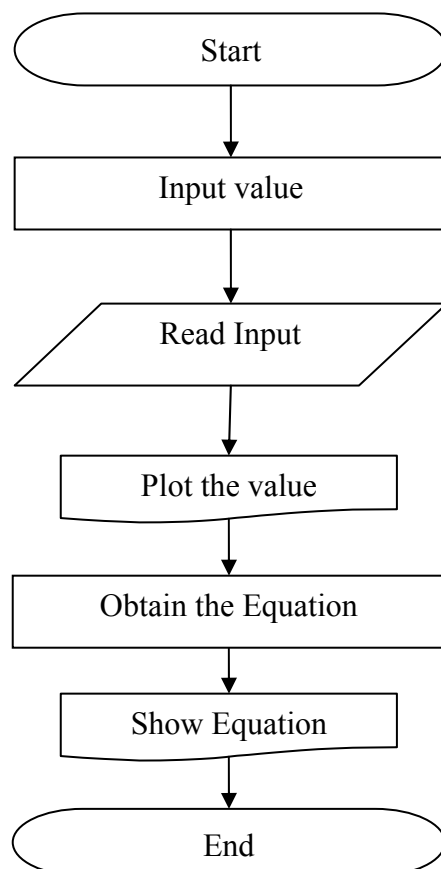
Figure 4.3: Flow Chart to Obtain Equation of State

4.2.2   Organic Rankine Cycle Selection

From all the data obtained in ORC programming, these data will be plotted and curve-fitted to obtain equation representing the line. Differentiation of the equation and maximum point is obtained. The peak point will be the optimized pressure that gives the highest work output. Organic compound selection will be based on the efficiency and TIT of the corresponding ORC. Selection will be primarily decided by whichever organic fluid that is able to provide a better efficiency. However, due to the limitation of heat source temperature from the solar thermal cycle, the sole choice will be the organic fluid that gives an achievable TIT.

4.3 Heat Transfer Fluid Programming

In this programming, the optimized pressure from the ORC programming will be used to calculate the required heat input for the power cycle. The heat input is used to calculate the highest and lowest temperature of the HTF in order to have the heat transfer from solar thermal cycle to the power cycle. The selection of the HTF will be based on the heat transfer fluid the gives the smallest temperature difference, highest temperature minus lowest temperature, for the heat transfer fluid. The highest temperature of HTF should not go beyond 230˚C because the highest temperature that is able to be achieved by flat plate collector is 250˚C.

4.4 Solar Radiation Simulation

There will be 2 programs involved in this solar radiation simulation, the first is a conversion program, which will converts unit from MJ m^{-2} to kWh m^{-2}. The second program, breakdown the diffuse and beam component in the solar radiation.

For the first program, the flow chart is as shown in Figure 4.4. The function of this program is to convert all the solar radiation data which is in the unit of MJ m^{-2} into kWh m^{-2}. In the program, variable, *I,* equals to the solar radiation in MJ m^{-2} and *II* is the solar radiation in kWh m^{-2}. First, *I* is set to 0 and the value of *I* will change as it reads the data from the solar radiation from Malaysia Metrological Department. For each value of *I*, it will be divided with 3.6 as it is converted into radiation in kWh

m^{-2}. For this programming, Microsoft Excel will be used because the data from Metrological Department is in Microsoft Excel format.

```
                    ┌─────────────────────┐
                    │        Start         │
                    └─────────────────────┘
                              │
                              ▼
                    ┌─────────────────────┐
                    │        I = 0         │
                    └─────────────────────┘
                              │
                              ▼
                    ┌─────────────────────┐
                    │       Read I         │
                    └─────────────────────┘
                              │
                              ▼
                    ┌─────────────────────┐
                    │   II = f(I) [Eq 3.1] │
                    └─────────────────────┘
                              │
                              ▼
                    ┌─────────────────────┐
                    │      Print II        │
                    └─────────────────────┘
                              │
                              ▼
                    ┌─────────────────────┐
                    │         End          │
                    └─────────────────────┘
```
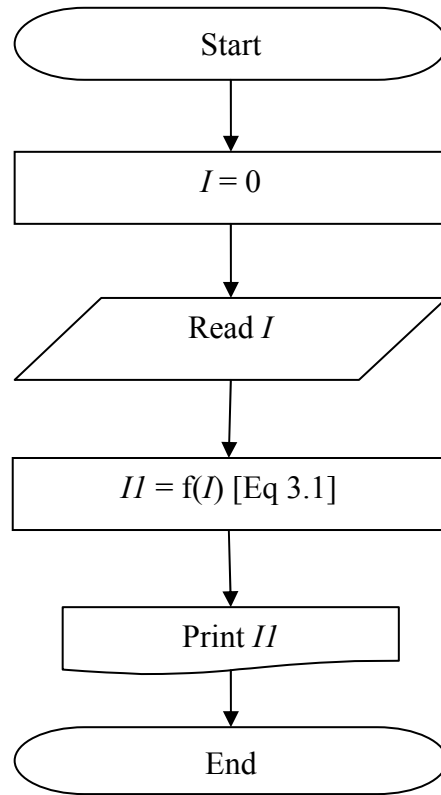
Figure 4.4: Solar Radiation Conversion Flow Chart

Figure 4.5 depicts the flow chart for the second program; the objective of this program is to get the diffuse and beam radiation form total radiation. The input of the program will depends on the location as it requires the latitude, ϕ and longitude, L_{loc} of the place in study. Other location dependent input include the standard meridian for local time zone, L_{st}, which in Malaysia is 105° in the east or GMT +8. Besides location of the place in question, the program also requires the time and day of the collected set of data, where n is day in a year. I is the total solar radiation collected from the Malaysia Metrological Department. This program will be done in MATLAB. The solar radiation data from Microsoft Excel will be imported into MATLAB.
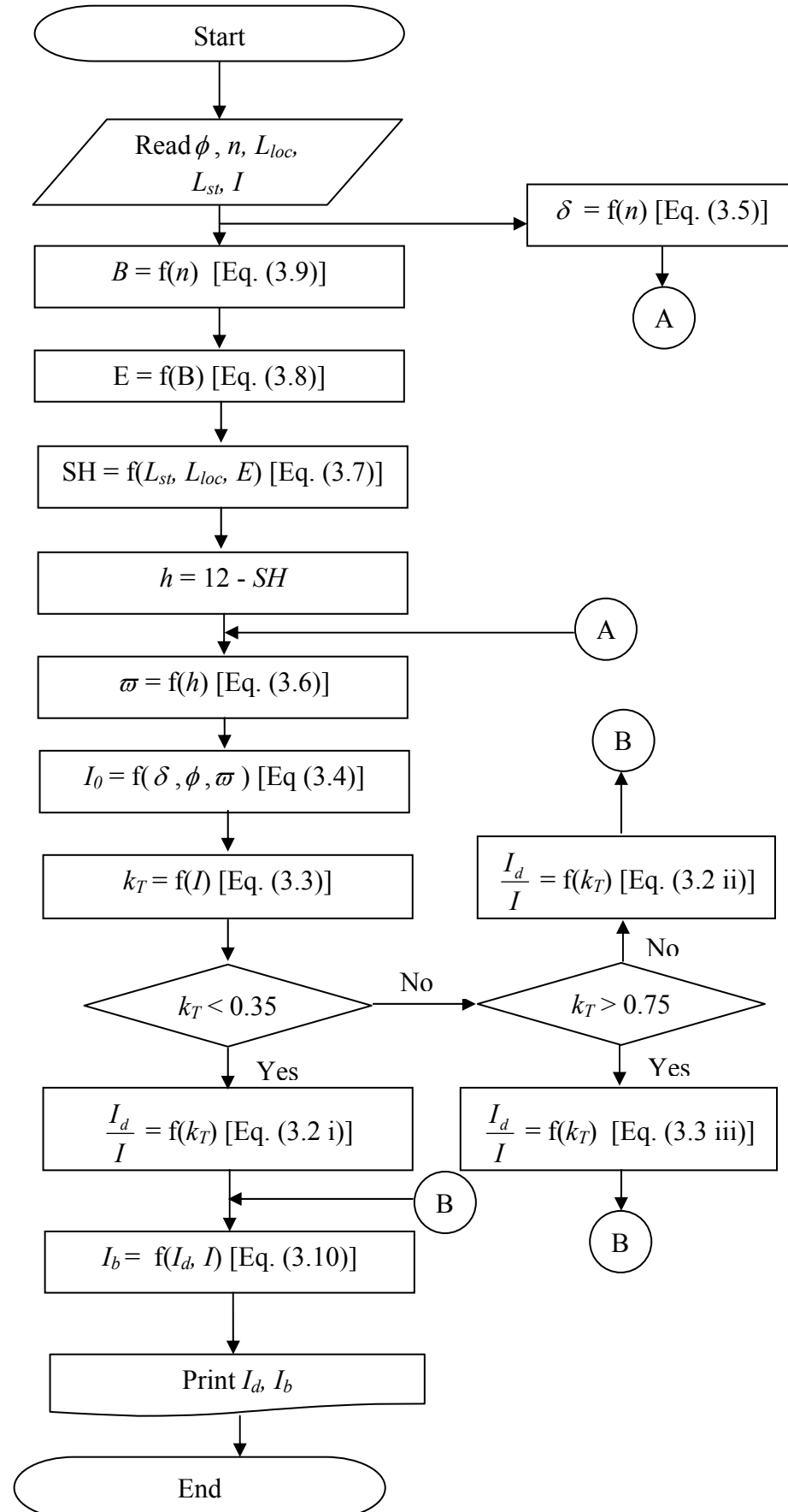
Figure 4.5: Flow Chart of the Diffuse and Direct Radiation

4.5   Solar Parabolic Trough Test Rig - Testing

The primary reason for testing the performance of the solar parabolic trough is to optimize the heat transfer from the received radiation to the absorber. Usually to get the maximum outlet temperature from the absorber independently is quite difficult. This is due to the fact that these components attached to the thermal system are easily affected by environmental factors such as wind, scattered clouds and cloudy weather.

Since environmental effects are a highly faced problem the testing configurations play an important role in the design of the model. In this case the effects of environmental factors and the ways to overcome it in on order to optimize the performance of the solar parabolic collector are investigated. To compare the data of those configurations, the test rig has to be designed in such a way that it is similar to those in use currently for the purpose of power generation.
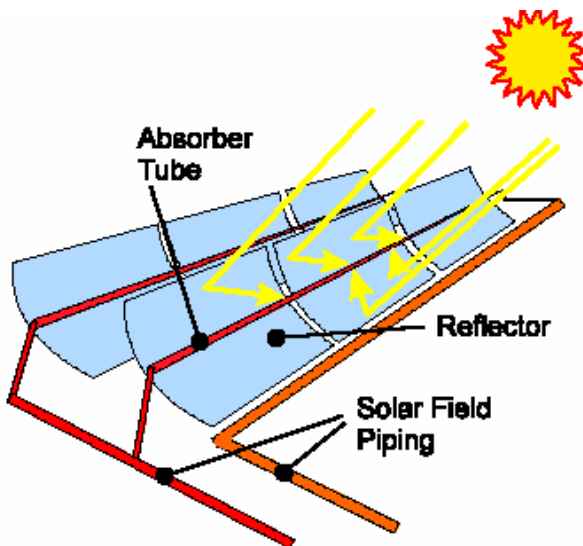
Figure 4.6: Principles of Parabolic Trough Systems [25]

Figure 4.6 above shows the principles of the parabolic trough system which is currently in use. The figure explains the parabolic trough system which consists of long parallel rows of identical concentrator modules, typically using trough shaped glass mirrors. Tracking the sun from East to West by rotation on one axis, the trough collector concentrates the direct solar radiation onto an absorber pipe located along

its focal line. A heat transfer medium, typically oil at temperature up to 400°C is circulated through the pipes. The hot oil evaporates water and the generated steam drives the steam turbine generator of a conventional power block [25]. The designed solar parabolic test rig in this study will carry out a sequence of testing based on the concept mentioned above.

4.6   Solar Parabolic Collector Test Rig Design and Installation.
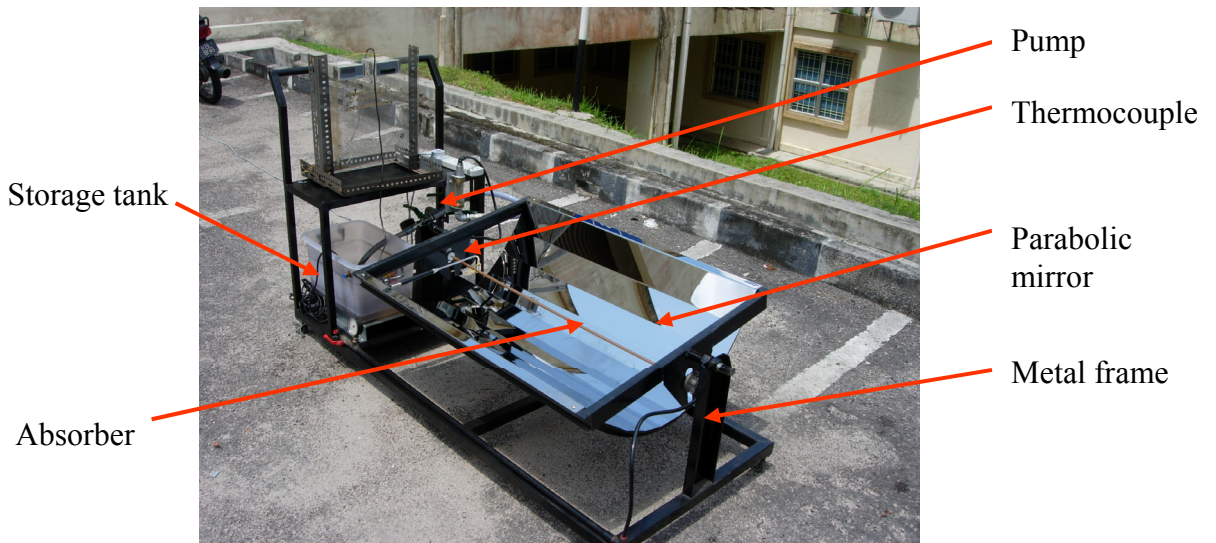
Figure 4.7: Solar Parabolic Collector Test Rig

Before fabricating the test rig, the technical drawing of the solar parabolic test rig was prepared (refer appendix A).The design and installation of the line-focus parabolic trough collector is carried out successfully according to strength, dynamic pressure and collector's weight. The solar parabolic trough collector consists of several main parts namely the metal frame, parabolic mirror, the solar radiation absorption system, pump, storage tank and the thermocouple as shown in Figure 4.7.

4.6.1 Metal Frame

The metal frame is the structure that supports the parabolic mirror, the solar radiation absorption system, pump, storage tank and temperature sensing system. This metal frame as shown in Figure 4.8 is designed in such away that it has the ability to track the sun's daily orbit. This can be achieved by the rotation of the collector axis. These movements can be achieved by sliding the collector's frame up and down manually.
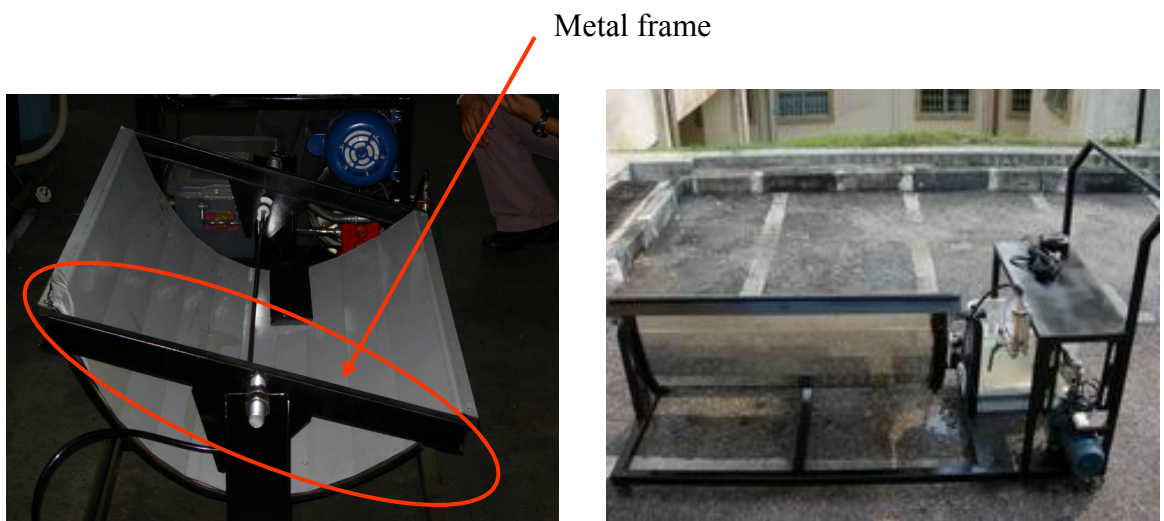
Figure 4.8: Test Rig Metal Frame

4.6.2 Parabolic Mirror

The active collector surface on this test rig consists of one parabolic mirror measuring (0.7 m^2).The placement of the mirror on the platform should be symmetrical with reference to the axis of rotation. The total incoming solar radiation is focused on a line which is parallel to the axis or rotation and at a distance of 0.14m. This mirror has a high reflection capability. The view of the parabolic mirror is shown in Figure 4.9.

Figure 4.9: Parabolic Mirror

4.6.3 Solar Radiation Absorption System

The heat pipe absorber as shown in Figure 4.10 in this solar collector system is made of copper and it has a good heat conduction using a minimum amount of material, resulting in a quick response to changes in radiation intensity. The developed system consists of a copper pipe, placed parallel to the axis of rotation and at distance of 0.14 m. The position where the maximum solar concentration is achieved coincides with the pipe position. The pipe's length is 1m. The most important part of the absorption system is the evacuated envelope which surrounds the heat pipe absorber. The vacuum between the glass and copper pipe reduces the rate of heat loss. A flexible pipe, through which the heat transfer fluid is supplied, is connected to the copper pipe. The evacuated envelope is not included in this system due to the high cost and fabrication complexity constraints.

Absorber
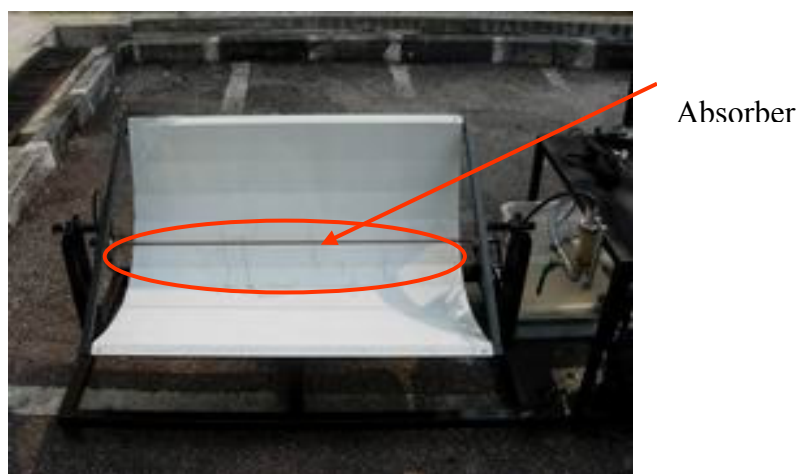
Figure 4.10: Collector Heat Absorption System

4.6.4 Pump

A pump is attached with the solar test rig for the purpose of suction and delivery of the heat transfer fluid which is stored in the storage tank. A pump with small flow rate is required to obtain maximum heat absorption.

The designed specification of the pump is as stated below:

Power   = 50-60 Watts

Flow rate   = 0.1 L/min – 0.2 L/min

RPM   = 6-600 rpm

Support pressure   = 1 bar – 5 bar

Flow Tube Diameter   = 10mm

Working fluid temperature = 25 – 150 (^{o}C)

4.6.5 Temperature Sensing System

The solar parabolic trough collector has a set of thermocouple attach to the storage tank and to the copper pipe wall as shown in Figure 4.11. The thermocouple is used to monitor the most critical parameter in the solar thermal cycle that is the temperature profile around the copper absorber pipe during system operation. The individual thermocouple will be connected to a digital data logger that will display the temperature of the absorber as shown in Figure 4.12.

Figure 4.11: Thermocouple attached on Absorber

Figure 4.12: Digital Data Logger

4.7 Description of Solar Test Rig Experiment Methods and Techniques.

The approach that is taken to conduct this research is to carry out various test techniques on the solar parabolic test rig. The performance of the designed solar parabolic test rig will be analyzed using the appropriate test methods and techniques. The experimentally evaluated readings and observations gained will be compared with each other to obtain the best performance out of the solar parabolic collector test rig. Among the test methods which will be carried out in this experimental study to analyze the performance of the solar parabolic trough rig and to optimize the heat transfer rate to the absorber are as stated and described below:

4.7.1 Dry Test - (Non-operating thermal cycle & no reflection effects) – Method 1

This test will be carried out when the solar parabolic collector is not in operating condition or given the term dry test in this study. During this test, the parabolic mirror surface will be covered up with a sheet of white paper to obtain the absorber temperature reading without the solar concentration effects.

4.7.2 Dry Test - (Non-operating thermal cycle & with reflection effects) –
Method 2

This test will also be carried out when the solar parabolic collector is not in operating condition. However during this test, the solar concentration effects by the parabolic mirror on the absorber will be taken into consideration. The absorber temperature with the effects of solar concentration on it will be taken in this case.

4.7.3 Testing for Suitable Pump Size

Here, two pumps with different capacity or sizes will be analysed. The purpose of this test is to check on the severity of friction between the pump rotation and the working fluid. A high powered pump with a capacity of 0.5hp (368 Watts) and a lab sized pump with a capacity of 0.1hp (75 Watts) will be tested here. The storage tank temperature will be monitored here as both this pump operates for a certain period of time. An increase of temperature in the storage tank will determine or show the severity of friction between the pump rotation and the working fluid. A minimum value of increase in the storage tank temperature is the desired value here.

4.7.4 Flow Profile Test

Once the suitable pump size is being selected, the flow profile of the fluid in the absorber will be determined. In this test, the copper absorber tube will be replaced with a Perspex tube to see the flow character in the Perspex tube. The pump speed will be set until it gives a minimal flow of working fluid and at the same the working fluid is to cover the overall circumference area of the Perspex tube. Once this condition is observed, the flow rate of the fluid will be taken and from this, the flow profile of the working fluid will be determined using the Reynolds's number formulation.

4.7.5 Operating Thermal Cycle - (Wrapping solar collector and with tilting effects)

Here in this test, the aperture area of the solar parabolic collector test rig will be wrapped or covered up with a thin plastic sheet to minimize as much as possible the external wind effect on the solar collector when the experiment is being carried out. Besides that, during this test, the collector will also be tilted in order for it to track the sun movement. In this test, both the storage tank temperature and the absorber temperature will be taken to see the effects given by this set up.

4.7.6 Operating Thermal Cycle - (Wrapping solar collector and no tilting effects)

In this test, the exact same set up as described earlier will be remained. The only difference upon carrying out this test is that the solar collector will not be tilted in order for it to track the sun movement. The solar collector surface will be fixed static facing upwards. Here, both the storage tank temperature and also the absorber temperature will be taken and the readings obtained from this test will be compared with the readings taken when the collector is tilted as mentioned in the subtopic above.

4.7.7 Dry Test (Non-operating thermal cycle, with effects of wrapping and insulation) – Method 3

This test will be carried out when the solar thermal system is not in operating condition. In this test method, the aperture area of the solar parabolic collector test rig will be wrapped with a thin plastic sheet and the bottom surface of the parabolic collector will be insulated with an insulation sheet. The purpose of this insulation sheet here is to minimize the heat loss to the environment and also to maximize the utilization of heat captured by the solar collector. The effects from this set up to the absorber temperature will be investigated.

4.7.8 Operating Thermal Cycle- (With effects of wrapping, insulation and tracking sun)

This test will be carried out with the same set up as described in subtopic 4.7.7, but with the solar thermal cycle in operating condition. During this test, the solar parabolic collector will also be tilted to track the sun movement. The effects of wrapping, insulating and tilting the solar collector will be studied and investigated here by analyzing the absorber temperature readings.

4.7.9 Operating Thermal Cycle- (Outlet temperature with different flow rates)

This test will be carried out using the same set up on the solar parabolic collector as mentioned in subtopic 4.7.8 above. Here, the system will be tested with two different flow rates operating on the solar thermal cycle which will be discussed in chapter five later on. The temperature difference (dT) between the absorber outlet temperature (T_{out}) and the absorber inlet temperature (T_{in}) is the area of interest in this testing. Both the absorber outlet temperature (T_{out}) and the absorber inlet temperature (T_{in}) readings will be taken here to determine the temperature differences. This temperature differences will then be used to determine the collector efficiency and also to carry out the analysis on the Organic Rankine Cycle (ORC) to determine the possible power generation by this testing.

All results, discussions and complete details including figures of the test which are being carried out based on the test technique described in the subtopics above, will be presented in chapter five.

CHAPTER V

RESULT & DISCUSSION

Introduction

In this chapter the results from both the parametric study and experimental study are presented and discussed in detail. The results shown in each subprogram in each subtopic will be used to construct the final model.

5.1 Organic Rankine Cycle

The power cycle, ORC, is important because the ORC result is used to evaluate the feasibility of the system. The measure of worth for the ORC will be based on the thermal efficiency of the whole cycle and also the turbine inlet temperature (TIT). The TIT has priority over the efficiency of the cycle. Though thermal efficiency is important and often used to measure the practicability of a thermodynamic cycle, but in this study the TIT is more important due to the temperature limitations of solar thermal collectors. The limited operating temperature is especially significant for flat plate collectors due to the constraint of the maximum temperature of 250°C. After considering the TIT, the system efficiency will be taken into consideration.

R123 and isobutane are studied parametrically to compare the thermal efficiency of both cycles. The ORC study will be conducted in the subcritical heating region. The effect of turbine inlet pressure along the saturated vapour line and turbine inlet temperature in the superheated region on system efficiency will be explored. Thermophysical properties of the two working fluids are listed in Table 5.1. Figure 5.1 depicts the general T-s diagram for both fluids.

Table 5.1: Thermophysical Properties of R123 and Isobutane [38]

Parameters	R123	Isobutane
Chemical Formula	$CHCl_2 - CF_3$	C_4H_{10}
Molecular weight (g/mol)	152.93	58.125
Slope of saturated vapour line	Isentropic	Negative
Critical temperature (K)	456.831	407.85
Critical Pressure (MPa)	3.6618	3.64
Boiling point at 1 atm (K)	300.82	261.44
Maximum Pressure (MPa)	NA	35
Maximum Temperature (K)	NA	600
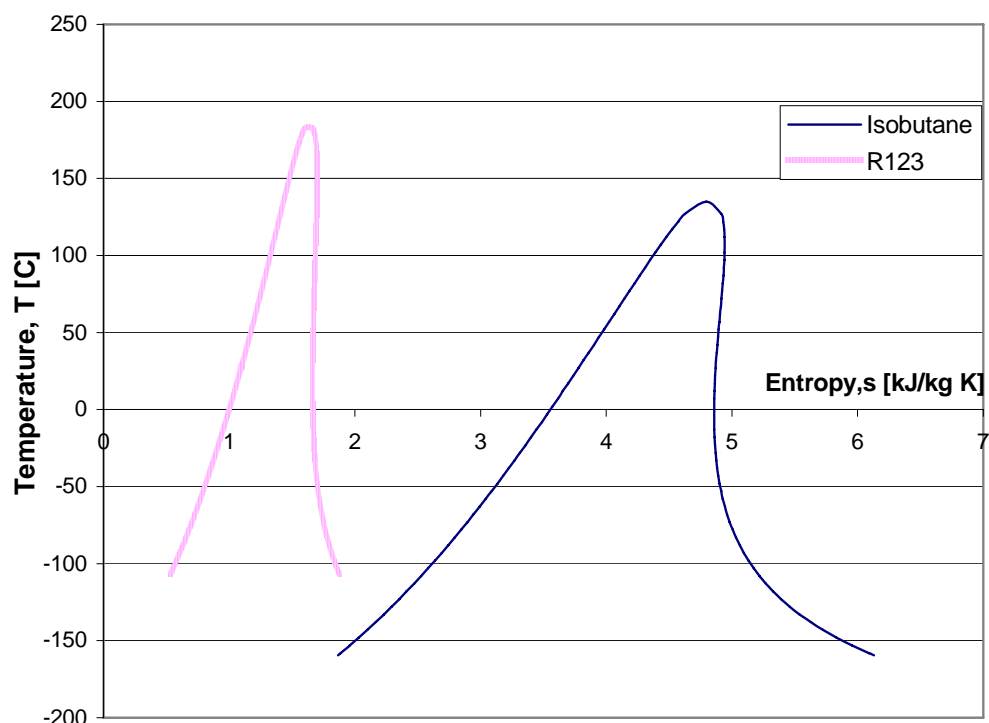
Figure 5.1: T-s Diagram of Isobutane and R123.

5.1.1   Isobutane

The effect of turbine inlet pressure (TIP) on efficiency and work is investigated. The result of the study is plotted and shown as in Figure 5.2. In the figure, it is shown that the efficiency and work is a quadratic function of turbine inlet pressure with a maximum point, after which both work and efficiency will decrease as the pressure increases. The maximum value of work and efficiency occur at different pressures however, they are close to each other.
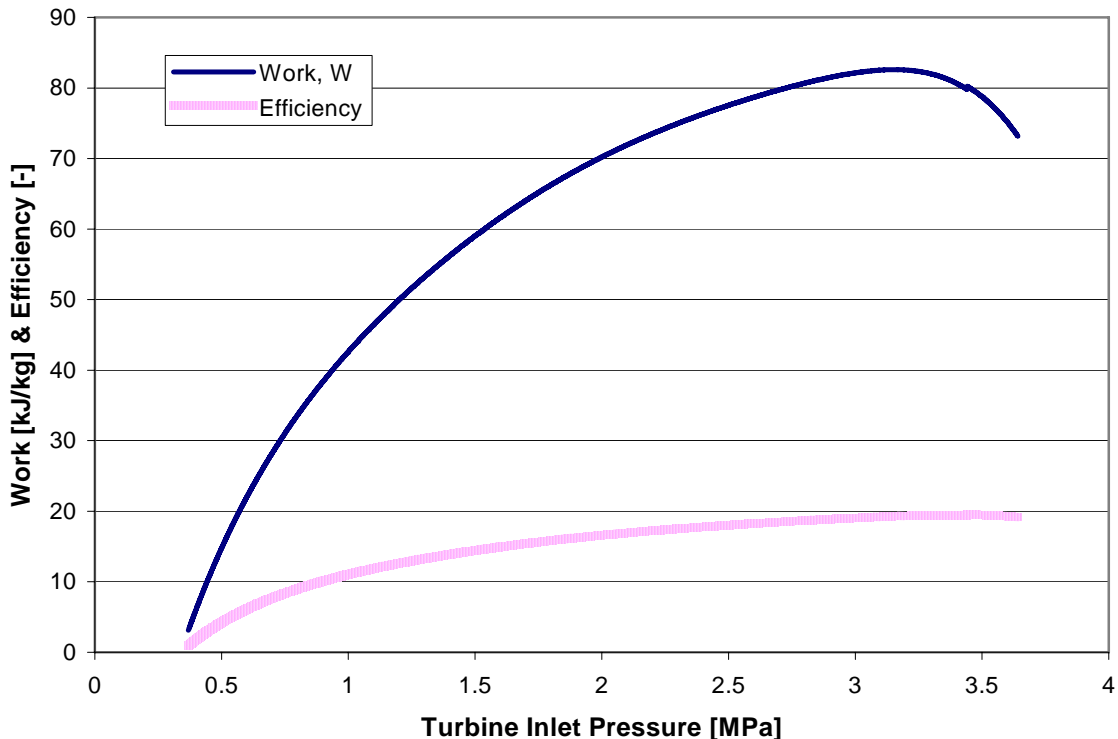
Figure 5.2: Work & Efficiency vs. Turbine Inlet Pressure.

Table 5.2: Conversion Characteristics for Isobutane ORC System.

Working Fluid	Isobutane		
Condition	Max Work	Max Efficiency	Corrected Pres.
Min. cycle pres. [MPa]	0.38	0.38	0.38
Min cycle temp. [˚C]	28	28	28
Max. cycle pres. [MPa]	3.16	3.40	2.25
Max. cycle temp. [˚C]	127	132	107
Turbine expansion ratio	8.32	8.95	5.9
Turbine vol. flow ratio	12.5	17.6	7.0
Isen. exp. work [kJ/kg]	77.65	75.78	69.2
Wettest vapour quality	0.95	0.86	NA
Exhaust vapour quality	Superheated	Superheated	Superheated
Turbine mass flow [kg/s]	1	1	16.6
Cycle Efficiency [%]	18.57	18.85	20.72
Carnot Efficiency [%]	24.74	25.62	0.38

Table 5.2 displays the relevant parameters which give the maximum value of work and efficiency from the graph in Figure 5.2. The highest work output obtained is 77.65 kJ/kg with a cycle thermal efficiency of 18.57 % while the maximum

thermal efficiency is 18.85 % and the work output at this maximum efficiency is 75.78 kJ/kg.

From the T-s diagram plotted in Figure 5.3, the turbine expansion line indicates that the vapour is wetter in the working section of turbine than at the turbine outlet. In Table 5.2, the term of wettest vapor quality is used. This term, wettest vapor quality, is to indicate the highest moisture content in the working section of the ORC turbine. When the pressure is optimized along the saturated vapor line, it is found that when the pressure approaches the critical pressure, fluid expansion in the turbine will lead to higher moisture content as compared to the turbine outlet. This occurs due to the saturated vapor line curvature in the T-s diagram of the fluid, at higher pressures the gradient of the saturated vapor line changes from isentropic or positive to negative.
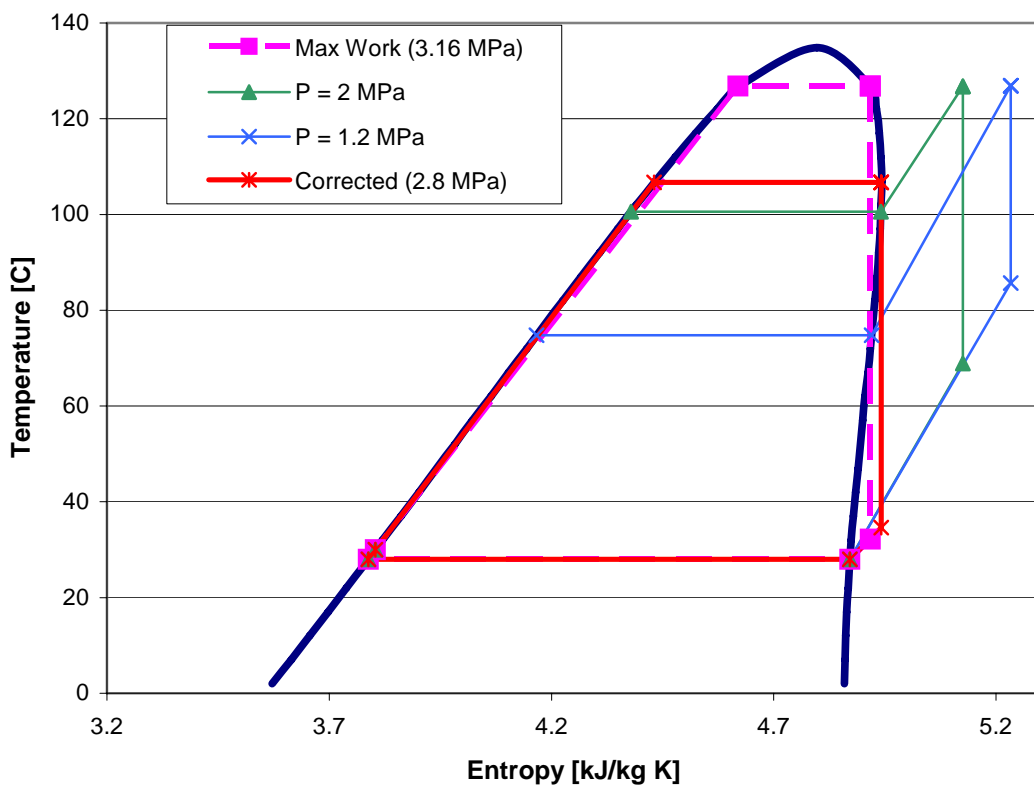
Figure 5.3: T-s Diagram of Isobutane at Maximum Work; Superheating at P = 1.2 MPa and P = 2 MPa; and Corrected Pressure

Therefore, to make sure that the vapor is dry in the turbine, it is recommended that the TIP be set at the turning point of the saturated vapor line in the T-s diagram. The turning point is situated between the point of inflexion and the

critical point. By changing the maximum cycle pressure, the efficiency and work output will drop to a lower value but the working fluid will be dry in the working section of the turbine. Last column in Table 5.3 shows the work delivered after correcting the pressure and temperature to the turning point of the saturated vapor line. The T-s diagram for the maximum work output cycle, corrected pressure cycle and superheating the fluid at 2 different pressures, 1.2 MPa and 2 MPa, are revealed in Figure 5.3.
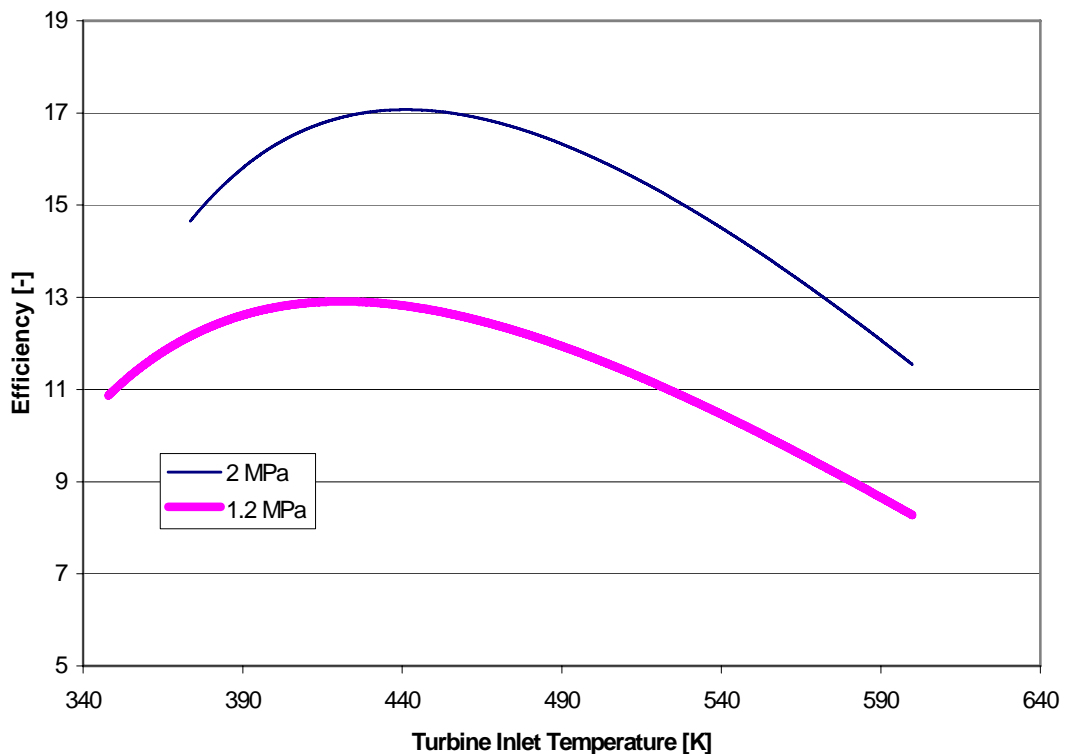
Figure 5.4: The Effect of TIT to the Efficiency for Isobutane in Superheated Region.

The effect of superheating isobutane is also studied parametrically. Figure 5.4 indicates the effect of turbine inlet temperature in the superheated vapour region on the efficiency of the ORC. Isobaric heating is done. The effect of turbine inlet temperature at a pressure between these two pressures can be obtained through interpolation. From Figure 5.4, it is identified that both lines are nearly parallel to each other. Initially the efficiency increases with an increase in the TIT but after it reaches the maximum point, any further increase of temperature will result in a drastic drop of efficiency. Therefore, an ORC that uses isobutane as working fluid can be operated in the superheated region but within a temperature limit.

5.1.2   R123

Similarly for R123, the effect of turbine inlet pressure on the efficiency and work output of the ORC is studied. Figure 5.5 indicates that work and efficiency is related to the turbine inlet pressure along the saturated vapour line. Both work and efficiency are quadratic functions of turbine inlet pressure. Compared to isobutane, R123 shows a higher efficiency but gives a lower work output. Similar to isobutane, the maximum work and efficiency are located at different pressures.
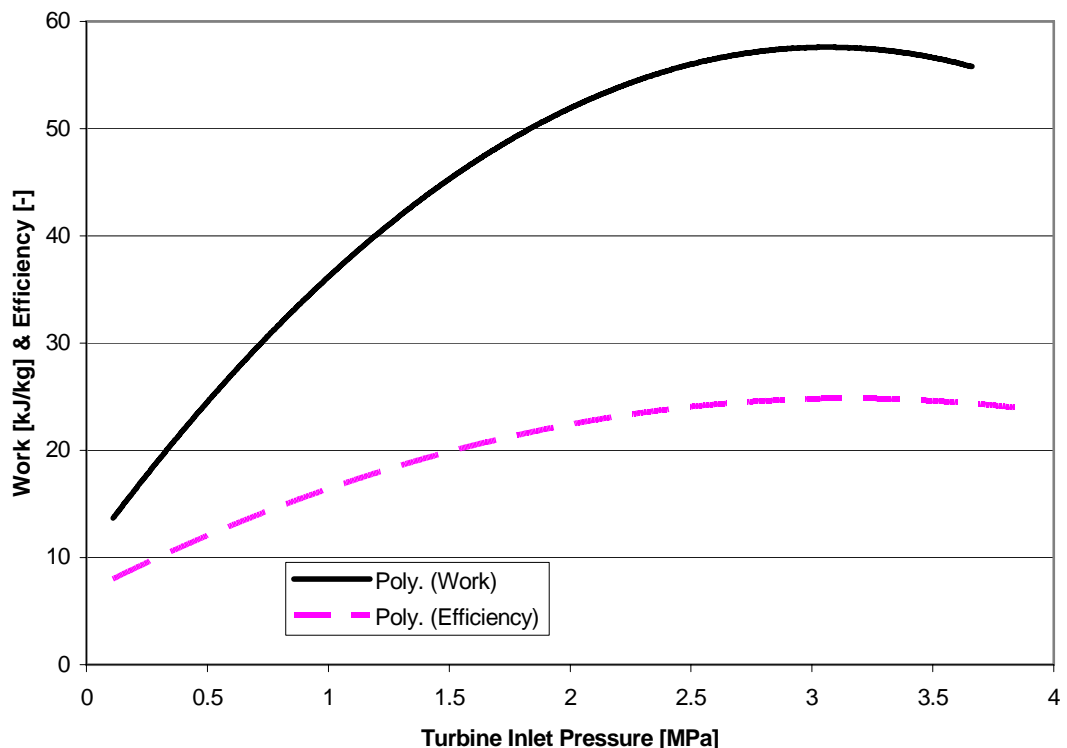
Figure 5.5: Work & Efficiency vs. Turbine Inlet Pressure.

Relevant parameters of the maximum work and pressure cycles using R123 are tabulated in Table 5.3. The maximum work output, 58.99 kJ/kg occurs when the pressure is at 3.4 MPa and the efficiency is rated at 25.63 % which is 8 % lower than the Carnot efficiency. At 3.54 MPa, the R123 ORC will achieve the maximum efficiency of 25.9 % which is 7 % lower than the Carnot efficiency and the work output is 58.54 kJ/kg. Comparing to the isobutane ORC, it is found that the same

phenomenon high moisture at high pressure also occurs in this R123 cycle. This phenomenon can be clearly seen in the T-s diagram of the R123 ORC at maximum work output in Figure 5.6. As a result, the pressure is also lowered, similar to isobutane, in order to ensure the fluid is always dry in the turbine. Relevant parameters are tabulated in Table 5.3 and the cycle is drawn in Figure 5.6.

Table 5.3: Conversion Characteristics for R123 ORC System

Working Fluid	R123		
Condition	Max Work	Max Efficiency	Corrected Pres.
Min. cycle pres. [MPa]	0.10	0.10	0.10
Min. cycle temp. [˚C]	28	28	28
Max. cycle pres. [MPa]	3.40	3.54	2.08
Max. cycle temp. [˚C]	180	182	150
Turbine expansion ratio	34	35.4	20.8
Turbine volume flow ratio	50.6	60.2	71.2
Isen. exp. work [kJ/kg]	58.99	58.54	51.6
Wettest vapour quality	0.84	0.78	Superheated
Exhaust vapour quality	1	0.98	Superheated
Turbine mass flow [kg/s]	1	1	1
Cycle Efficiency [%]	25.63	25.90	22.15
Carnot Efficiency [%]	33.82	33.55	28.88
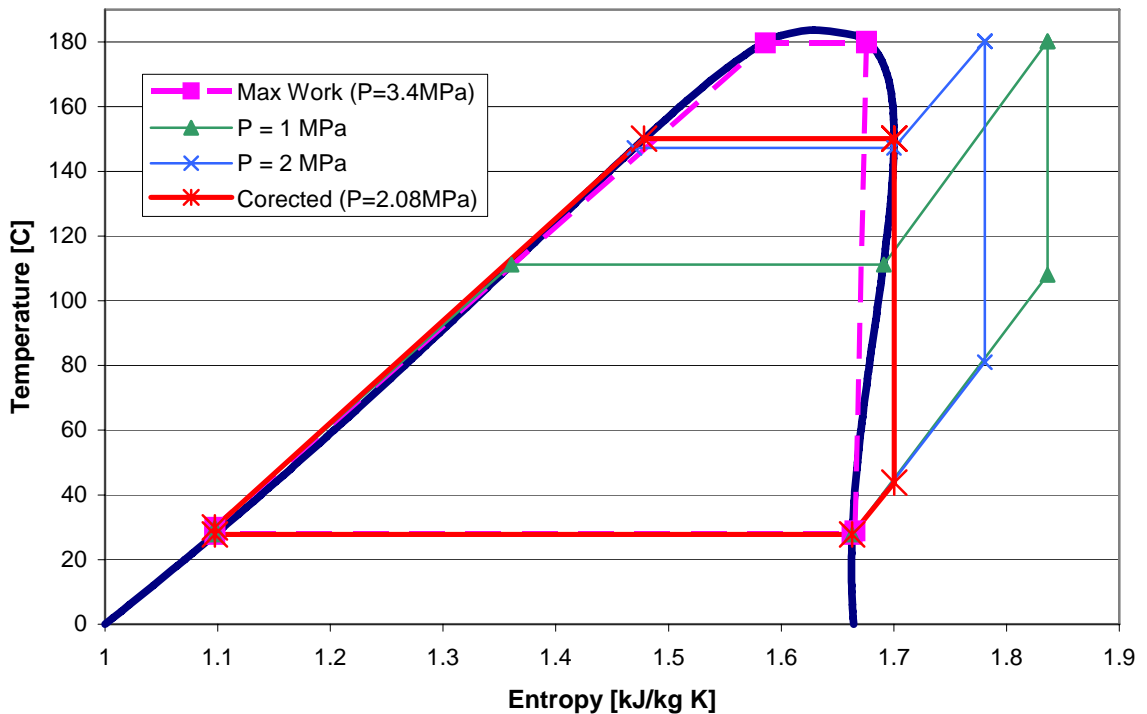
Figure 5.6: T-s Diagram of ORC R123 at Maximum Work; Superheat at P = 1 MPa and P=2 MPa; and Corrected Pressure.

R123, being an isentropic organic fluid as the gradient of the saturated vapour line is nearly isentropic, shows a drop of efficiency when the turbine inlet temperature is further increased to the superheated region. This is especially true for high turbine inlet pressures. At lower turbine inlet pressures, a slight increase of efficiency in the range of 0.5% can be seen. The graphical representation of the effect of TIT on the efficiency is shown in Figure 5.7. From this figure, superheating is found to be not suitable for R123. From the two pressure lines, it can be shown at higher pressure, the drop of efficiency is linear with temperature but at lower pressure, the efficiency line is quadratic. The change of the efficiency is nominal when compared with isobutane.
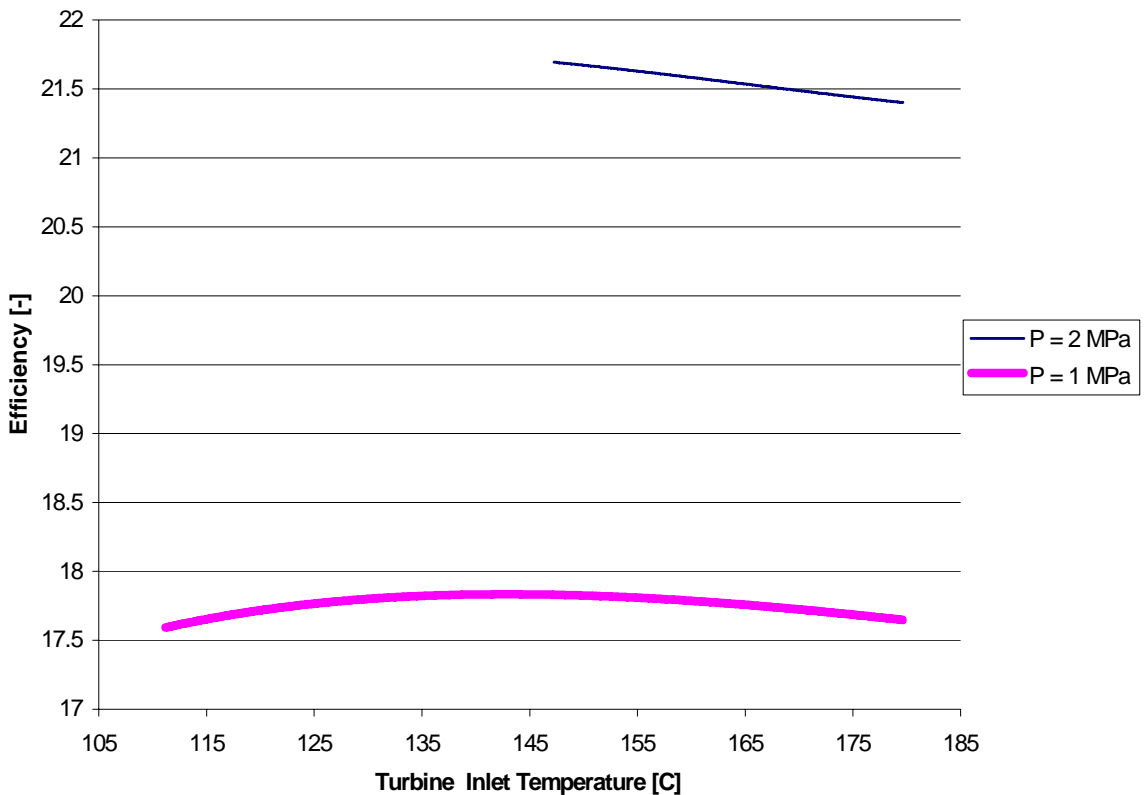
Figure 5.7: The Effect of Turbine Inlet Temperature to Efficiency at Superheated Region for R123.

5.2 Heat Transfer Fluid

In this subtopic, the results from the heat transfer fluid (HTF) in the heat exchanger programming will be presented. The input for this study is the heat input of the ORC cycles. The output from the programming will be the maximum and minimum temperature of the HTF. Only the corrected pressure cycle from both fluids are chosen for analysis. The choice of HTF will depend on the overall temperature obtained from the study. A lower overall temperature is preferred, since lower temperature implies smaller temperature difference between the ORC and the HTF. Small temperature differences mean less heat loss in the heat exchanger. The pinch point will be set at 5 ˚C. The effectiveness of the heat exchanger is set to 1.

5.2.1 R123 Organic Rankine Cycle
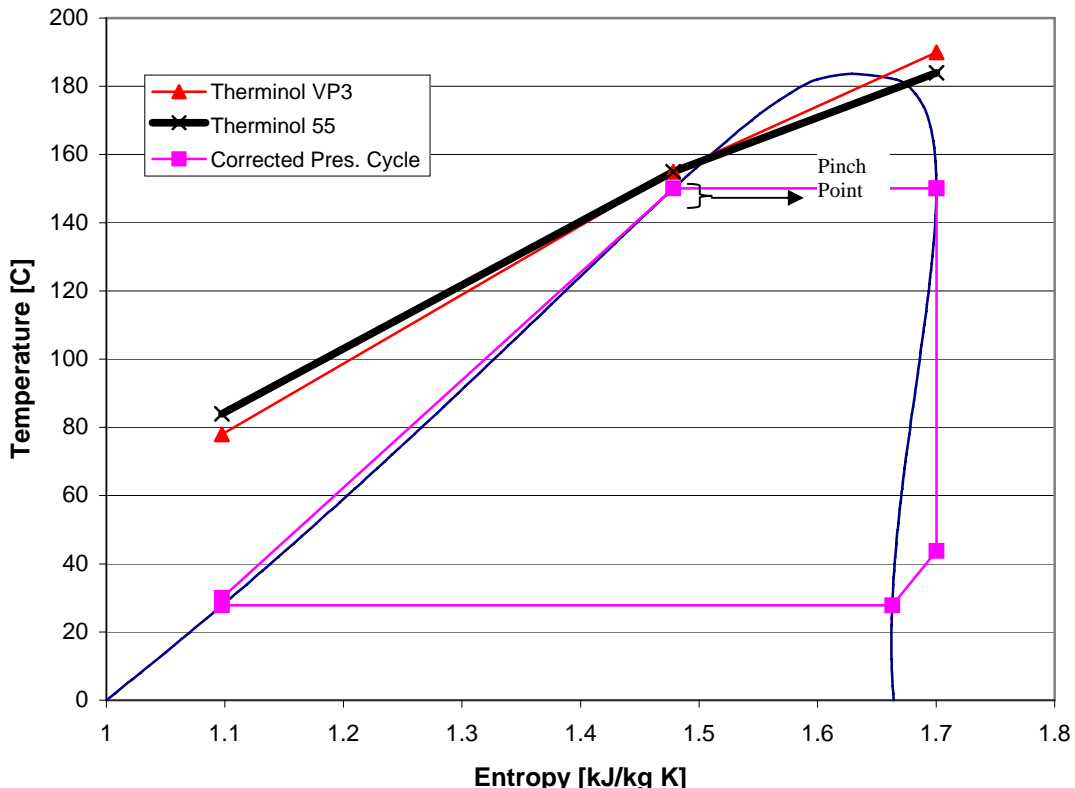
Figure 5.8: Maximum and Minimum HTF Temperature for R123 ORC.

Referring to Figure 5.8, the pinch point notes the nearest temperature gap between the ORC and the HTF. The pinch value is set at 5˚C. From the pinch, maximum and minimum temperatures can be found. An arbitrary mass flow rate of 1 kg/s is chosen for both fluids. The exact temperatures of both fluids are tabulated in Table 5.4. The heat capacity of the fluid is obtained by averaging the heat capacity at the maximum and minimum temperature. This averaging method is used as the heat capacity of the fluid is linearly proportional to the temperature. Therminol VP 3 gives a lower minimum temperature but a higher maximum temperature as compared to Therminol 55. The difference between the maximum temperatures of the two HTFs is 5˚C but the difference between the minimum temperatures is 6˚C. Therefore for R123 ORC, Therminol VP3 is chosen though it has higher maximum temperature but overall, this HTF line is nearer to the ORC.

Table 5.4: HTF Temperature, Mass Flow and Average Heat Capacity (R123)

HTF	Temperature, T_{max} (˚C)	Temperature, T_{min} (˚C)	Average HeatCapacity C_p^{ave} (kJ/kg K)	Mass Flow Rate $\dot{m}$ (kg/s)
Therminol VP3	190	78	2.0824	1
Therminol 55	185	84	2.3111	1

5.2.2 Isobutane Organic Rankine Cycle
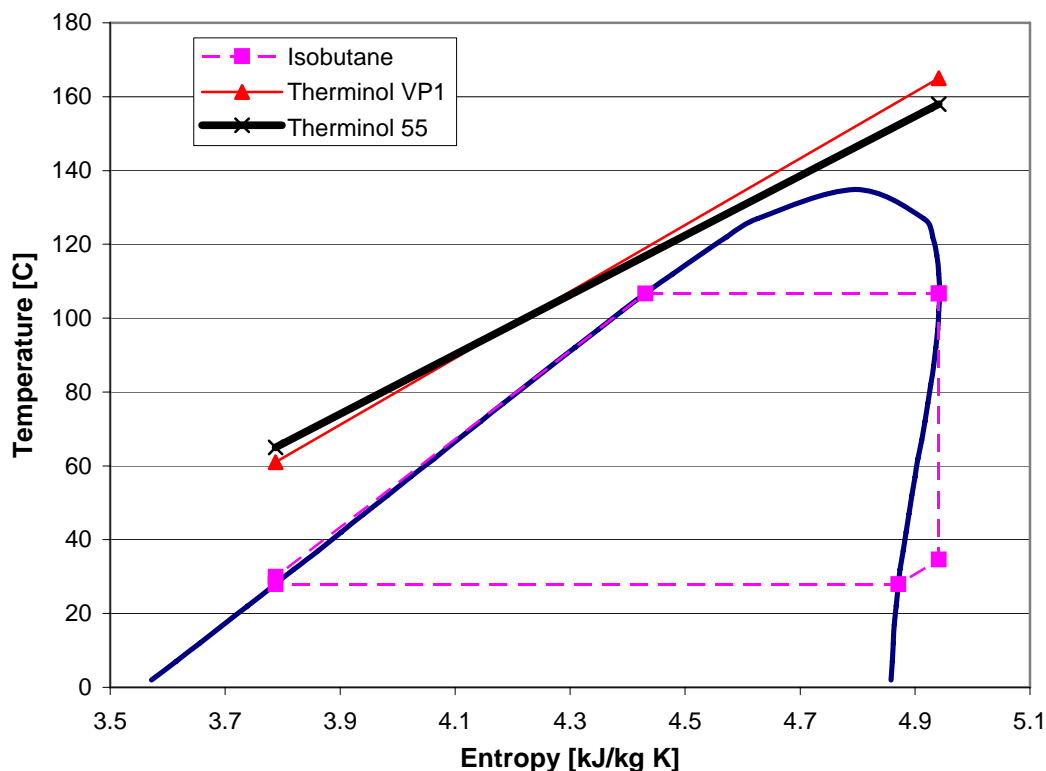
Figure 5.9: Maximum and Minimum HTF Temperature for Isobutane ORC.

The HTF lines in the T-s diagram of the isobutane ORC is drawn in Figure 5.9. Using the same method, the maximum and minimum temperature is calculated and tabulated in Table 5.5. First, the mass flow rate of the HTF is set to 1 kg/s but from calculations, temperature cross-over because the HTF minimum temperature is

lower than the cycle temperature. As a result, the mass flow rate is increased to 2 kg/s in order to transfer the required heat input for the economizer of the ORC. In the isobutane ORC, the same condition happens where Therminol 55 gives a lower maximum temperature but a higher minimum temperature as compared to Therminol VP3. For isobutane, Therminol 55 is chosen because it has a lower overall temperature.

Table 5.5: HTF Temperature, Mass Flow and Average Heat Capacity (Isobutane)

HTF	Temperature, T_{max} (˚C)	Temperature, T_{min} (˚C)	Average HeatCapacity C_p^{ave} (kJ/kg K)	Mass Flow Rate $\dot{m}$ (kg/s)
Therminol VP3	165	61	2.0024	2
Therminol 55	158	65	2.2296	2

5.3 Solar Radiation

In this subtopic, the result of average value of total solar radiation or global radiation and components of the beam radiation for a year in Chuping, Kedah and Kota Kinabalu, Sabah is presented. In the calculation, it is assumed that the total solar radiation received in a year for that particular place is constant every year.

5.3.1   Chuping

Chuping is situated at latitude 6˚ 29' N, longitude 100˚ 16' E and is 21.3 m above sea level. In the solar programming, the data used for the calculation is for the year 1999. This is because the data from 2003 is corrupted with frequent device failures. Whenever the device fails a negative value will be recorded. For the year 2003, there are over 1000 occurrences of device failure, while in year 1999, there are only 8 occurrences. Using data from year 1999, it is calculated that the yearly average global radiation is 1.50 MJm^{-2} per hour and the yearly average beam radiation is 0.90 MJm^{-2} per hour.
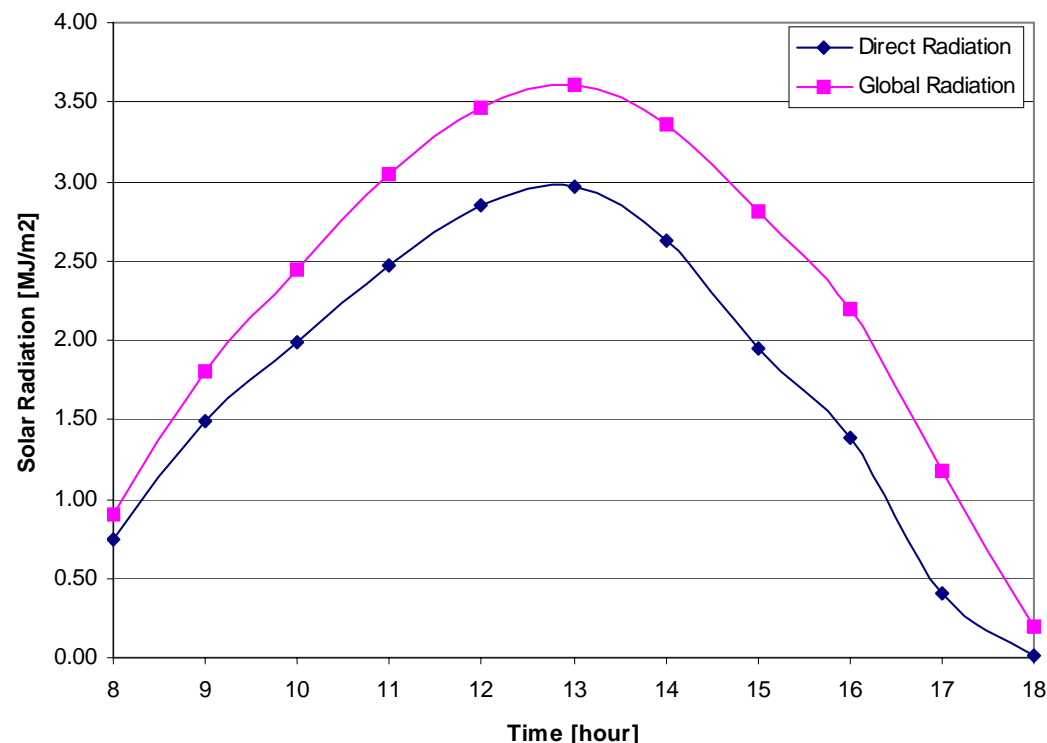
Figure 5.10: Hourly Average Global Radiation and Direct Radiation on 20th February 1999
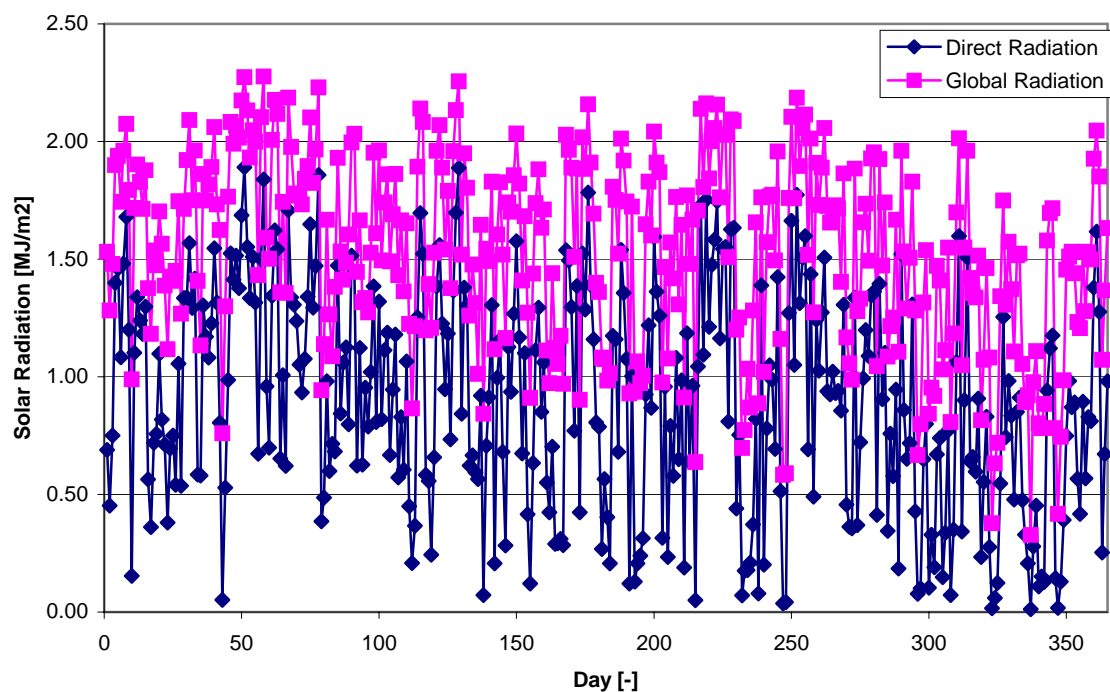
Figure 5.11: Global and Direct Solar Radiation in 1999.

Figure 5.10 shows the global radiation and direct component of solar radiation for 20th February 1999, which has the highest daily average of beam radiation for the year. By calculation, the beam component is 1.89 MJ m^{-2} per hour while the global radiation is 2.27 MJ m^{-2} per hour in the day. In a typical day, the solar radiation will gradually increase from the morning, peak in the afternoon, around 12 to 2, and drop to zero in the evening, around 6 p.m. Depicted in Figure 5.11 is the daily average of global radiation and direct radiation. From the figure, it is concluded that both direct and global radiation are inconsistent and vary greatly on a day to day basis.

5.3.2   Kota Kinabalu

Kota Kinabalu is located at latitude 5° 56'N, longitude 116° 3'E and is 2.3m above sea level. The data studied for Kota Kinabalu was collected in the year 2003 by the Malaysia Metrological Department and there was no device failure recorded. From the correlation, it is estimated that the hourly average beam radiation for the year in Kota Kinabalu is 1.01 MJ m^{-2} per hour out of the hourly average global radiation of 1.60 MJ m^{-2} per hour. Figure 5.12 depicts the global and beam radiation over a period of 11 hours on 24th March 2003. This day has the highest estimated hourly average beam radiation of 1.75 MJ/m^2 per hour, while the hourly average of global radiation is 2.38 MJ/m^2 per hour. Figure 5.13 indicates the hourly average of global radiation and direct radiation for every day in 2003.
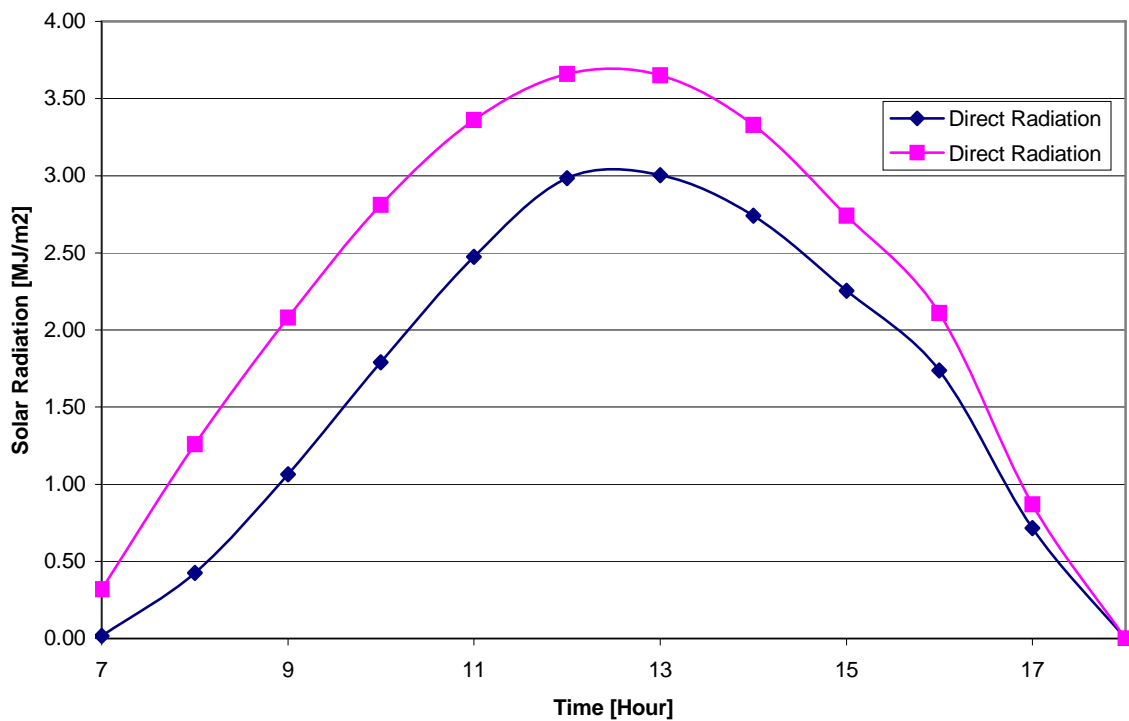
Figure 5.12: Global Radiation and Direct Radiation on 24th March 2003.
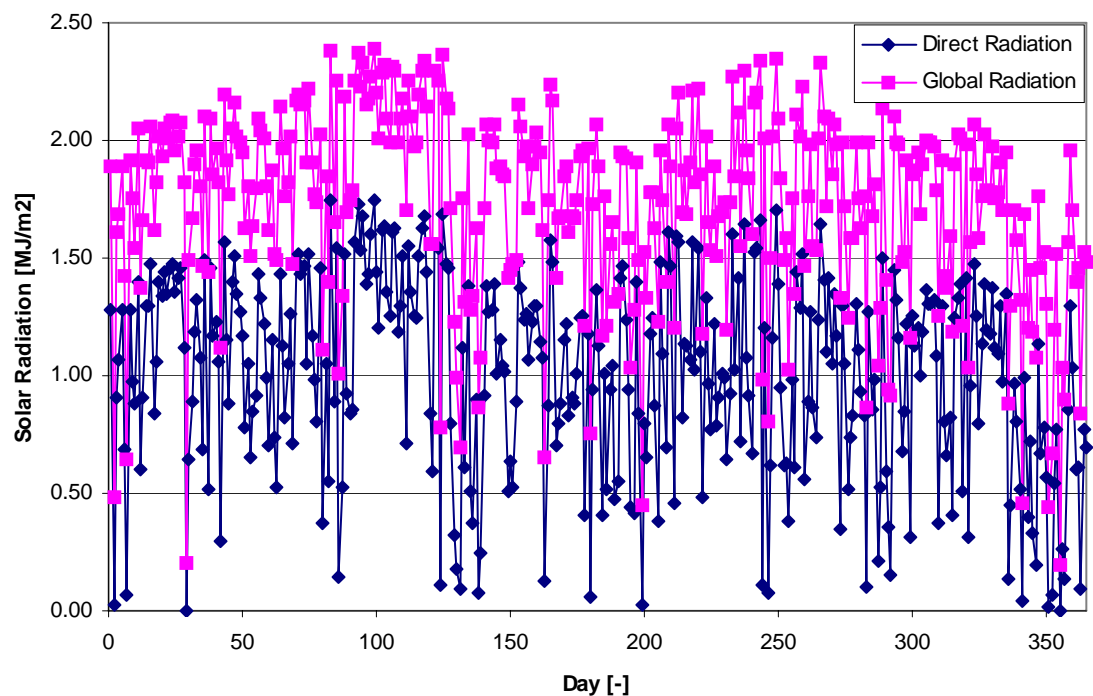
Figure 5.13: Global and Direct Radiation for 2003.

5.4 Solar Collector

The solar collector area is presented and discussed in the following subsections organized by type of collectors. The collector area is estimated from the hourly average solar radiation in a year and heat input of ORC discussed in previous subsections. In this subsection, specific work is obtained to justify the ORC system for power generation. Higher specific work will allow smaller solar collector arrays. Specific work refers to the work, W, produced by every 1 m^2 of collector area. Since work generated is dependent on the organic compound used, therefore, the area of collector calculated will be the determination factor. Work is inversely proportional to the collector area. As a result, smaller collector area will mean a higher specific work can be obtained.

5.4.1   Parabolic Trough

The collector efficiency of 68% as mentioned in literature review, the collector area is obtained. The average direct radiation for Kota Kinabalu as 1.01 MJ m^{-2} per hour and for Chuping it is 0.90 MJ m^{-2}. Table 5.6 shows the parabolic trough collector area according to the location, organic compound and heat transfer fluid used. From the table, the lowest collector area, 1121 m^2, is the R123 ORC using Therminol 55 as the working fluid with the specific work of 52.62 W/m^2. For Isobutane ORC, the highest collector area is 2 214m^2 located in Kota Kinabalu and with Therminol VP3 as the working fluid.

Table 5.6: Parabolic Trough Collector Area and Specific Work

Location	ORC	HTF (Therminol)	Area, A (m^2)	Work, W (W)	Specific Work, $\frac{W}{A}$ (W/m²)
Kota Kinabalu	R123	VP3	1,223	51 660	42.26
Kota Kinabalu	R123	55	1,224	51 660	42.22
Kota Kinabalu	Isobutane	VP3	2,183	69 200	31.70
Kota Kinabalu	Isobutane	55	2,174	69 200	31.83
Chuping	R123	VP3	1,372	51 660	37.65
Chuping	R123	55	1,373	51 660	37.62
Chuping	Isobutane	VP3	2,450	69 200	28.25
Chuping	Isobutane	55	2,439	69 200	28.37

5.4.2 Flat Plate Collector

The flat plate collector efficiency for this study is taken as 67%. To calculate the flat plate collector area, total or global radiation is used. Average global radiation for Kota Kinabalu is 1.60 MJ m² per hour, while for Chuping it is 1.50 MJ m^{-2} per hour. Relevant data, collector area and specific work, are tabulated in Table 5.7. The R123 ORC in Kota Kinabalu using Therminol 55 gives the highest overall specific work, 82.16 W m^{-2}, with a collector area of 718 m². Highest specific work for the Isobutane ORC is 58.21 W m^{-2}.

Table 5.7: Flat Plate Collector Area and Specific Work

Location	ORC	HTF (Therminol)	Area, A (m^2)	Work, W (W)	Specific Work, $\frac{W}{A}$ (W/m²)
Kota Kinabalu	R123	VP3	783	51 660	65.96
Kota Kinabalu	R123	55	784	51 660	65.90
Kota Kinabalu	Isobutane	VP3	1399	69 200	49.48
Kota Kinabalu	Isobutane	55	1393	69 200	49.69
Chuping	R123	VP3	835	51 660	61.83
Chuping	R123	55	836	51 660	61.78
Chuping	Isobutane	VP3	1492	69 200	46.38
Chuping	Isobutane	55	1486	69 200	46.58

5.5   Final Model

From the data and the rigorous discussion presented in the previous subtopic, the choice of working fluid for the ORC is R123. R123 is chosen due to the higher efficiency outcome of the system as compared to the isobutane. Of the three cycles shown, corrected pressure cycle for R123 is preferred to ensure the fluid is dry within the turbine. The TIT is in the reasonable range of 150˚C which is less than the flat plate operating temperature limit of 220˚C. Superheating is not beneficial for R123 ORC as the study demonstrates a decrease in efficiency with the increase in turbine inlet temperature. In order to obtain the highest specific work in the study, the R123 ORC will be used with HTF Therminol VP3 and the optimal location is Kota Kinabalu. This ORC will have an efficiency of 22.15 % and it is close to Carnot Cycle, the difference is just 6.73 %. The collector efficiency is 67 %, as a result giving an overall system efficiency of 14.84 %.

Introduction to Experimental Analysis

In these following subtopics, the results from the experimental study on the solar thermal cycle are presented and discussed in detail. The results shown in this chapter are based on the test methods and techniques carried out throughout the whole semester.

5.6 Solar Thermal Cycle

The thermal cycle is the area of interest in this study because the experimental results from this study will be used to evaluate the suitability of the system in our climate. The measure of worth for the thermal cycle will be based on a few parameters which are the absorber temperature, absorber outlet temperature (T_{out}), collector efficiency ($\eta_{collector}$) of the cycle and also the useful energy gained by the test fluid ($\dot{Q}_{used}$). The useful energy gained by the test fluid has priority over the power that will be generated by the Organic Rankine Cycle (ORC). Though the ORC power output is important and often used to measure the practicability of a thermodynamic cycle, but in this study the absorber temperature and the absorber outlet temperature (T_{out}), is more important due to the temperature limitations of solar thermal collector. Here, the effects and results of the variety of test being carried out to enhance the performance of the system will be explored. Water with flow rate 0.14 L/min is chosen as the working fluid in all test methods carried out in this topic. Any changes in flow rate will be stated.

5.7   Various Test Results and Discussions on Solar Parabolic Collector Rig

5.7.1   Dry Test (Non-operating cycle & no reflection effects) – Method 1

Figure 5.14: Solar Test Rig without Reflection Effects

The direct effect of solar radiation without the parabolic mirror reflection in heating the absorber and water in the storage tank are investigated. Figure 5.14 shows the set up of the solar test rig for this test.

The results of this study is plotted and shown as in Figure 5.15. In the figure, it is shown that there is an increase in the storage tank temperature as it is placed under the sun for a period of time. The (dT) of storage tank from the start of experiment till the end of experiment noticed in this case is 5 ^{o}C.The figure also shows the absorber temperature fluctuation through out the test. The unstable temperature condition is due to sudden weather changes such as windy and scattered clouds situations.The maximum temperature that is 51 ^{o}C in this particular case occurs when the weather is sunny and the temperature drops when there are scattered clouds condition.
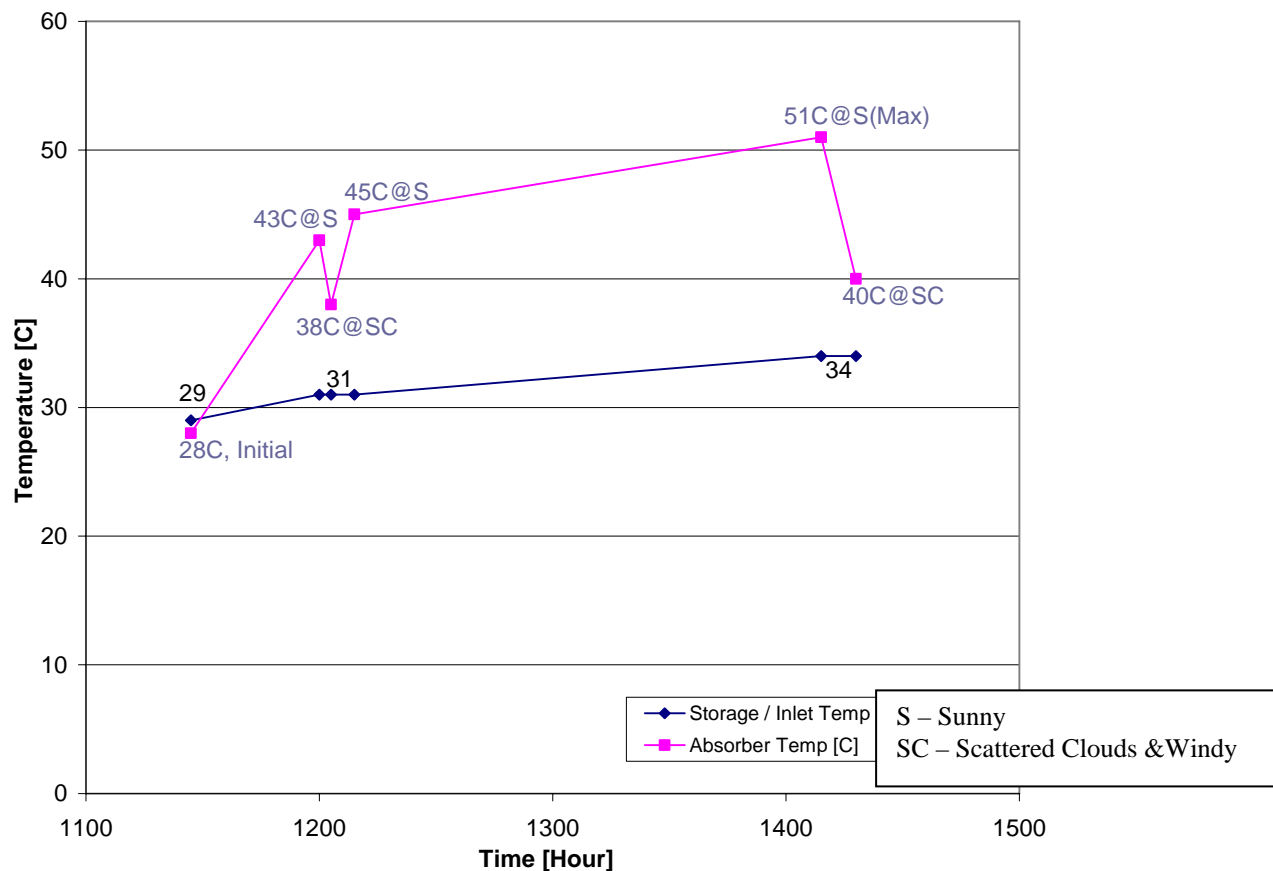
Figure 5.15: Comparison of Storage Tank Temp and Absorber Temperature [^{o}C]

The sunny weather and scattered clouds condition when the experiment is being
carried out is showed in Figure 5.16 and 5.17.
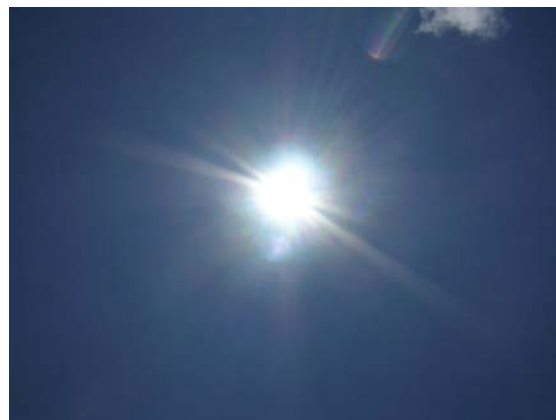
Figure 5.16: Sunny Condition

Figure 5.17: Scattered Clouds

5.7.2 Dry Test (Non-operating cycle & with reflection effects) – Method 2

Figure 5.18: Solar Test Rig with Mirror Reflection Effects

The effect of solar radiation with parabolic mirror reflection in heating the absorber is investigated. Figure 5.18 shows the set up of the solar test rig for this test.

The comparison of results between the reflection effects and without the reflection effects on the absorber is plotted and shown as in Figure 5.19. In the figure, it is clearly shown that there is an increase in the absorber temperature when the solar radiation is focused on the absorber by the collector mirror surface. From this, we can see that the (dT) given by the effects of the mirror surface is approximately $10\,^{\circ}\text{C}$.The figure also shows both the absorber temperature fluctuation through out the test.The maximum value of absorber temperature with the effects of mirror reflection is $62\,^{\circ}\text{C}$ in this case. From this we can also clearly see that the losses in temperature occur due to the scattered clouds condition and strong wind factor.
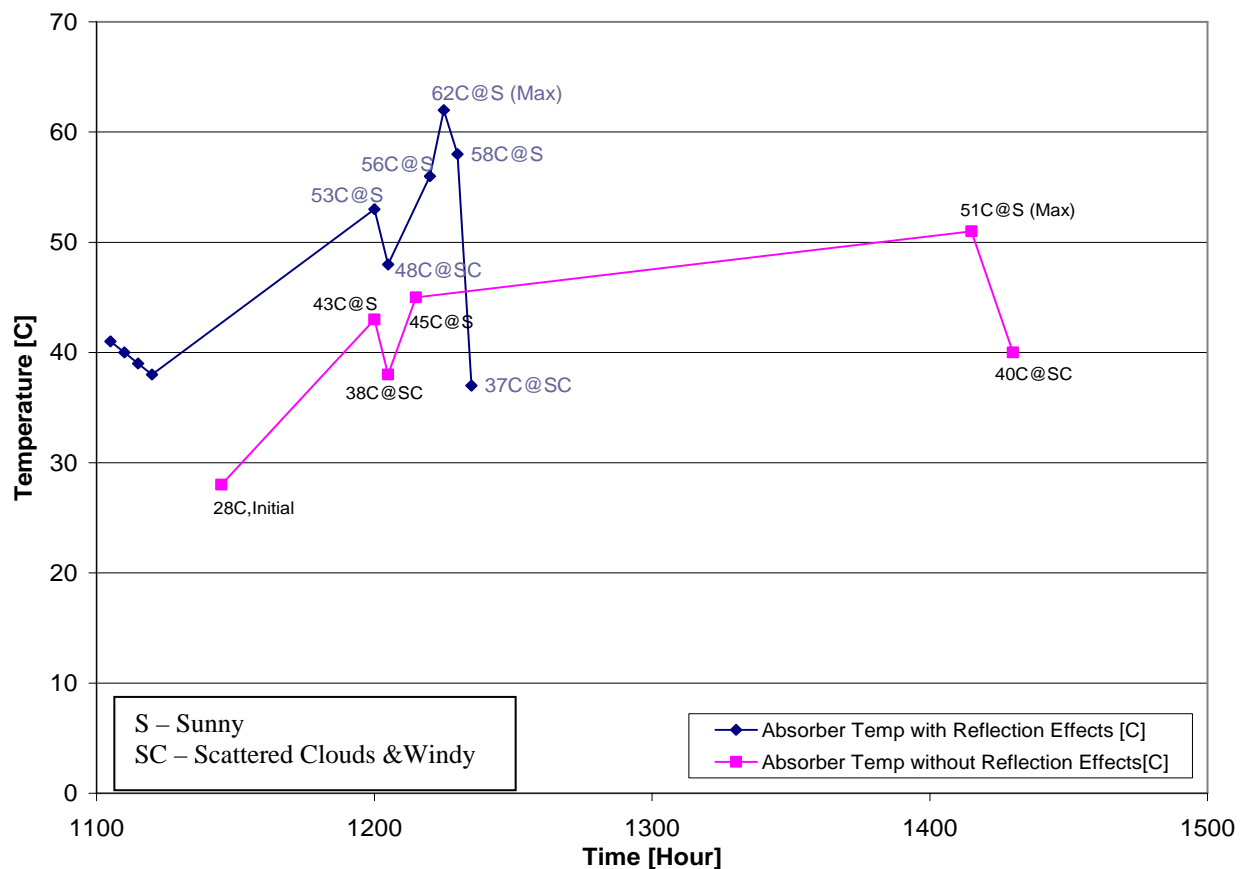
Figure 5.19: Absorber Temp with Reflection vs. Temp without Reflection Effects [^{o}C]

5.7.3 Testing for suitable pump size

Figure 5.20: Pump capacity 0.5hp

Figure 5.21: Pump capacity 0.1hp

The proper pump size is an important parameter to be determined as it may bring an unwanted rise on the temperature of the test fluid upon carrying out this study. Two types of pump with a horsepower (hp) of 0.5 hp (368 Watts) and a lab sized pump with the capacity of 0.1 hp (75 Watts) as shown in Figure 5.20 and Figure 5.21 respectively are being tested here to see it's suitably on the solar parabolic collector test rig designed. The comparison of results on the storage tank temperature during the operation of these two pumps are plotted and shown in Figure 5.22. In the figure, it is shown that there is a proportional increase of temperature compared to time in the storage tank when the higher powered pump is in use. The figure also shows that the storage tank temperature is constant when the 0.1 hp (75 Watts) pump is in use. Looking into these results, the 0.1hp pump is chosen to be use through out this study.
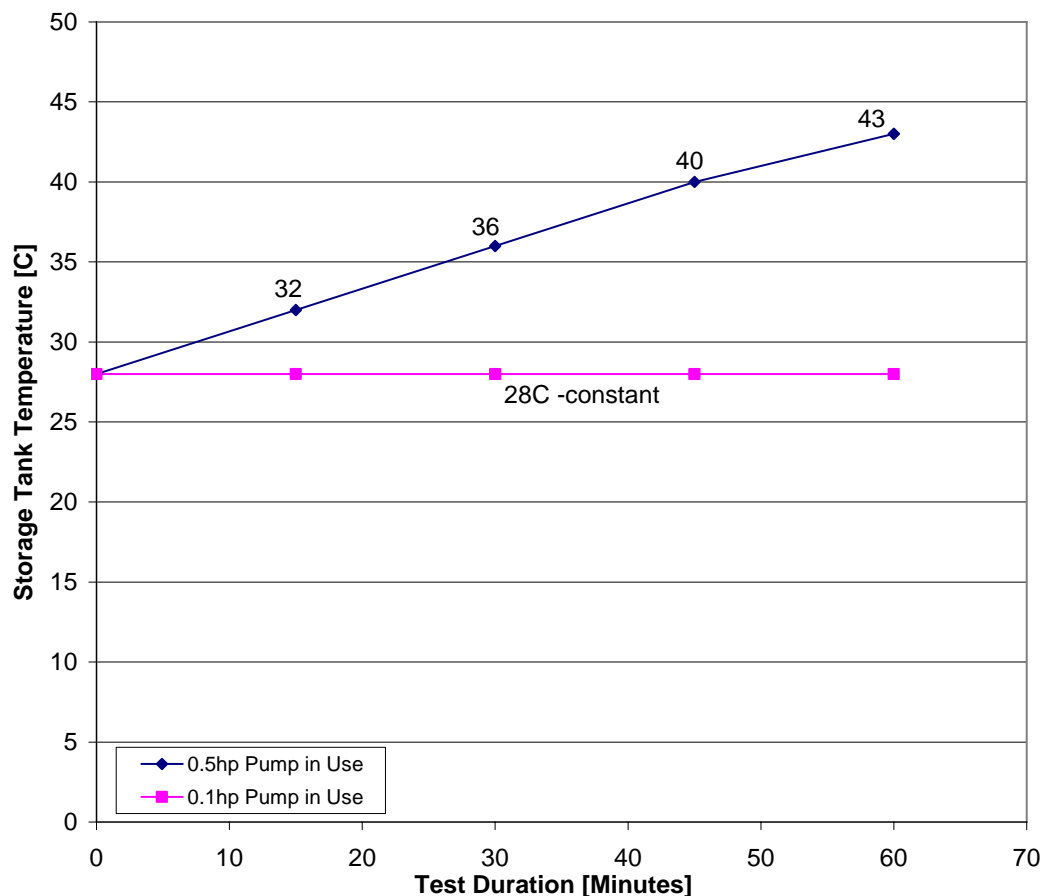
Figure 5.22: Tank Temp with 0.5Hp Pump vs. Tank Temp with 0.1Hp Pump

5.7.4 Flow Profile Test

Before carrying out further test on the solar collector rig when the thermal cycle is being operated, a suitable flow rate is being set or tested first. This test is carried out by using a Perspex tube to replace the copper absorber. Figure 5.23 shows the set up of the solar test rig for this test.
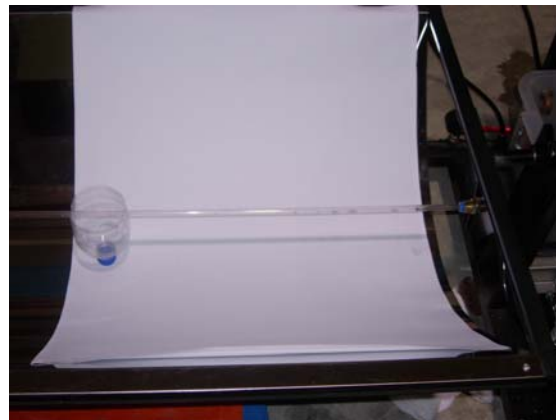
Figure 5.23: Copper Absorber Tube replaced with Perspex Tube

A minimum flow of water is released into the Perspex tube ensuring the water flow fills the entire tube surface. The flow rate at this condition is taken and used to determine the flow profile to see if it's a laminar flow or turbulent flow. This analysis is being done using the Reynolds number formulation. The value of R_e obtained is 260.56. Since the value of Reynolds number is less than 2000, the flow profile of HTF which will be flowing in the absorber will be a Laminar flow. (Refer appendix B for calculation steps)

5.7.5 Operating Thermal Cycle- (Wrapping Parabolic Collector and Tilting Effects)

A new test approach has been taken to further increase the absorber temperature and also the storage / inlet temperature referring to the results which has been collected from the test methods stated previously. Here, the test rig is been wrapped up in order to prevent it from the external wind factor which leads to heat loss. The effects from the tilted collector angle upon carrying out this test and the wind velocity factor are also taken into consideration here. Figure 5.24 and 5.25 shows the set up on the solar test rig and the anemometer which is used to take the wind velocity reading during this test.

Figure 5.24: Test Rig Wrapped and Tilted

Figure 5.25: Anemometer

The absorber temperature, storage tank / inlet temperature and external wind velocity reading is plotted and shown as in Figure 5.26. The figure also shows the absorber temperature fluctuation through out the test. Looking into the graph, the temperature fluctuation is related to the scattered clouds conditions. When scattered clouds or cloud covers are formed in the sky, the parabolic collector does not reflect any radiation to the absorber. Hence, the absorber temperature decreases instantly. From this we can see that the losses in temperature occur due to the scattered clouds condition creating diffuse radiation.

The maximum value of absorber temperature with the minimum effects of external wind is 56 $^{\circ}$C in this case. The figure also shows the storage tank / inlet temperature which increases relatively with time as it is being exposed to the ambient

temperature. However the storage tank / inlet temperature is also being affected by the scattered clouds condition. This situation can be seen on the graph when the storage tank temperature decreases from 39 °C to 37 °C due to the scattered cloud condition labelled (SC).By analysing the wind flow obtained from the graph, it shows that the temperature increases as the wind velocity decreases and the absorber temperature decreases when the wind velocity rises. The average wind velocity obtained is 1 m/s. In whole, it can be seen that the peak radiation is captured from time ranging from 1230hour to 1530hour.The radiation level decreases as the time passes 1530hour.
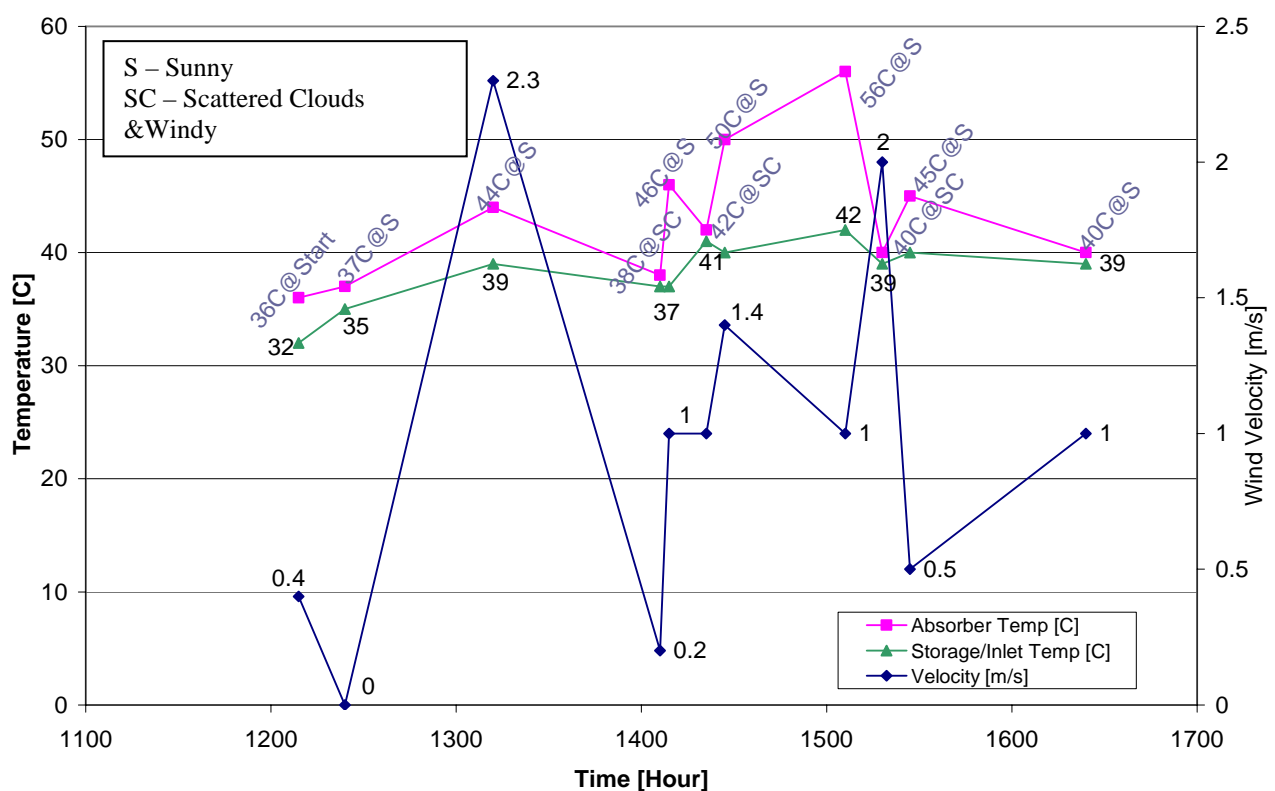
Figure 5.26: Comparison of Absorber Temp, Storage Tank / Inlet Temp [°C] and External Wind Velocity [m/s] when Test Rig Tracks Sun and Wrapped

5.7.6 Operating Thermal Cycle- (Wrapping Solar Collector and No Tilting Effects)

A slight improvement is done on the test method as stated in subtopic previously. Now, with the same existing set up, the experiment is carried out but with the solar collector not tracking the movement of sun. The effect from the untitled collector angle upon carrying out this test is taken into consideration in this case. Figure 5.27 shows the set up of the test rig during this test.

Figure 5.27: View of Solar Test Rig Wrapped and Not Tilted

The absorber temperature, storage tank / inlet temperature and external wind velocity is plotted and shown as in Figure 5.28. In the figure, it is shown that there is a very minimum increase in the absorber maximum temperature when the solar collector is not tilted. The (dT) observed here is $2\,^{o}$C compared to the condition when the test rig is being tilted to track the sun movement. The maximum absorber temperature in this case is $58\,^{o}$C. This minimal increase of temperature is most likely due to the higher value of solar radiation at the time the reading was taken.

The figure also shows the absorber temperature fluctuation through out the test. The occurrence of temperature fluctuation in this case is similar to the explanation given in the subtopics discussed previously, where it is influenced by the scattered clouds condition and diffuse radiation.

The figure also shows the storage tank / inlet temperature which increases relatively with time as it is being exposed to the ambient temperature. However the storage tank / inlet temperature is also being affected by the scattered clouds condition. This situation can be seen on the graph when the storage tank temperature decreases from 42 ^{o}C to 39 ^{o}C due to the scattered cloud conditions labelled (SC).The average wind velocity observed here is 0.2 m/s.
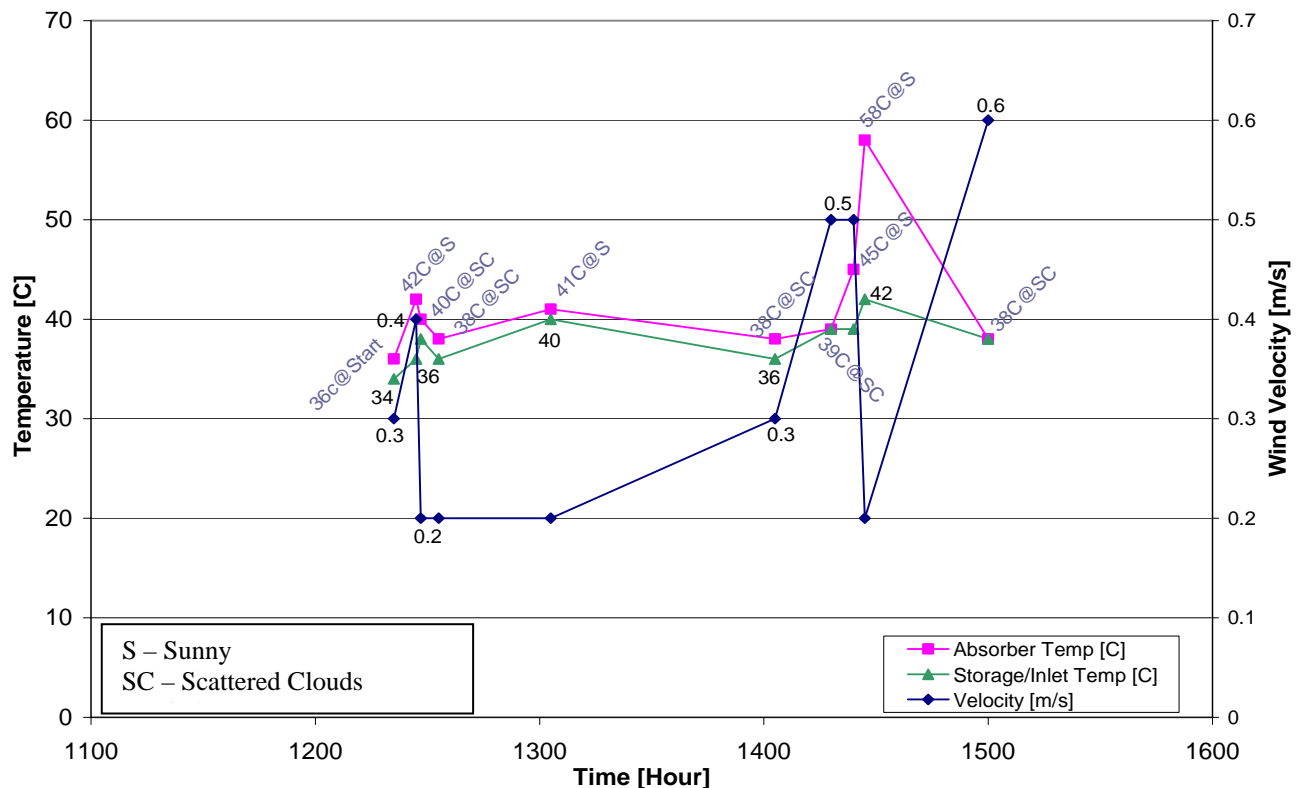
Figure 5.28: Comparison of Absorber Temp, Storage Tank / Inlet Temp [^{o}C] and Wind Velocity [m/s] when Test Rig is Wrapped and Not Tracking Sun

5.7.7 Dry Test (Non-operating thermal cycle, with Effects of Wrapping and Insulation) – Method 3

Looking into the influence of external wind condition and environmental effects which causes heat loss to the overall thermal system, the approach to insulate the bottom surface of the parabolic collector is taken. In this test method, the test rig is also wrapped as explained in the previous subtopics above. The purpose of wrapping and insulating the test rig is to minimize the effects of external wind and to maximize the utilization of heat captured by the collector. Figure 5.29 shows the setup of the test rig for this method.

Figure 5.29: View of Solar Test Rig Wrapped and Insulated

The effects of wrapping and insulating the thermal system are investigated. The comparison of results between the wrapping and insulating effects to without any of these effects on the absorber temperature is plotted and shown as in Figure 5.30. In the figure, it is clearly shown that there is a drastic increase in the maximum absorber temperature when the thermal cycle is wrapped and insulated. From this, we can see that the (dT) on the maximum absorber temperature is 45 ^{o}C upon carrying these improvement on the thermal cycle.The figure also shows both the absorber temperature fluctuation through out the test.The maximum value of absorber temperature with these improvement effects is 107 ^{o}C . From this we can justify that the losses in temperature occur due to the scattered clouds condition and strong wind factor.
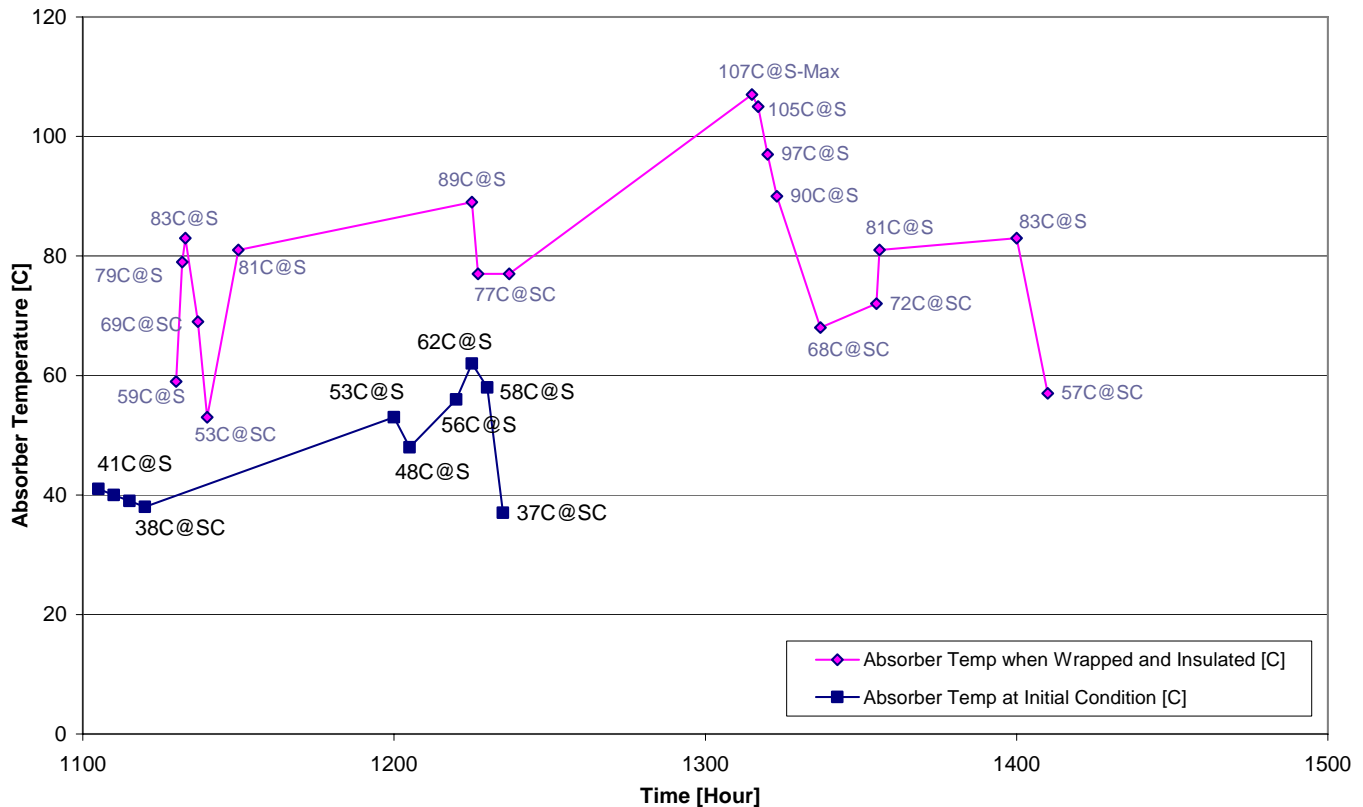
**Figure 5.30:** Absorber Temp when Wrapped and Insulated vs.Temp when Not Wrapped and Insulated [^{o}C]

5.7.8 Operating Thermal Cycle- (With Effects of Wrapping, Insulation and Tracking Sun)

The effects of temperature on the absorber surface when the solar parabolic collector is being wrapped, insulated and tilted to track the sun gives a high range of temperature reading when the dry test is carried out as explained..

Now, with this same set up, the system is being operated and the absorber surface temperature readings are being collected. The result of the study is plotted in Figure 5.31. The absorber surface temperature observed in this study gives the highest reading compared to all other test methods done when the system is being operated. The maximum value of absorber temperature surface obtained from this test is 61°C when the weather is hot or sunny. The high maximum value of absorber surface temperature observed in this test is most likely due to the set up of the solar

test rig. This set up on the solar parabolic collector not only helps in protecting the test rig against external wind factor but also to capture more heat collected by the solar test rig.

Looking into the sunny weather condition through out the test period, there is still absorber temperature fluctuation noticed. This fluctuation of temperature could occur due to the inconsistent solar radiation effects by the sun. As this set up gives the highest absorber surface temperature, the following test methods which will be discussed in the subtopics below will use this rig set up and further improvements will be done on it to enhance it's performance.
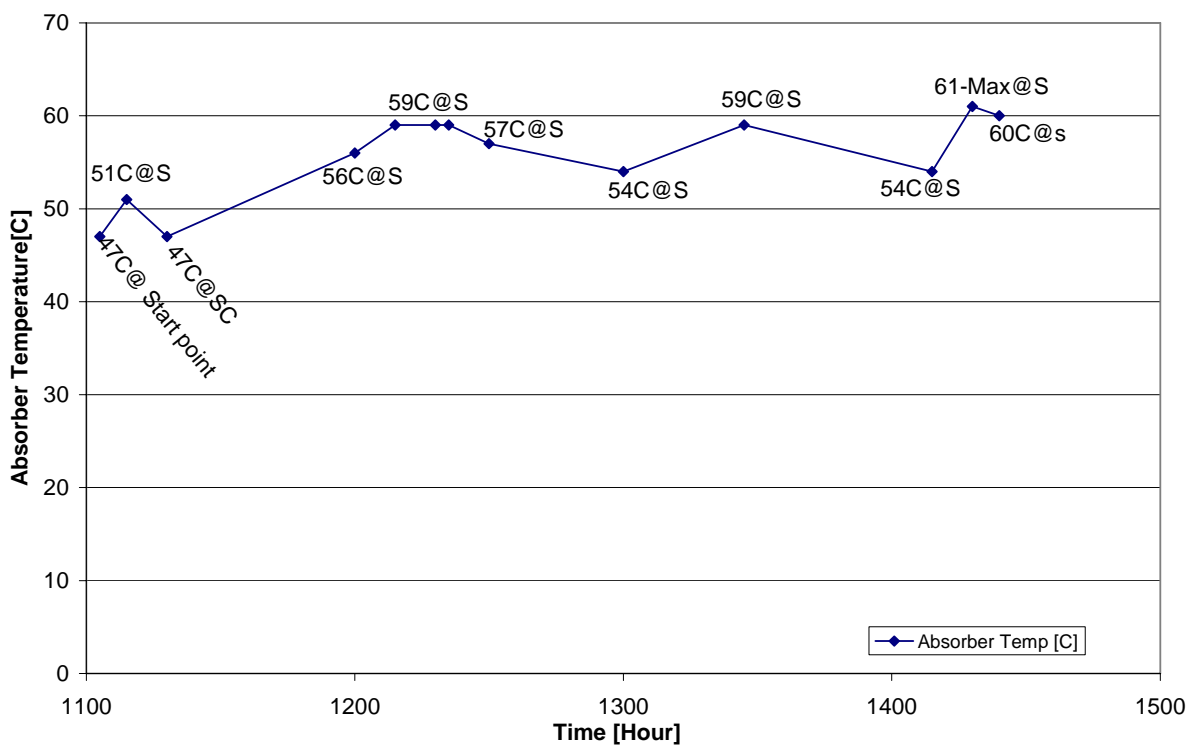
Figure 5.31: Absorber Temp when Solar Collector is Wrapped, Insulated and Tilted

5.7.9 Operating Thermal Cycle- (Outlet Temperature with Different Flow Rates)

The outlet temperature (T_{out}) and inlet / tank temperature (T_{in}) of test fluid from the thermal cycle is an important parameter in determining the ORC work output. Upon carrying out the test with the same set up as in subtopic 5.7.8, the absorber outlet temperature (T_{out}) and inlet / tank temperature (T_{in}) were analysed to determine the temperature differences (dT). The absorber outlet temperature (T_{out}) and inlet / tank temperature (T_{in}) of two different flow rates which are 0.14 L/min and 0.13 L/min respectively are collected here. Figure 5.32 shows the absorber outlet flow temperature (T_{out}) being taken using a thermocouple. The comparison of results between the absorber outlet temperatures (T_{out}) and inlet temperature (T_{in}) for both cases are plotted and shown as in Figure 5.33 and Figure 5.34.

Figure 5.32: Absorber Outlet Temperature (T_{out}) Taken Using a Thermocouple

5.7.9.1 Results for Flow Rate - 0.14 L/min

Figure 5.33 , shows both the inlet temperature (T_{in}) and absorber outlet temperature (T_{out}) for the test fluid with flow rate 0.14 L/min. The absorber surface temperature is also plotted here in this figure. It is shown that there is a maximum absorber outlet temperature (T_{out}) of 40 ^{o}C when the inlet temperature (T_{in}) is 28 ^{o}C.The maximum value of (dT) observed here is 12 ^{o}C. This maximum outlet temperature (T_{out}) is achieved at the time the absorber temperature stabilises and not at the time where the absorber is picking up heat. In the figure, it is shown that there

is an increase in the inlet / tank temperature (T_{in}) as it is exposed to the ambient temperature.

The figure also shows the absorber temperature fluctuation through out the test. The occurrence of temperature fluctuation in this case is similar to the explanation given in the previous subtopics in this chapter where it is influenced by the scattered clouds condition and diffuse radiation. From the figure, we can also see that the value of outlet temperature (T_{out}) correlates with the fluctuation of the absorber surface temperature.
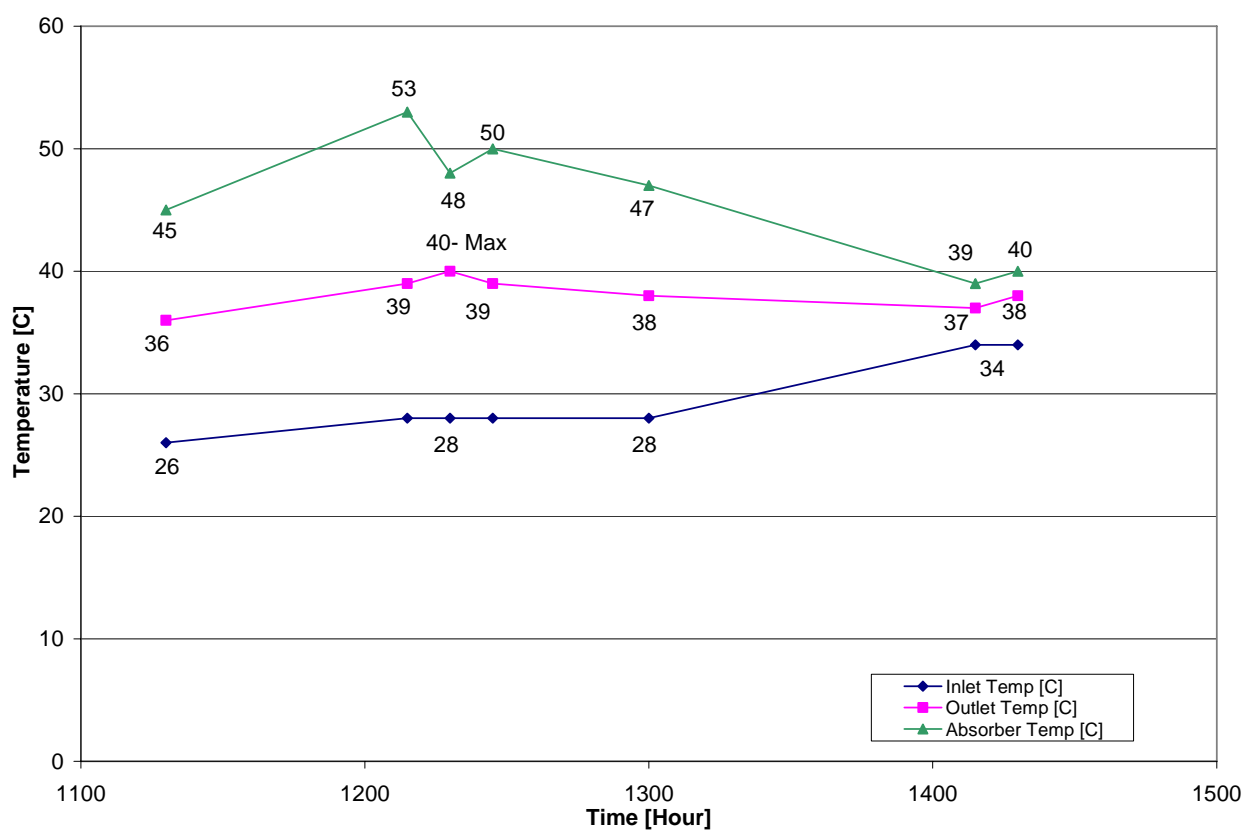
Figure 5.33: Outlet, Inlet and Absorber Temperatures at 0.14 L/min

5.7.9.2 Results for Flow Rate - 0.13 L/min

The data's collected upon carrying out the similar type of test but with changes of flow rate from 0.14 L/min to 0.13 L/min is explained in Figure 5.34. The fundamentals of flow rate reduction are discussed here. Both inlet temperature (T_{in}) and absorber outlet temperature (T_{out}) for the test fluid with flow rate 0.13 L/min is plotted here in this figure. The absorber surface temperature is also taken into consideration here in this study.

It is shown that there is a maximum absorber outlet temperature (T_{out}) of 44 ^{o}C when the inlet temperature (T_{in}) is 29 ^{o}C. The maximum value of (dT) observed here is 15 ^{o}C. This maximum outlet temperature (T_{out}) is also achieved at the time the absorber temperature stabilises and not at the time where the absorber is picking up heat. In practical, the fluctuation of the absorber temperature occurs almost every minute due to the often scattered cloud conditions and this gives effects to the value of absorber outlet temperature (T_{out}). In the figure, it is also shown that there is an increase in the inlet / tank temperature (T_{in}) as it is exposed to the ambient temperature.

The increase in absorber outlet temperature (T_{out}) when the flow rate is reduced is most likely due to the condition where the slow flowing test fluid absorbs or captures more heat as it passes through the heated absorber.
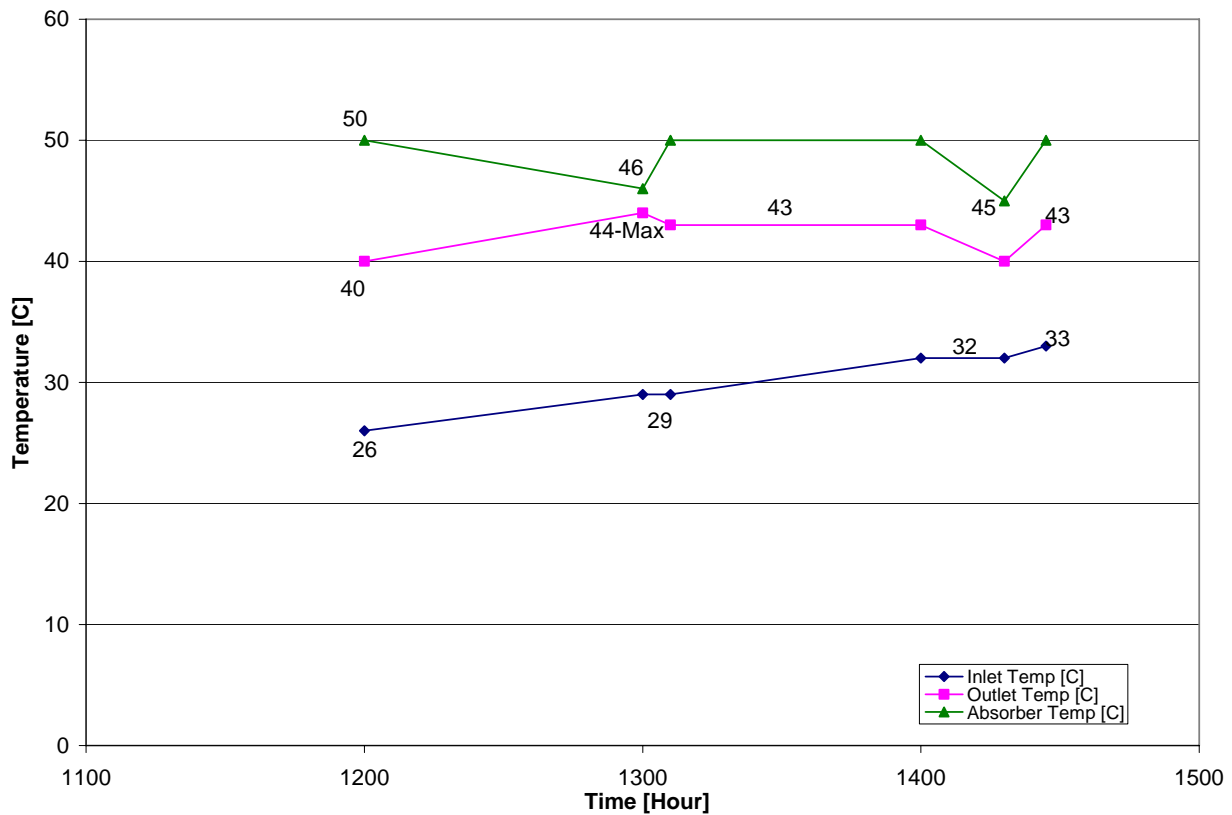
Figure 5.34: Outlet, Inlet and Absorber Temperatures at 0.13 L/min

5.7.10 Analysis on Collector Efficiency,($\eta_{collector}$)

In this subtopic, the efficiency of the solar parabolic trough collector test rig ($\eta_{collector}$) is being investigated. The collector efficiency at different outlet temperatures (T_{out}) and inlet temperatures (T_{in}) are plotted in Figure 5.35. All absorber outlet temperatures and inlet temperatures are based on the values obtained from the test as explained in subtopic 5.7.9.2 above.

The value of beam radiation component, (I_b) in this analysis is taken as 1.01 MJ m^{-2} per hour . This is the estimated value of beam radiation calculated referring to the hourly average global radiation of 1.60 MJ m^{-2} per hour in Kota Kinabalu produced by the Malaysia Metrological Department for year 2003[23]. The aperture area is set at 0.7m^2.

Referring to Figure 5.35 , it is observed that the value of collector efficiency increases as the temperature difference (dT) between the absorber outlet temperature (T_{out}) and absorber inlet temperature increases (T_{in}).Looking at the collector efficiency value which is analysed using the experimental temperature difference values, the maximum collector efficiency obtained is 0.2. This value of collector efficiency could be increased up to any desired value by making an attempt to increase the (dT) of absorber outlet temperature (T_{out}) and inlet temperature (T_{in}).
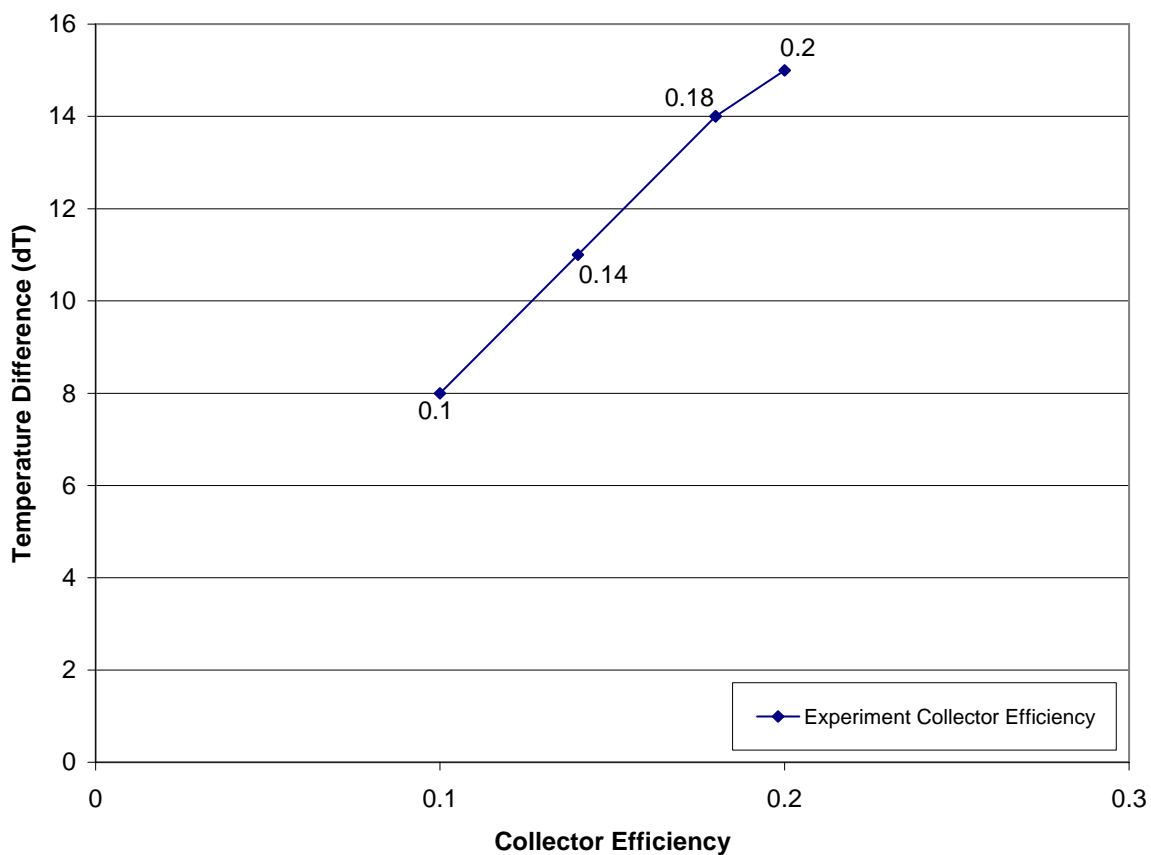
Figure 5.35: Solar Parabolic Collector Efficiency

5.8 Analysis on Power Output by Solar Parabolic Collector Assisted ORC

The power cycle, ORC is important because the result is used to evaluate the feasibility of the system which is assisted by the solar parabolic through collector. In this topic, the results from the experimental study will be used to calculate the amount of power generated by the Organic Rankine Cycle, ORC or power cycle. Isobutane and R123 are studied parametrically to compare the capability of the ORC to generate power with these different organic compounds.

5.8.1 Isobutane Organic Rankine Cycle.
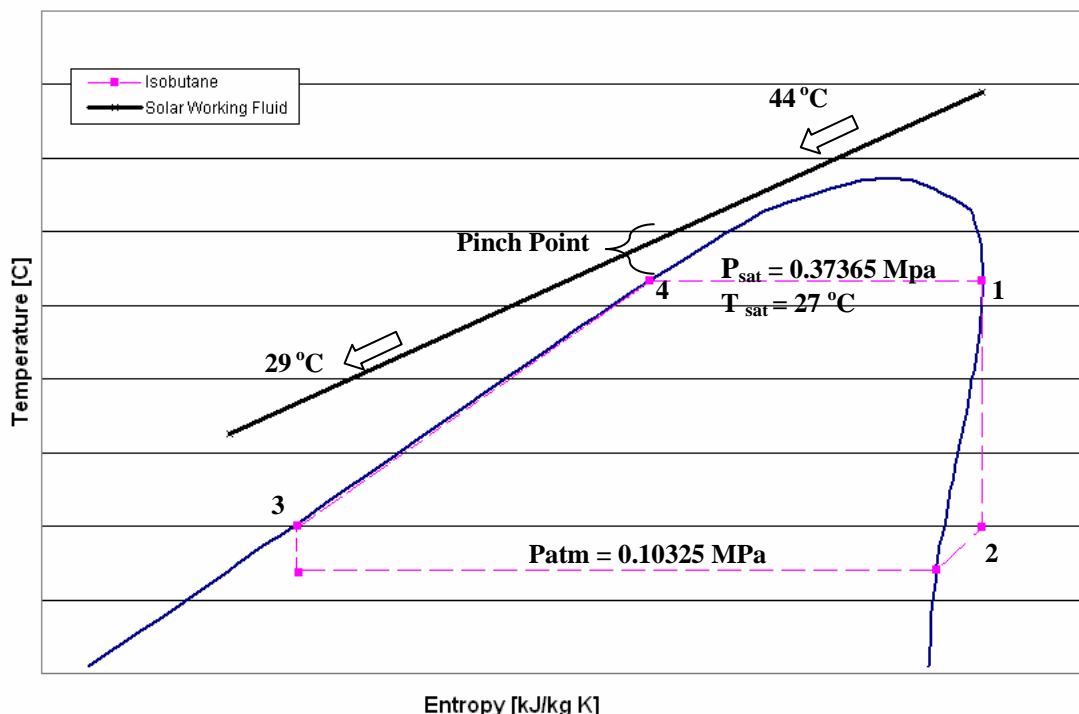
Figure 5.36: T-s Diagram of Isobutane ORC

Isobutane will be used as the organic compound in this study. The T-s diagram in Figure 5.36 displays the relevant thermodynamic parameters which are involved in analysing the power output from the ORC. Referring to the highest value

of temperature difference (dT) between the absorber inlet temperature (T_{in}) and absorber outlet temperature (T_{out}) which is 15 °C obtained from the test method as stated in subtopic 5.7.9.2, the energy gained by the working fluid ($\dot{Q}_{used}$) is calculated. The mass flow rate of the working fluid is set at 2.167 x 10^{-3} kg/s. The value of energy gained by the working fluid ($\dot{Q}_{used}$) in this case is 0.14 kW which is calculated using equation (3.18).

The ORC saturated pressure and saturated temperature is set at 0.37365 Mpa and 27 °C respectively. The useful energy gained ($\dot{Q}_{used}$) is assumed to be the energy in (Q_{in}) to the ORC. The mass flow rate of organic compound in this case is 3.3866 x 10^{-4} kg/s. The refrigerant inlet temperature (point 3) is set at -9 °C which is above the condenser outlet temperature at -11 °C for Isobutane set at atmospheric pressure. Referring to Figure 5.36, the pinch point notes the nearest temperature gap between the ORC and the working fluid. The pinch point value is set at 5 °C. The differences of enthalpy between point 1 and point 2 multiplied by the mass flow rate of Isobutane gives the ORC power output. All enthalpy and entropy values at this point are obtained from the Isobutane refrigerant properties table (refer appendix B).

In this study, the power generated by the ORC which is assisted with a solar parabolic trough collector of 1 meter in length is 2kWh for the period of one month. Looking into this, the power generated by the ORC could be increased to any desired value by just increasing the mass flow rate of the working fluid in the thermal cycle or by increasing the overall length of the solar parabolic trough collector in this research. (Please refer appendix B for the complete calculation steps)

5.8.2 Effects of Superheating Isobutane
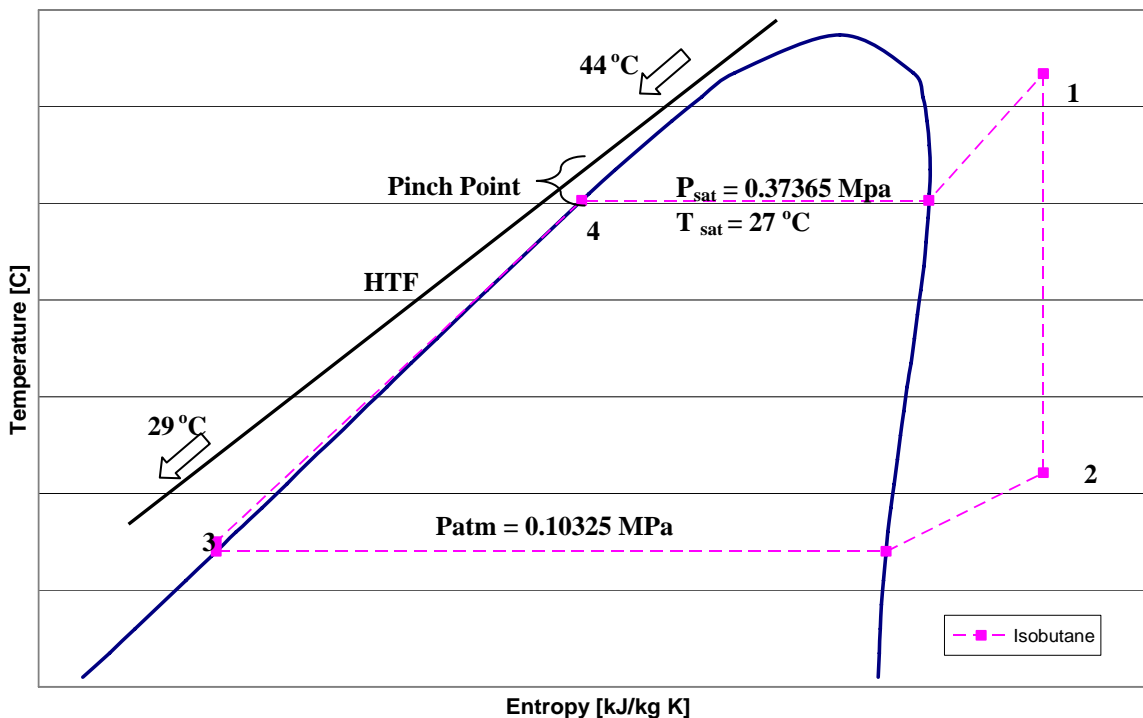
Figure 5.37: T-s Diagram of Isobutane ORC Working at Superheated Region

Here, the effect of superheating Isobutane is studied parametrically. The T-s diagram in Figure 5.37 displays the relevant thermodynamics parameters which are involved in analysing the power output from the ORC considering the effects of superheating the organic compound.

In this case, the same value of useful energy gained ($\dot{Q}_{used}$) obtained by the working fluid in the solar thermal cycle from the experimental study which is 0.14 kW is assumed to be the energy in (Q_{in}) to the ORC as given in equation (3.26). The ORC saturated pressure and saturated temperature is set at 0.37365 Mpa and 27 °C respectively. Referring to this saturated pressure value, the turbine inlet temperature at point 1 is being further increased to the superheated region. The turbine inlet temperature at the superheated region is set at 37 °C. The mass flow rate of the organic compound in this case is 3.218 x 10^{-4} kg/s.

The refrigerant inlet temperature at point 3 is set at -9 °C. Referring to Figure 5.37 the pinch point notes the nearest temperature gap between the ORC and the

HTF. The pinch point value is set at 5 ^{o}C. Using all the relevant data obtained, the ORC power output is calculated. All enthalpy and entropy values at this point are obtained from the pressure – enthalpy diagram and properties table of Isobutane (refer appendix B).

In this study on the ORC which considers the superheating effects of Isobutane at the turbine inlet, the value of power generated obtained is similar to the case when there are no superheating effects. The power generated in this ORC which is assisted with a parabolic trough collector of 1 meter in length is also 2kWh for the period of one month. (Please refer appendix B for the complete calculation steps)

5.8.3 R123 Organic Rankine Cycle
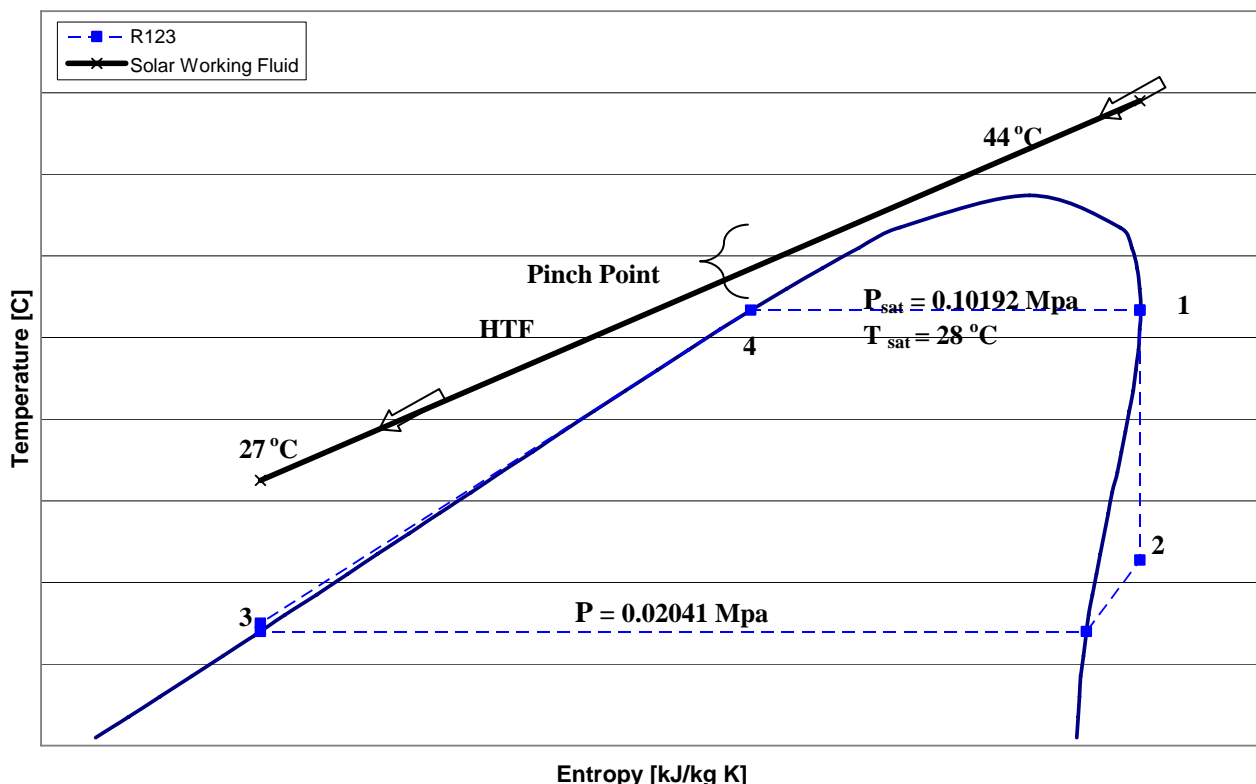
Figure 5.38 : T-s Diagram of R123 ORC

The effects of R123 on the ORC will be investigated here. The T-s diagram in Figure 5.38 displays the relevant thermodynamics parameters which are involved in analysing the power output from the ORC.

Referring to Figure 5.38, the pinch point notes the nearest temperature gap between the ORC and the HTF. The pinch value is set at 3^oC. The ORC saturated pressure and saturated temperature is set at 0.10192 Mpa and $28\,^o$C respectively. The refrigerant inlet temperature into the ORC (point 3) is set at $-10\,^o$C similar to the condenser temperature at a pressure of 0.02041 Mpa. The same value of useful energy gained ($\dot{Q}_{used}$) obtained by the working fluid in the solar thermal cycle from the experimental study which is 0.14 kW is assumed to be the energy in (Q_{in}) to the ORC as given in equation (3.26). The mass flow rate for R123 obtained is 6.6225 x 10^{-4} kg/s. The differences of enthalpy between point 1 and point 2 which is the turbine inlet and outlet respectively when multiplied by the mass flow rate of R123, gives the ORC power output. All enthalpy and entropy values at this point are obtained from the R123 refrigerant properties table (please refer appendix B).

The power output for a period of one month, obtained upon the analysis on this R123 Organic Rankine Cycle which is assisted by the solar parabolic collector test rig is 2kWh (please refer appendix B for complete calculation steps). Comparing the results which are gave by both the R123 ORC and Isobutane ORC, it can be seen that this solar assisted ORC used in this experimental study is definite to produce a monthly power of 2kWh. However the power generated by the ORC could be increased to any desired value by just increasing the mass flow rate of the working fluid in the thermal cycle or by increasing the overall length of the solar parabolic trough collector in this case.

CHAPTER VI

CONCLUSION & SUGGESTION

Conclusion

As a conclusion, this study found R123 is a more suitable working fluid for the ORC due to the higher efficiency as compared to isobutane. The overall efficiency of the R123 ORC using solar as heat source is 14.84 %. The thermal efficiency of the ORC only is 22.15 %, which is 6.73 % lower than the Carnot efficiency evaluated at the same temperatures. The Carnot cycle is an ideal cycle and a difference in efficiency of less than 10 % shows that the ORC is close to an ideal cycle. The difference in thermal efficiency between a fossil fuel based Rankine Cycle and Carnot cycle at the same temperature is normally around 15 % or more. Therefore, the ORC is better compared to the fossil fuel Rankine Cycle as the efficiency of the ORC is closer to that of the Carnot Cycle.

In the study, the specific work for R123 ORC is 65.96 W/m^2. A specific work of 89.9 W/m^2 was reported for the commercialised SEGS plant in America. Although the specific work found in this study is less, but the value are close at about 8.6% of difference.

Referring to the results and discussions of the various test methods on the solar parabolic collector test rig as presented in chapter V, it can be concluded that the environmental factor plays a major role in the performance analysis of the solar collector. Environmental or weather conditions such as wind and scattered clouds conditions are factors that bring down the efficiency of the solar collector. Besides that, the incomplete system on the absorber tube which is without an evacuated glass envelope due to its high cost and fabrication complexity constraints is also a contributing factor towards the poor performance of the solar collector test rig.

In the study, the power output for the Isobutane and R123 ORC which generates 2kWh per month could be increased by adding the length of the test rig. This is to allow more mass flow rate passing through the solar collector. However this method may not be cost effective. In whole, this study found that the cloudy conditions in Malaysia do not allow the maximum performance of the solar parabolic collector to take place. The SEGS plant uses the Rankine Cycle coupled with parabolic collectors and it is placed in a desert.Therefore the main contributors to the lower specific work are due to the lower quantity and quality of solar radiation in Malaysia. Quantity refers to the value of solar flux whereas, quality refers to the type of radiation – beam or diffuse, with the former is considered of a higher quality.

6.2 Suggestion

After reviewing this study, several suggestions for further study have been formulated. The first suggestion is to design, fabricate and test a compound parabolic collector (CPC) in the Malaysian context (please refer appendix C for design of proposed CPC). By designing, fabricating and testing the new compound parabolic collector (CPC), a comparison of test results between the CPC and the parabolic trough collector (PTC) can be obtained. The comparison of both this results can be used to improve the overall system efficiency for both the collectors. Besides that, the absorber of the new designed compound parabolic collector (CPC) and also the existing parabolic collector (PTC) needs to be equipped with an evacuated glass envelope. All necessary techniques which could increase the temperature difference (dT) between the absorber outlet temperature (T_{out}) and absorber inlet temperature (T_{in}) are encouraged to be applied in the experimental study on the solar collector, for example, insulating the inlet storage tank and other relevant techniques.

In terms of the analysis on the power output by the solar assisted ORC it is suggested that this analysis includes more organic compounds as the efficiency of the ORC is greatly influenced by the choice of working fluid. Besides that, other improvements to the ORC should be considered, for example, superheating and heat recuperation in the ORC.

Lastly, an economic feasibility study on the solar parabolic collectors should be done. This study should be done, as it seen that the solar parabolic collector has a potential use as a home water heating system. This alternative can be taken if in the case the parabolic collectors are not feasible to be used as a unit in the ORC power generation system looking at the Malaysian weather context in this research.

REFERENCE

1. National Energy Education Development. www.need.org. USA. 2003.

2. Energy Information Administration. www.eia.doe.gov. USA. 2004

3. Tenaga Nasional Berhad. *Annual Report 2003*. K.L. 2004

4. Eighth Malaysia Plan. Government of Malaysia. K.L. 2000

5. Campbell, C.J. *The Imminent Peak of World Oil Production*. Presentation to British House of Commons All-Party Committee. U.K.1999

6. Bloomberg Channel News, 8th October 2004

7. U.S. Dept of Energy. *Energy Efficiency and Renewable Energy*. www.eere.energy.gov. U.S.A. 2004

8. Fisher, U., Sugarmen, C., Ring, A. and Sinai J., *Gas Turbine "Solarization"-Modifications for Solar/Fuel Hybrid Operation*. 2004. 126: 872-878.

9. Nag, P.K. *Power Plant Engineering*. 2nd Ed. Singapore: Mc-Graw Hill. 2002.

10. Larjola, J. Int. J. Production Economics: *Electricity from Industrial Waste Heat Using High-Speed Organic Rankine Cycle (ORC)*.1995. 41: 227-235.

11. Hung, T.C., Shai, T.Y. and Wang, S.K. Energy: *A Review of Organic Rankine Cycles (ORCs) for the Recovery of Low-Grade Waste Heat.* 1997. 22(7):661-667.

12. Larson, D.L. Solar Energy: *Operational Evaluation of the Grid-Connected Coolidge Solar Thermal Electricity Power Plant.* 1987. 38(1): 11-24.

13. Verschoor, M.J.E. and Brouwer, E.P. Energy: *Description of SMR Cycle, Which Combines Fluid Elements of Steam and Organic Rankine Cycles.* 1995. 20(4):195-303

14. Yang, W.J., Kuo, C.H. and Orhan, A. Int. J. of Energy Research: *A Hybrid Power Generation System: Solar-Driven Rankine Engine-Hydrogen Storage.* 2001. 25: 1107-1125.

15. Yamamoto, T., Furuhata, T., Arai, N. and Mori, K. Energy: *Design and Testing of the Organic Rankine Cycle.* 2001. 26:239-251.

16. Maizza, V. and Maizza, A. Applied Thermal Engineering: *Unconventional Working Fluids in Organic Rankine-cycles for Waste Energy Recovery Systems.* 2001. 21(3):381-390.

17. Liu, B.T., Chien, K.H. and Wang, C.C. Energy: *Effect of Working Fluids on Organic Rankine Cycle for Waste Heat Recovery.* 2004. 29:1207-1217.

18. Angelino, G., Invernizzi, C. and Molteni, G. Proc Instn Mech Engrs: *The Potential Role of Organic Bottoming Rankine Cycles in Steam Power Stations.* 1999. 213(A):75-91

19. Hung T.C. Journal of Engineering for Gas Turbines and Power: *Triple Cycle: A Conceptual Arrangement of Multiple Cycle Toward Optimal Energy Conversion.* 2002. 124:429-436

20. Zyhowski G.J. Opportunities for HFC-245fa Organic Rankine Cycle Appended to Distribute Power Generation Systems. *21st IIR International Congress of Refrigeration.* August 17-22, 2003. Washington, D.C: IIR.

21. DiPippo, R. Geothermics: *Second Law Assessment of Binary Plants Generating Power from Low-temperature Geothermal Fluids.* 2004. Article in Press.

22. Duffie, J.A. and Beckman, W.A. *Solar Engineering of Thermal Processes.* 2nd Ed. U.S.A.: John Wiley and Sons, Ltd. 1991.

23. Metrological Department of Malaysia. Selangor. 2004. Unpublished

24. Markvart T. *Solar Electricity.* 2nd Ed. West Sussex, London: John Wiley and Sons, Ltd. 2000.

25. Patel, M.K. *Wind and Solar Power Systems.* U.S.A: CRC Press Ltd. 1999

26. Cengel, Y.A. and Boles, M.A. *Thermodynamics: An Engineering Approach.* 4th Ed. U.S.A.: McGraw-Hill. 2002.

27. Solar Research Design Sdn. Bhd. (2004). *Microsolar Coaxial Multivalve Vacuum Tube.* Selangor: Catalogue.

28. Solutia Hong Kong Ltd. (Malaysia Branch) (2004). *Therminol® Heat Transfer Fluid.* Selangor: Catalogue.

29. Riffelmann, K.J., Kruger, D., Pitz-Paal, R. *Solar Thermal Plants – Power and Process Heat.* 1999.

30. Cooper, P. I. Solar Energy: *The Absorption of Solar Radiation Stills.*1969. 12:3.

31. Klein, S.A. Solar Energy: *Calculation of Monthly Average Insolation on Tilted Surfaces.* 1977. 19:325.

32. Ong, K.S. *Solar Water Heaters, Engineering and Applications*. K.L.: University Malaya Press. 1994.

33. Hsieh, J.S. *Solar Energy Engineering*. New Jersey: Prentice-Hall Inc. 1986.

34. Riffelmann, K.J. et al. Solar Thermal Power Plant. *6th International Summer School Solar Energy 2000*. July 24 – August 4, 2000. University of Klagenfurt, Austria.

35. Jones, S.A., Pitz-Paal, R., Schwarzboezl, P., Blair, N. and Cable, R. TRNSYS Modelling of the SEGS VI Parabolic Trough Solar Electric Generating System. *Solar Forum 2001: Solar Energy: The Power to Choose*. April 21-25, 2001. Washington, D.C.

36. Younglove, B.A. and McLinden, M.O. J. Phys. Chem. Ref. Data: *An International Standard Equation of State for the Thermodynamic Properties of Refrigerant 123 (2,2-Dichloro-1,1,1-Trifluoroethane)*. 1994. 23(5):731-765.

37. Younglove, B.A. and Ely, J.F. J. Phys. Chem. Ref. Data: *Thermodynamical Properties of Fluids. II. Methane, Ethane, Propane, Isobutane, and Normal Butane*. 1987. 16(4):577-797.

38. National Institute of Standard and Testing. http://www.nist.gov. USA. 2004

APPENDIX A

SOLAR PARABOLIC COLLECTOR TECHNICAL DRAWINGS

Section X-X

F = 100 - 140 mm (Adjustable)

(Ø 9.53)

(15°)

Trough is able to rotate at an angle of 15 degrees

(F)

(90)

(70)

(50)

(30)

(10)

(70)

(70)

(70)

(70)

(70)

UNLESS OTHERWISE SPECIFIED:
DIMENSIONS ARE IN MILLIMETERS
TOLERANCES:
LINEAR:
ANGULAR:

	NAME	SIGNATURE	DATE
DRAWN			
CHK'D			
APPV'D			
MFG			
Q.A			

FINISH:

DEBUR AND
BREAK SHARP
EDGES

DO NOT SCALE DRAWING

REVISION

TITLE:

utm
Parabolic Trough

MATERIAL:

DWG NO.

WEIGHT:

SCALE:1:1

SHEET 1 OF 1

A4

Solar thermal Cycle Circuitry

utm

No	Particulars
1	Surge Tank
2	Pressure Gauge
3	Valve (Globe)
4	Pump (2.5 W, 4m)
5	Storage Tank
6	Flow meter
7	Temperature Gauge
8	Vacuum Tube
9	Parabolic Trough
10	Connectors

No	Pipe (Nominal size)
A	Steel Pipe (20mm 40ST)
B	Steel Pipe (10mm 40ST)
C	Flexible Pipe (10mm)
D	Cooper Pipe (1/4 in L)

L = 1 m

UNLESS OTHERWISE SPECIFIED:
DIMENSIONS ARE IN MILLIMETERS

FINISH:

DEBUR AND
BREAK SHARP
EDGES

DO NOT SCALE DRAWING

REVISION

	NAME	SIGNATURE	DATE
DRAWN	Eng Cong		
CHK'D	Dr. Sanjay		
APPV'D	Dr. Sanjay		
MFG			
Q.A			

MATERIAL:

WEIGHT:

TITLE:

Solar thermal Cycle Circuitry

DWG NO.

SCALE:1:1

SHEET 1 OF 1

A4

APPENDIX B

MATLAB PROGRAMMING &
RELATED SOLAR PARABOLIC TROUGH COLLECTOR
CALCULATIONS

```
%R123 Programming
%The following are the initial value to start the program
P = 0.11;
%P = Pressure in MPa
data = [];
h3 = 228.03;
% h3 is the enthalpy at the condenser, which is fixed at 28C
PP = 0;
x = 1;
x2 = 0;
%x is the dryness fraction at the turbine outlet, x2 is the dryness fraction at the
%turbine working section
%Programming start here until the program reach critical point at P=3.6618MPa
%Equations are obtained from Ms Excel by curve-fitting data, t is temperature in C
%Value of enthalpy, h and entropy, s is in kJ/kg and kJ/kg K respectively
%Value of Heat, Q and Work, W are in kJ/kg
while PP < 3.6618
    h1 = -1.2239*P^6 + 14.167*P^5 - 65.324*P^4 + 153.17*P^3 - 199.3*P^2 +
158.96*P + 384.71;
    s = -0.0004*P^6 + 0.0035*P^5 - 0.0127*P^4 + 0.0252*P^3 - 0.0389*P^2 +
0.0565*P + 1.6574;
    t1 = -1.4544*P^6 + 18.006*P^5 - 88.161*P^4 + 218.58*P^3 - 297.39*P^2 +
255.09*P + 6.0898;
% When the entropy is less than 1.663, the turbine outlet go into the 2 phase region
% in T-s diagram, therefore this subroutine is needed to check on this
    if s > 1.663
        h2 = 254.49*s^2 - 551.96*s + 612.52;
        t2 =  181.26*s^2 - 172.31*s - 186.91;
    elseif s <= 1.663
        x = (s - 1.0975)/(1.663 - 1.0975);
        h2 = x*(398.22 - 228.03) + 228.03;
        t2 = 27.82;
    end
% When the temperature at the turbine inlet is higher than 150C, the working section
% will be in the 2 phase region of the T-s diagram
    if t1 > 150
        x2 = (s - 1.4782)/(1.7003 - 1.4782);
    end
% The following is the saving of values into the a single name - data
    W = h1 - h2;
    Q = h1 - h3;
    eff = 100*(W/Q);
    eps = abs(eff - effold);
    data = [data; P Q h1 s h2 x x2 t1 t2 W eff];
    PP = P;
    P = P + 0.001;end
```

```matlab
%Isobutane Programming
%The following are the initial value to start the program
P = 0.381;
%P = Pressure in MPa
data = [];
h3 = -1651.2;
% h3 is the enthalpy at the condenser, which is fixed at 28C
x = 1;
x2 = 0;
%x is the dryness fraction at the turbine outlet, x2 is the dryness fraction at the
%turbine working section
%Programming start here until the program reach critical point at P=3.641MPa
%Equations are obtained from Ms Excel by curve-fitting data, t is temperature in K
%Value of enthalpy, h and entropy, s is in J/mol and J/mol K respectively
%Value of Heat, Q and Work, W are in J/mol
while P < 3.641
    h1 = -125.09*P^6 + 1348.5*P^5 - 5857.2*P^4 + 13231*P^3 - 17500*P^2 +
15960*P + 13156;
    s = -0.2316*P^6 + 2.3139*P^5 - 9.0401*P^4 + 17.449*P^3 - 18.481*P^2 +
13.552*P + 279.84;
    t1 = -1.1856*P^4 + 11.983*P^3 - 47.537*P^2 + 110.39*P + 265.86;
% When the entropy is less than 283.14, the turbine outlet go into the 2 phase region
% in T-s diagram, therefore this subroutine is needed to check on this
    if s > 283.14
        h2 = 1.6351*s^2 - 632.74*s + 65422;
        t2 = 0.0029*s^2 + 1.2941*s - 303.3;
    elseif s <= 283.14
        x = (s - 220.16)/(283.14 - 220.16);
        h2 = x*(17318 - (-1651.2)) + (-1651.2);
        t2 = 301;
    end
% When the temperature at the turbine inlet is higher than 380K, the working section
% will be in the 2 phase region of the T-s diagram
    if t1 > 380
        x2 = (s - 257.7)/(287.22 - 257.7);
    end
% The following is the saving of values into the a single name – data. Value of W is
% divided by molecular weight, 58.123 to change from J/mol into kJ/kg
% The following is the saving of values into the a single name - data
    W = (h1 - h2)/58.123;
    Q = (h1 - h3)/58.123;
    eff = 100*(W/Q);
    data = [data; P Q h1 s h2 x x2 t1 t2 W eff];
    P = P + 0.001;
    PP = P;
end
```

```
% R123 Superheating Programming
%The following are the initial value to start the program
P = 1;
%Pressure, P is chosen as 1MPa for first stage superheating
data1 = [];
h3 = 224.12;
% h3 is the enthalpy at the condenser, which is fixed at 28C
Tit = 0;
T = 111.15;
% This temperature, T is the temperature at the saturated vapour line at this pressure
x = 1;
x2 = 0;
%x is the dryness fraction at the turbine outlet, x2 is the dryness fraction at the
%turbine working section
%Programming start here until the program reaches max temperature at 250C
%Equations are obtained from Ms Excel by curve-fitting data, t is temperature in K
%Value of enthalpy, h and entropy, s is in kJ/kg and kJ/kg K respectively
%Value of Heat, Q and Work, W are in kJ/kg
while Tit < 250
    h1 = 0.8903*T + 346.62;
    s =  (-2E-06)*T^2 + 0.0027*T + 1.4148;
    h2 = 256.43*s^2 - 563.75*s + 624.06;
% When the entropy is less than 1.663, the turbine outlet go into the 2 phase region
% in T-s diagram, therefore this subroutine is needed to check on this
    if s > 1.663
        h2 = 254.49*s^2 - 551.96*s + 612.52;
        t2 =  181.26*s^2 - 172.31*s - 186.91;
    elseif s <= 1.663
        x = (s - 1.0975)/(1.663 - 1.0975);
        h2 = x*(398.22 - 228.03) + 228.03;
        t2 = 27.82;
    end
% When the temperature at the turbine inlet is higher than 150C, the working section
%might be in the 2 phase region of the T-s diagram
    if T > 150
        x2 = (s - 1.4782)/(1.7003 - 1.4782);
    end
% The following is the saving of values into the a single name - data
    W = h1 - h2;
    Q = h1 - h3;
    eff = 100*(W/Q);
    data1 = [data1; P Q h1 s h2 x x2 T t2 W eff];
    T = T + 0.1;
    Tit = T;
end

%The following are the initial value to start the second stage superheating at 2MPa
P = 2;
data2 = [];
h3 = 224.12;
```

```
% h3 is the enthalpy at the condenser, which is fixed at 28C
Tit = 0;
T = 147.25;
% This temperature, T is the temperature at the saturated vapour line at this pressure
x = 1;
x2 = 0;
%x is the dryness fraction at the turbine outlet, x2 is the dryness fraction at the
%turbine working section
%Programming start here until the program reaches max temperature at 250C
%Equations are obtained from Ms Excel by curve-fitting data, t is temperature in K
%Value of enthalpy, h and entropy, s is in kJ/kg and kJ/kg K respectively
%Value of Heat, Q and Work, W are in kJ/kg
while Tit < 250
    h1 = 0.9893*T + 316.15;
    s =  (-4E-06)*T^2 + 0.0037*T + 1.2438;
    h2 = 256.43*s^2 - 563.75*s + 624.06;
% When the entropy is less than 1.663, the turbine outlet go into the 2 phase region
% in T-s diagram, therefore this subroutine is needed to check on this
    if s > 1.663
        h2 = 254.49*s^2 - 551.96*s + 612.52;
        t2 =  181.26*s^2 - 172.31*s - 186.91;
    elseif s <= 1.663
        x = (s - 1.0975)/(1.663 - 1.0975);
        h2 = x*(398.22 - 228.03) + 228.03;
        t2 = 27.82;
    end
% When the temperature at the turbine inlet is higher than 150C, the working section
%might be in the 2 phase region of the T-s diagram
    if T > 150
        x2 = (s - 1.4782)/(1.7003 - 1.4782);
    end
% The following is the saving of values into the a single name - data
    W = h1 - h2;
    Q = h1 - h3;
    eff = 100*(W/Q);
    data2 = [data2; P Q h1 s h2 x x2 T t2 W eff];
    T = T + 0.1;
    Tit = T;
end
```

```
%Isobutane Superheating Programming
%The following are the initial value to start the program
P = 1.2;
%Pressure, P is chosen as 1.2MPa for first stage superheating
data = [];
h3 = -1651.2;
% h3 is the enthalpy at the condenser, which is fixed at 28C
x = 1;
x2 = 0;
T = 347.786;
% This temperature, T is the temperature at the saturated vapour line at this pressure
Tit = T;
%x is the dryness fraction at the turbine outlet, x2 is the dryness fraction at the
%turbine working section
%Programming start here until the program reaches max temperature at 600K
%Equations are obtained from Ms Excel by curve-fitting data, t is temperature in K
%Value of enthalpy, h and entropy, s is in J/mol and J/mol K respectively
%Value of Heat, Q and Work, W are in J/mol
while Tit < 600
    h1 = 0.0881*T^2 + 64.724*T - 12249;
    s = 0.3179*T + 177.05;
% When the entropy is less than 283.14, the turbine outlet go into the 2 phase region
% in T-s diagram, therefore this subroutine is needed to check on this
    if s > 283.14
        h2 = 1.6351*s^2 - 632.74*s + 65422;
        t2 = 0.0029*s^2 + 1.2941*s - 303.3;
    elseif s <= 283.14
        x = (s - 220.16)/(283.14 - 220.16);
        h2 = x*(17318 - (-1651.2)) + (-1651.2);
        t2 = 301;
    end
% When the temperature at the turbine inlet is higher than 380K, the working section
%might be in the 2 phase region of the T-s diagram
    if T > 380
        x2 = (s - 257.7)/(287.22 - 257.7);
    end
% The following is the saving of values into the a single name – data. Value of W is
% divided by molecular weight, 58.123 to change from J/mol into kJ/kg
% The following is the saving of values into the a single name - data
    W = (h1 - h2)/58.123;
    Q = (h1 - h3)/58.123;
    eff = 100*(W/Q);
    data = [data; P Q h1 s h2 x x2 T t2 W eff];
    T = T + 0.1;
    Tit = T;
end

%The following are the initial value to start the second stage superheating at 2MPa
P = 2;
data1 = [];
```

```
h3 = -1651.2;
% h3 is the enthalpy at the condenser, which is fixed at 28C
x = 1;
x2 = 0;
T = 373.6;
% This temperature, T is the temperature at the saturated vapour line at this pressure
Tit = T;
%x is the dryness fraction at the turbine outlet, x2 is the dryness fraction at the
%turbine working section
%Programming start here until the program reaches max temperature at 600K
%Equations are obtained from Ms Excel by curve-fitting data, t is temperature in K
%Value of enthalpy, h and entropy, s is in J/mol and J/mol K respectively
%Value of Heat, Q and Work, W are in J/mol
while Tit < 600
    h1 = 0.0515*T^2 + 105.39*T - 23986;
    s = 0.3272*T + 167.12;
% When the entropy is less than 283.14, the turbine outlet go into the 2 phase region
% in T-s diagram, therefore this subroutine is needed to check on this
  if s > 283.14
      h2 = 1.6351*s^2 - 632.74*s + 65422;
      t2 = 0.0029*s^2 + 1.2941*s - 303.3;
    elseif s <= 283.14
      x = (s - 220.16)/(283.14 - 220.16);
      h2 = x*(17318 - (-1651.2)) + (-1651.2);
      t2 = 301;
  end
 % When the temperature at the turbine inlet is higher than 380K, the working
%section might be in the 2 phase region of the T-s diagram
  if T > 380
      x2 = (s - 257.7)/(287.22 - 257.7);
    end
% The following is the saving of values into the a single name – data. Value of W is
% divided by molecular weight, 58.123 to change from J/mol into kJ/kg
% The following is the saving of values into the a single name - data
    W = (h1 - h2)/58.123;
    Q = (h1 - h3)/58.123;
    eff = 100*(W/Q);
    data1 = [data1; P Q h1 s h2 x x2 T t2 W eff];
    T = T + 0.1;
    Tit = T;
end
```

Calculation Steps in Determining HTF Flow Profile

The Reynolds number formulation used in determining the HTF flow profile in this study is:

$$R_e = \frac{\rho v d}{\mu}$$

Where,

ρ = density of heat transfer fluid = 1000 kg /m^3

v = velocity of heat transfer fluid = 0.0297 m/s with flow rate 0.14 L/min

d = absorber tube diameter = 0.01 m

μ = coefficient of heat transfer fluid dynamic viscosity = 1.14 x 10^{-3} Ns m^{-2}

Now replacing all values in the Reynolds number formulation:

$$R_e = \frac{1000 \text{ kg /m}^3 \text{ x } 0.0297 \text{ m/s x } 0.01 \text{ m}}{1.14 \text{ x } 10^{-3} \text{ Ns m}^{-2}}$$

= 260.56

Referring to the principals of the Reynolds number formulation,
when R_e < 2000, the flow profile is laminar.

Calculations for Isobutane ORC

Analysis on the thermal cycle:
Q (flow rate of HTF) = 0.13 L/min
$p = \dot{m} / Q$
p for water(HTF) = 1000 kg/m^3

From here we get $\dot{m} = 2.167 \times 10^{-3}$ kg/s

Now to calculate the energy gained by HTF:
$$\dot{Q}_{used} = \dot{m} c_p \left(T_{HTF,out} - T_{HTF,in} \right)$$
$$= 2.167 \times 10^{-3} \text{kg/s} \times 4.2 \times (44\,^{\circ}\text{C} - 29\,^{\circ}\text{C})$$
$$= 0.14 \text{kW}$$

Analysis on the ORC
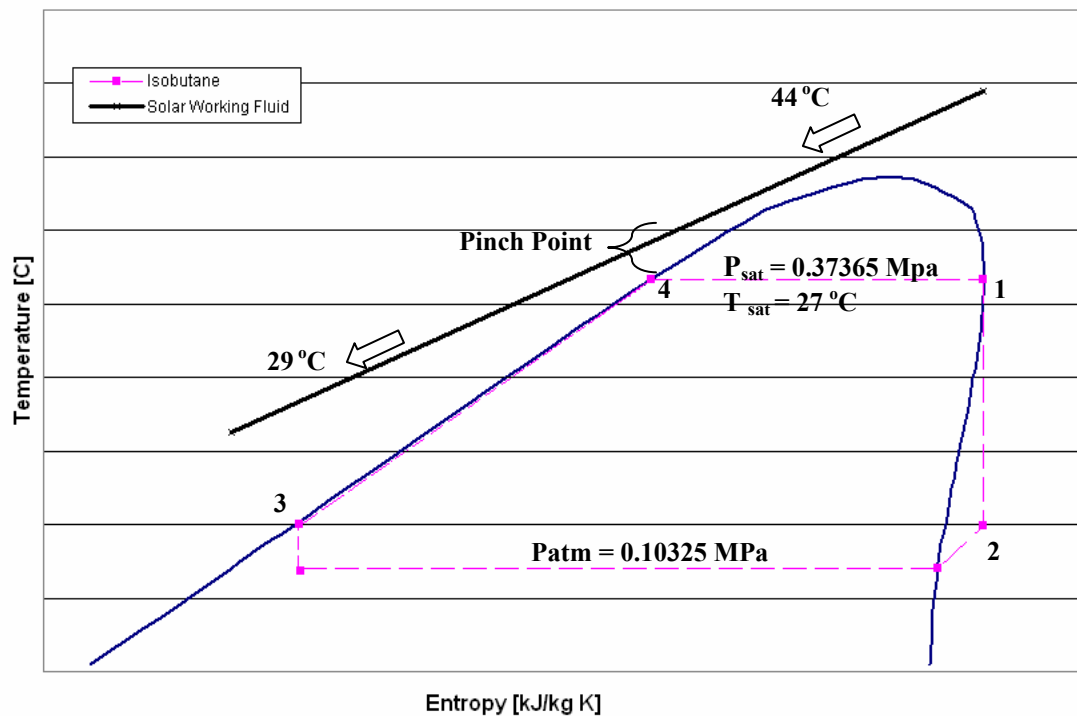
Figure: T-s Diagram of Isobutane ORC

At point 1
$P_{sat} = 0.37365$ Mpa
$T_{sat} = 27\,^{\circ}$C
$h_g = h_1 = 708.36$ kJ/kg
$s_g = 4.8739$ kJ/(kg.K) $= s_1$

Point 3 (ORC inlet)
$T_3 = -9\,^{\circ}$C
$h_3 = 294.97$ kJ/kg $= h_f$

At point 4
$h_f = 381.09$ kJ/kg $= h_4$

(all values are obtained from Isobutane properties table)

Knowing that, $\dot{Q}_{used} = \dot{Q}_{in}$
We obtain:
$0.14\text{kW} = \dot{m}_{ref}\left(h_1 - h_3\right)$
$\dot{m}_{ref} = 3.386 \times 10^{-4}\text{kg/s}$

Method for calculating pinch temperature between HTF and Isobutane based at saturated press (0.37365 Mpa) & saturated temp(27°C) line:

$\dot{Q} = \dot{m}_{ref}\left(h_1 - h_4\right)$
$\dot{Q} = 3.386 \times 10^{-4}\text{kg/s}\ (708.36\text{kJ/kg} - 381.09\ \text{kJ/kg})$
$\quad = 0.1108\ \text{kW}$

Using this concept, $\dot{Q}_{used} = \dot{Q}_{in}$
$0.1108\text{kW} = 2.167\times10^{-3}\text{kg/s} \times 4.2 \times (44\,^{\circ}\text{C}- \text{A}\,^{\circ}\text{C})$
$\qquad \text{A}\,^{\circ}\text{C} = 32\,^{\circ}\text{C}$
Hence;
Pinch point $= 32\,^{\circ}\text{C} - 27\,^{\circ}\text{C}$
$\qquad\qquad = 5\,^{\circ}\text{C}$

Amount of power generated:

Due to the isentropic process, we know that $s_1 = s_2 = 4.8739\ \text{kJ/(kg.K)}$
Referring to the value of s_g at point 2, $s_g = 4.8625\ \text{kJ/(kg.K)}$, it is found that $s_2 > s_g$
From this we know that point 2 falls in the superheated region.
Looking at the Isobutane superheated properties table, the h_2 value is 660 kJ/kg

Hence,

Power generated $(W_{out}) = \dot{m}_{ref}\ (h_1 - h_2)$
$\qquad\qquad\qquad\quad = 0.016\text{kW}$

0.016kW x 4 hours of estimated sunny weather condition per day gives us 0.065 kWh of power a day.

Therfore,the estimated power to be generated for a month is:
0.065 kWh x 30 days = 2kWh per month.

Calculations for Isobutane Superheating Effects

Analysis on the thermal cycle:

Q (flow rate of HTF) = 0.13 L/min
$p = \dot{m} / Q$
p for water(HTF) = 1000 kg/m^3

From here we get $\dot{m} = 2.167 \times 10^{-3}$ kg/s

Now to calculate the energy gained by HTF:
$$\dot{Q}_{used} = \dot{m}c_p\left(T_{HTF,out} - T_{HTF,in}\right)$$
$$= 2.167 \times 10^{-3} \text{kg/s} \times 4.2 \times (44\,^\circ C - 29\,^\circ C)$$
$$= 0.14 \text{kW}$$

Analysis on the ORC:
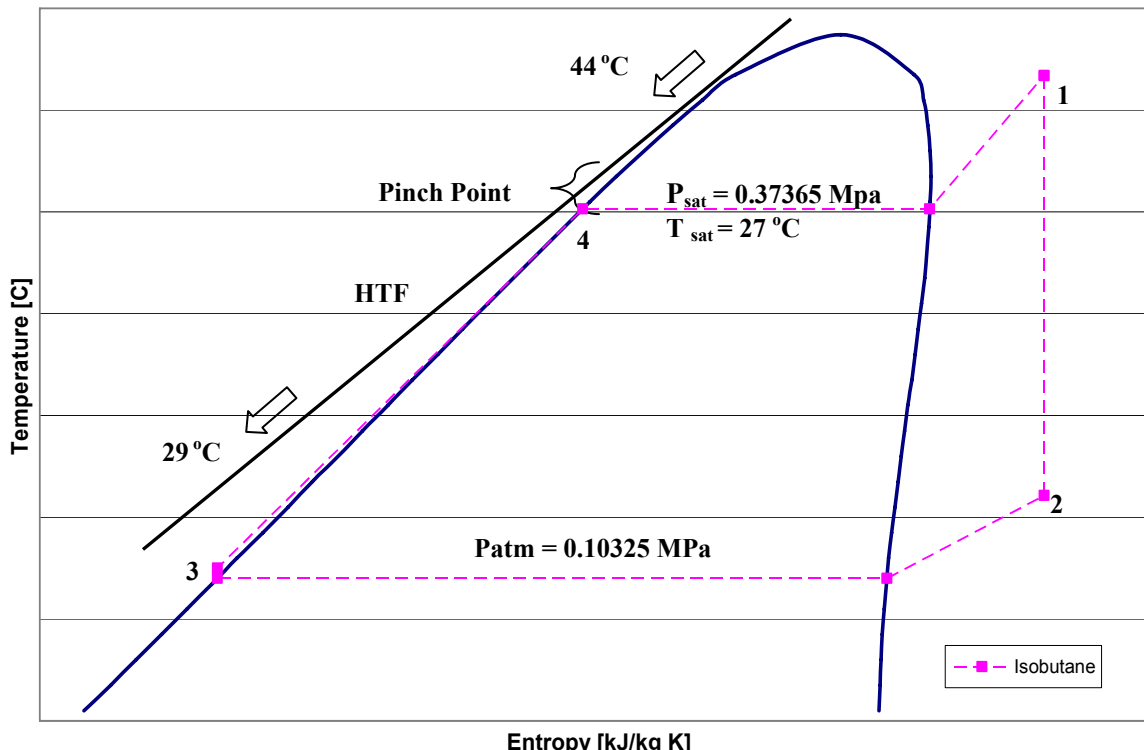
Figure: T-s Diagram of Isobutane ORC Working at Superheated Region

At point 1
$P_1 = 0.37365$ Mpa
$T_1 = 37\,^\circ C$
$h_g = h_1 = 730$ kJ/kg
$s_g = 4.95$ kJ/(kg.K) $= s_1$

Point 3 (ORC inlet)
$T_3 = -9\,^\circ C$
$h_3 = 294.97$ kJ/kg $= h_f$

At point 4
$h_f = 381.09$ kJ/kg $= h_4$

(all values are obtained from Pressure – Enthalpy Diagram and properties table of Isobutane)

Knowing that, $\dot{Q}_{used} = \dot{Q}_{in}$
We obtain:
$0.14\text{kW} = \dot{m}_{ref} \left(h_1 - h_3 \right)$
$\dot{m}_{ref} = 3.218 \times 10^{-4}\text{kg/s}$

Method for calculating pinch temperature between HTF and Isobutane based at saturated pressure (0.37365 Mpa) line:

$\dot{Q} = \dot{m}_{ref} \left(h_1 - h_4 \right)$
$\dot{Q} = 3.218 \times 10^{-4}\text{kg/s} (730 \text{ kJ/kg} - 381.09 \text{ kJ/kg})$
$\quad = 0.1123 \text{ kW}$

Using this concept, $\dot{Q}_{used} = \dot{Q}_{in}$
$0.1123\text{kW} = 2.167\times10^{-3}\text{kg/s} \times 4.2 \times (44\,^{\circ}\text{C} - A\,^{\circ}\text{C})$
$\qquad A\,^{\circ}\text{C} = 32\,^{\circ}\text{C}$
Hence;
Pinch point $= 32\,^{\circ}\text{C} - 27\,^{\circ}\text{C}$
$\qquad\qquad = 5\,^{\circ}\text{C}$

Amount of power generated:

Due to the isentropic process, we know that $s_1 = s_2 = 4.95$ kJ/(kg.K)
Referring to the value of s_g at point 2, $s_g = 4.8625$ kJ/(kg.K) , it is found that $s_2 > s_g$
From this we know that point 2 falls in the superheated region.
Looking at the Isobutane Pressure – Enthalpy Diagram, the h_2 value is 680 kJ/kg

Hence,

Power generated $(W_{out}) = \dot{m}_{ref} (h_1 - h_2)$
$\qquad\qquad\qquad\qquad = 0.016\text{kW}$

0.016kW x 4 hours of estimated sunny weather condition per day gives us 0.065 kWh of power a day.

Therfore,the estimated power to be generated for a month is:
0.065 kWh x 30 days = 2kWh per month.

Calculations for R123 Organic Rankine Cycle

Analysis on the thermal cycle:

Q (flow rate of HTF) = 0.13 L/min
$p = \dot{m} \, / \, Q$
p for water(HTF) = 1000 kg/m^3

From here we get $\dot{m} = 2.167 \times 10^{-3}$ kg/s

Now to calculate the energy gained by HTF:

$$\dot{Q}_{used} = \dot{m} c_p \left(T_{HTF,out} - T_{HTF,in} \right)$$
$$= 2.167 \times 10^{-3} \text{kg/s} \times 4.2 \times (44\,^{\circ}\text{C} - 29\,^{\circ}\text{C})$$
$$= 0.14 \text{kW}$$

Analysis on the ORC:
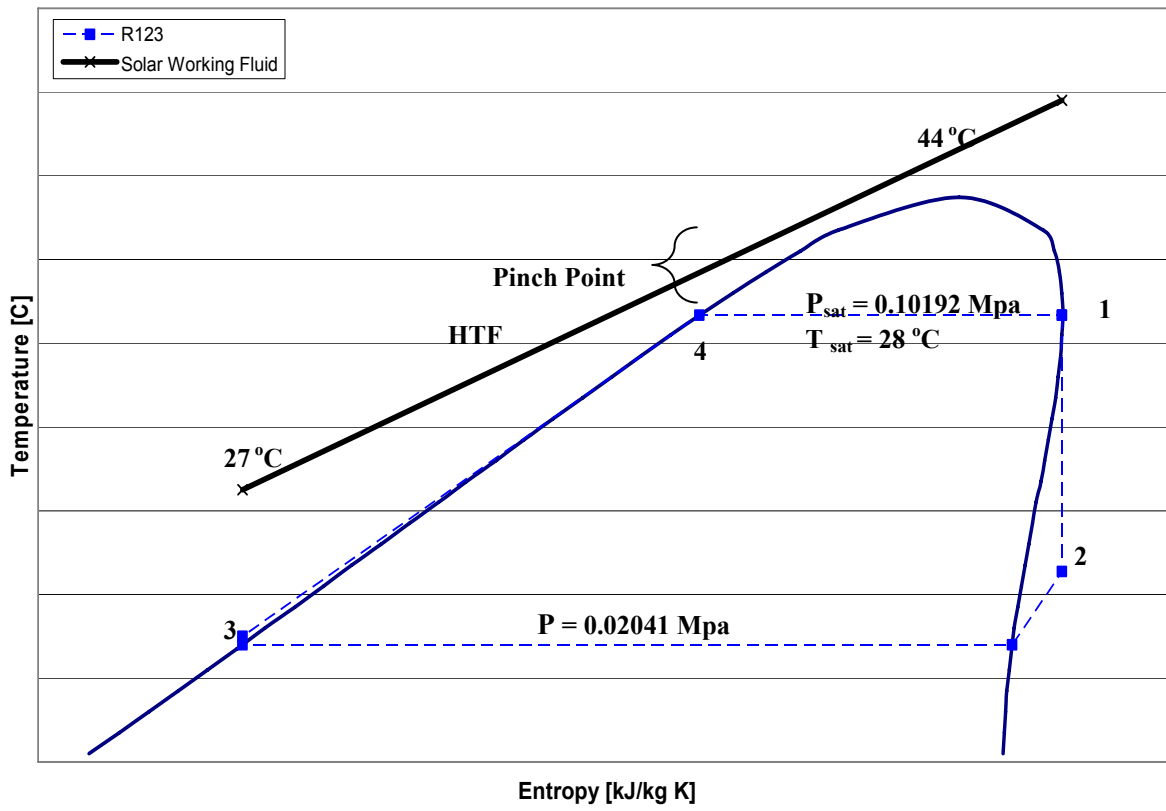
Figure : T-s Diagram of R123 ORC

At point 1
$P_1 = 0.10192$ Mpa
$T_1 = 28\,^{\circ}$C
$h_g = h_1 = 396.76$ kJ/kg
$s_g = 1.6574$ kJ/(kg.K) $= s_1$

Point 3 (ORC inlet)
$T_3 = -10\,^{\circ}$C
$h_3 = 191.48$ kJ/kg $= h_f$

At point 4
$h_f = 226.38$ kJ/kg $= h_4$

(all values are obtained from thermodynamics properties table of R123)

Knowing that, $\dot{Q}_{used} = \dot{Q}_{in}$
We obtain:
$0.14kW = \dot{m}_{ref}\left(h_1 - h_3\right)$
$\dot{m}_{ref} = 6.81995 \times 10^{-4} kg/s$

Method for calculating pinch temperature between HTF and Isobutane based at saturated pressure (0.10192 Mpa) line:

$\dot{Q} = \dot{m}_{ref}\left(h_1 - h_4\right)$
$\dot{Q} = 6.81955 \times 10^{-4} kg/s \ (396.76 \ kJ/kg - 226.38 \ kJ/kg)$
$= 0.1162 \ kW$

Using this concept, $\dot{Q}_{used} = \dot{Q}_{in}$
$0.1162kW = 2.167 \times 10^{-3} kg/s \times 4.2 \times (44\,^{\circ}C - A\,^{\circ}C)$
$\qquad A\,^{\circ}C = 13\,^{\circ}C$
Hence;
Pinch point $= 31\,^{\circ}C - 28\,^{\circ}C$
$\qquad\qquad = 3\,^{\circ}C$

Amount of power generated:

Due to the isentropic process, we know that $s_1 = s_2 = 1.6574 \ kJ/(kg.K)$
Referring to the value of s_g and s_f at point 2, $s_g = 1.6610 \ kJ/(kg.K)$
and $s_f = 0.9683 \ kJ/(kg.K)$, it is found that $s_f < s_2 < s_g$
From this we know that point 2 falls in the saturated mixture region.

Using the equation $s_2 = s_f + x \ (s_g - s_f)$
The value of quality,$(x) = 0.99$

Now using the equation $h_2 = h_f + x \ (h_g - h_f)$ the value of h_2 is calculated.
The value of $h_2 = 191.48 \ kJ/kg + 0.99 \ (373.77 \ kJ/kg - 191.48 \ kJ/kg)$
$\qquad\qquad = 371.95 \ kJ/kg$

Hence,
Power generated $(W_{out}) = \dot{m}_{ref} \ (h_1 - h_2)$
$\qquad\qquad\qquad = 0.016kW$

0.016kW x 4 hours of estimated sunny weather condition per day gives us 0.065 kWh of power a day.

Therefore, the estimated power to be generated for a month is:
0.065 kWh x 30 days = 2kWh per month.

Isobutane Refrigerant Saturated Properties Table

Refrigerant Properties 17.59

Refrigerant 600a (Isobutane) Properties of Saturated Liquid and Saturated Vapor

Temp, K	Pressure, MPa	Vapor Volume, m³/kg	Liquid Density, kg/m³	Enthalpy, kJ/kg Liquid	Enthalpy, kJ/kg Vapor	Entropy, kJ/(kg·K) Liquid	Entropy, kJ/(kg·K) Vapor
**113.55	0.19E-07	859732.	741.38	0.000	485.30	1.8625	6.1364
115	0.28E-07	597742.	739.99	2.470	486.58	1.8841	6.0938
120	0.93E-07	183981.	735.21	11.029	491.05	1.9570	5.9572
125	0.28E-06	62914.	730.44	19.654	495.63	2.0274	5.8352
130	0.79E-06	23603.	725.65	28.347	500.33	2.0956	5.7262
135	0.20E-05	9611.8	720.87	37.113	505.14	2.1617	5.6286
140	0.48E-05	4209.8	716.08	45.951	510.06	2.2261	5.5411
145	0.000011	1967.5	711.28	54.866	515.09	2.2886	5.4626
150	0.000022	974.60	706.47	63.858	520.22	2.3496	5.3921
155	0.000044	508.61	701.66	72.930	525.45	2.4092	5.3287
160	0.000082	278.20	696.84	82.082	530.78	2.4673	5.2717
165	0.000149	158.77	692.00	91.318	536.21	2.5242	5.2206
170	0.000258	94.158	687.15	100.64	541.73	2.5800	5.1746
175	0.000432	57.824	682.29	110.04	547.35	2.6345	5.1334
180	0.000701	36.656	677.42	119.54	553.04	2.6881	5.0965
185	0.001104	23.920	672.52	129.13	558.83	2.7407	5.0634
190	0.001690	16.028	667.61	138.81	564.70	2.7924	5.0339
195	0.002525	11.003	662.68	148.58	570.65	2.8432	5.0076
200	0.003685	7.7231	657.72	158.46	576.67	2.8932	4.9843
205	0.005266	5.5330	652.73	168.44	582.78	2.9425	4.9636
210	0.007380	4.0392	647.72	178.52	588.95	2.9910	4.9455
215	0.010156	3.0004	642.67	188.72	595.20	3.0389	4.9296
220	0.013744	2.2647	637.60	199.02	601.52	3.0862	4.9158
225	0.018313	1.7349	632.48	209.45	607.91	3.1330	4.9039
230	0.024053	1.3473	627.32	219.99	614.36	3.1791	4.8938
235	0.031170	1.0597	622.12	230.65	620.87	3.2248	4.8853
240	0.039893	0.84322	616.87	241.43	627.44	3.2700	4.8783
245	0.050466	0.67829	611.57	252.34	634.05	3.3147	4.8727
250	0.063153	0.55111	606.22	263.38	640.72	3.3590	4.8683
255	0.078231	0.45194	600.80	274.55	647.42	3.4028	4.8651
260	0.095995	0.37380	595.32	285.84	654.16	3.4463	4.8629
261.36	0.101325	0.35550	593.81	288.93	655.99	3.4581	4.8625
262	0.10392	0.34724	593.10	290.40	656.86	3.4636	4.8623
264	0.11234	0.32297	590.88	294.97	659.56	3.4809	4.8619
266	0.12129	0.30075	588.64	299.57	662.27	3.4980	4.8616
268	0.13077	0.28038	586.39	304.18	664.99	3.5152	4.8614

Temp, K	Pressure, MPa	Vapor Volume, m³/kg	Liquid Density, kg/m³	Enthalpy, kJ/kg Liquid	Enthalpy, kJ/kg Vapor	Entropy, kJ/(kg·K) Liquid	Entropy, kJ/(kg·K) Vapor
270	0.14081	0.26169	584.13	308.82	667.70	3.5322	4.8614
272	0.15144	0.24450	581.85	313.48	670.42	3.5493	4.8615
274	0.16267	0.22868	579.56	318.17	673.13	3.5662	4.8617
276	0.17452	0.21410	577.26	322.87	675.85	3.5831	4.8621
278	0.18703	0.20065	574.94	327.60	678.57	3.6000	4.8625
280	0.20020	0.18822	572.61	332.34	681.29	3.6169	4.8631
282	0.21406	0.17672	570.26	337.12	684.01	3.6336	4.8638
284	0.22863	0.16608	567.89	341.90	686.72	3.6504	4.8645
286	0.24394	0.15621	565.51	346.72	689.44	3.6671	4.8654
288	0.26001	0.14705	563.11	351.56	692.15	3.6837	4.8664
290	0.27686	0.13854	560.69	356.42	694.86	3.7004	4.8674
295	0.32256	0.11976	554.57	368.68	701.63	3.7418	4.8704
300	0.37365	0.10399	548.32	381.09	708.36	3.7830	4.8739
305	0.43048	0.090678	541.93	393.66	715.06	3.8240	4.8777
310	0.49344	0.079371	535.39	406.40	721.71	3.8649	4.8820
315	0.56289	0.069717	528.69	419.32	728.31	3.9057	4.8866
320	0.63921	0.061430	521.81	432.42	734.84	3.9463	4.8914
325	0.72279	0.054281	514.73	445.72	741.30	3.9870	4.8965
330	0.81400	0.048083	507.43	459.22	747.66	4.0276	4.9016
335	0.91327	0.042686	499.89	472.95	753.91	4.0682	4.9069
340	1.0210	0.037962	492.08	486.93	760.04	4.1089	4.9122
345	1.1376	0.033809	483.95	501.16	766.01	4.1497	4.9174
350	1.2636	0.030142	475.48	515.67	771.81	4.1907	4.9225
355	1.3995	0.026887	466.61	530.48	777.38	4.2319	4.9273
360	1.5457	0.023985	457.28	545.63	782.69	4.2733	4.9318
365	1.7029	0.021383	447.40	561.16	787.67	4.3151	4.9357
370	1.8719	0.019038	436.86	577.12	792.26	4.3574	4.9389
375	2.0532	0.016911	425.52	593.57	796.34	4.4004	4.9411
380	2.2479	0.014967	413.17	610.60	799.77	4.4442	4.9420
385	2.4571	0.013174	399.50	628.36	802.32	4.4891	4.9410
390	2.6820	0.011500	383.99	647.07	803.66	4.5357	4.9373
395	2.9242	0.0099050	365.69	667.16	803.18	4.5851	4.9294
400	3.1862	0.0083329	342.51	689.59	799.64	4.6394	4.9145
405	3.4709	0.0066269	307.19	717.73	789.12	4.7068	4.8831
*408.00	3.6549	0.00446	224.	752.5	752.5	4.791	4.791

**Triple point

*Critical point

Isobutane Superhated Properties Table

Thermophysical properties of iso-butane - Continued

Density kg/m³	Density mol/dm³	E J/mol	H J/mol	S J/(mol·K)	C_v J/(mol·K)	C_p J/(mol·K)	Sound m/s	Visc. μPa·s	Therm. W/(m·K)	Diel. Const.
0.6485	0.01116	44540.0	49020.0	375.8	149.8	158.2	285.1	13.2	0.0482	1.00068
0.6252	0.01076	47580.0	52230.0	381.7	154.0	162.4	290.1	13.7	0.0513	1.00066
0.6036	0.01038	50700.0	55520.0	387.4	158.1	166.5	295.1	14.1	0.0544	1.00064
0.5833	0.01004	53910.0	58890.0	393.1	162.1	170.4	300.0	14.5	0.0576	1.00061

				0.10 MPa isobar						
741.4	12.75	-23800.0	-23790.0	108.5	74.02	98.99	1728.0	9100.0	0.110	2.10782
735.2	12.65	-23160.0	-23150.0	113.9	74.24	100.1	1700.0	6160.0	0.116	2.09379
657.7	11.31	-14600.0	-14590.0	168.3	82.19	114.9	1319.0	546.0	0.135	1.93554
606.3	10.43	-8558.0	-8549.0	195.2	90.00	127.2	1069.0	263.0	0.117	1.84170
594.1	10.22	-7117.0	-7107.0	200.8	92.08	130.4	1010.0	229.0	0.112	1.82018
2.806	0.04828	12140.0	14210.0	282.4	80.33	90.64	196.5	6.63	0.0125	1.00302
2.746	0.04725	12450.0	14570.0	283.8	81.19	91.36	198.2	6.72	0.0129	1.00295
2.580	0.04439	13710.0	15960.0	288.9	84.76	94.51	204.4	7.08	0.0142	1.00277
2.391	0.04113	15470.0	17900.0	295.6	89.78	99.17	212.1	7.56	0.0161	1.00256
2.230	0.03836	17330.0	19930.0	302.2	95.01	104.1	219.4	8.04	0.0182	1.00238
2.091	0.03597	19290.0	22070.0	308.6	100.3	109.3	226.3	8.52	0.0205	1.00223
1.969	0.03387	21350.0	24300.0	315.0	105.7	114.5	233.0	9.01	0.0228	1.00210
1.861	0.03202	23520.0	26650.0	321.4	111.0	119.8	239.3	9.49	0.0253	1.00198
1.765	0.03037	25800.0	29100.0	327.6	116.3	125.0	245.5	9.97	0.0279	1.00188
1.679	0.02888	28180.0	31650.0	333.8	121.5	130.1	251.5	10.4	0.0306	1.00178
1.600	0.02754	30670.0	34300.0	340.0	126.6	135.1	257.4	10.9	0.0334	1.00170
1.529	0.02631	33250.0	37050.0	346.1	131.5	140.0	263.0	11.4	0.0362	1.00162
1.464	0.02520	35930.0	39900.0	352.2	136.3	144.8	268.6	11.9	0.0392	1.00155
1.405	0.02417	38700.0	42840.0	358.2	140.9	149.4	274.0	12.3	0.0421	1.00149
1.350	0.02323	41570.0	45880.0	364.1	145.4	153.9	279.4	12.8	0.0452	1.00143
1.300	0.02236	44520.0	49000.0	370.0	149.8	158.3	284.6	13.2	0.0482	1.00137
1.253	0.02155	47560.0	52200.0	375.9	154.0	162.5	289.7	13.7	0.0513	1.00132
1.209	0.02080	50690.0	55500.0	381.6	158.1	166.6	294.7	14.1	0.0545	1.00127
1.168	0.02010	53890.0	58870.0	387.4	162.1	170.5	299.7	14.6	0.0576	1.00123

				0.101325 MPa isobar						
741.4	12.75	-23800.0	-23790.0	108.5	74.02	98.99	1728.0	9100.0	0.110	2.10782
735.2	12.65	-23160.0	-23150.0	113.9	74.24	100.1	1700.0	6160.0	0.116	2.09379
657.7	11.31	-14600.0	-14590.0	168,3	82.19	114.9	1319.0	546.0	0.135	1.93554
606.3	10.43	-8558.0	-8549.0	195.2	90.00	127.2	1069.0	263.0	0.117	1.84171
593.7	10.21	-7074.0	-7064.0	201.0	92.15	130.5	1008.0	228.0	0.112	1.81954
2.841	0.04887	12170.0	14240.0	282.4	80.43	90.76	196.6	6.64	0.0126	1.00306
2.784	0.04790	12450.0	14570.0	283.7	81.22	91.41	198.1	6.72	0.0129	1.00299
2.615	0.04499	13710.0	15960.0	288.8	84.78	94.55	204.3	7.08	0.0142	1.00281
2.423	0.04169	15470.0	17900.0	295.5	89.80	99.19	212.1	7.56	0.0161	1.00260
2.260	0.03888	17320.0	19930.0	302.0	95.02	104.2	219.4	8.04	0.0182	1.00242
2.119	0.03645	19280.0	22060.0	308.5	100.3	109.3	226.3	8.53	0.0205	1.00226
1.995	0.03433	21350.0	24300.0	314.9	105.7	114.5	232.9	9.01	0.0228	1.00213
1.886	0.03245	23520.0	26650.0	321.2	111.0	119.8	239.3	9.49	0.0253	1.00201
1.789	0.03077	25800.0	29090.0	327.5	116.3	125.0	245.5	9.97	0.0279	1.00190
1.701	0.02927	28180.0	31650.0	333.7	121.5	130.1	251.5	10.4	0.0306	1.00181
1.622	0.02790	30670.0	34300.0	339.9	126.6	135.1	257.3	10.9	0.0334	1.00172
1.550	0.02666	33250.0	37050.0	346.0	131.5	140.0	263.0	11.4	0.0362	1.00164
1.484	0.02553	35930.0	39900.0	352.1	136.3	144.8	268.6	11.9	0.0392	1.00157
1.424	0.02449	38700.0	42840.0	358.1	140.9	149.4	274.0	12.3	0.0421	1.00151
1.368	0.02354	41570.0	45870.0	364.0	145.4	153.9	279.4	12.8	0.0452	1.00145
1.317	0.02266	44520.0	49000.0	369.9	149.8	158.3	284.6	13.2	0.0482	1.00139
1.269	0.02184	47560.0	52200.0	375.8	154.0	162.5	289.7	13.7	0.0513	1.00134
1.225	0.02108	50690.0	55490.0	381.5	158.1	166.6	294.7	14.1	0.0545	1.00129
1.184	0.02037	53890.0	58870.0	387.2	162.1	170.5	299.7	14.6	0.0576	1.00125

124

Pressure – Enthalpy Diagram for Isobutane
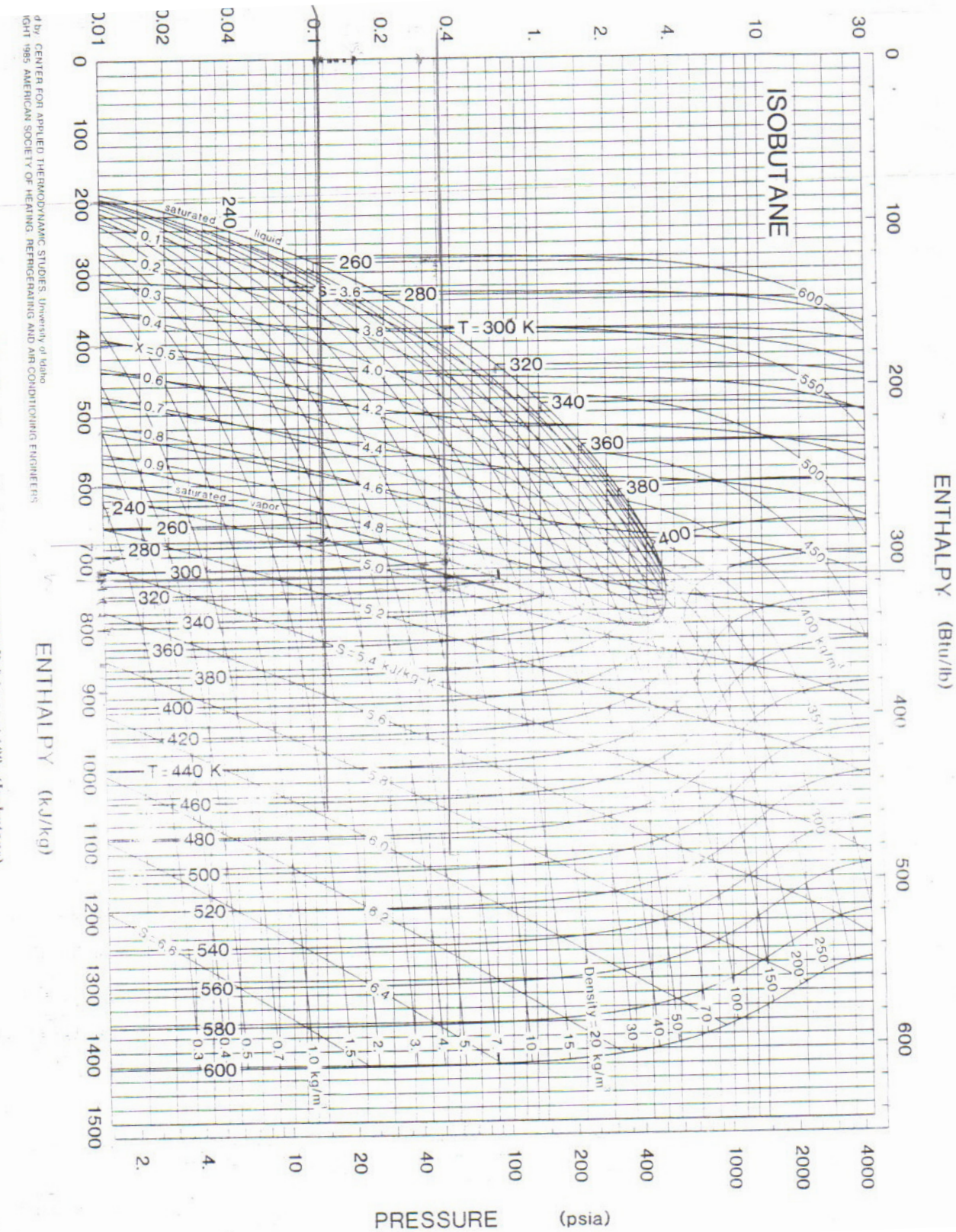
Fig. 28   Pressure-Enthalpy Diagram for Refrigerant 600a (Isobutane)

R123 Refrigerant Properties Table

Refrigerant Properties 17.23

Refrigerant 123 (1,1-dichloro-2,2,2-trifluoroethane) Properties of Saturated Liquid and Saturated Vapor

Temp, °C	Pressure, MPa	Density, kg/m³ Liquid	Volume, m³/kg Vapor	Enthalpy, kJ/kg Liquid	Enthalpy, kJ/kg Vapor	Entropy, kJ/(kg·K) Liquid	Entropy, kJ/(kg·K) Vapor	Specific Heat c_p, kJ/(kg·K) Liquid	Specific Heat c_p, kJ/(kg·K) Vapor	c_p/c_v Vapor	Velocity of Sound, m/s Liquid	Velocity of Sound, m/s Vapor	Viscosity, μPa·s Liquid	Viscosity, μPa·s Vapor	Thermal Cond, mW/(m·K) Liquid	Thermal Cond, mW/(m·K) Vapor	Surface Tension, mN/m	Temp, °C
−40.00	0.00378	1613.2	3.3365	167.23	356.30	0.8704	1.6814	—	0.594	1.106	—	118.	1048.8	—	—	—	23.49	−40.00
−30.00	0.00698	1591.5	1.8798	175.47	362.04	0.9050	1.6723	—	0.611	1.105	—	120.	884.0	—	—	—	22.20	−30.00
−20.00	0.01221	1569.5	1.1145	183.38	367.87	0.9369	1.6657	—	0.629	1.105	—	122.	755.0	—	89.7	—	20.93	−20.00
−10.00	0.02041	1546.9	0.69040	191.48	373.77	0.9683	1.6610	—	0.648	1.104	—	124.	652.4	—	86.8	—	19.68	−10.00
0.00	0.03273	1523.8	0.44453	200.00	379.75	1.0000	1.6581	0.875	0.667	1.104	786.	125.	569.6	—	83.9	—	18.43	0.00
2.00	0.03581	1519.1	0.40879	201.76	380.95	1.0064	1.6577	0.885	0.670	1.105	778.	126.	555.0	—	83.3	—	18.19	2.00
4.00	0.03912	1514.3	0.37644	203.54	382.16	1.0129	1.6573	0.895	0.674	1.105	770.	126.	541.0	—	82.7	—	17.94	4.00
6.00	0.04267	1509.6	0.34709	205.34	383.37	1.0193	1.6571	0.905	0.678	1.105	762.	126.	527.5	—	82.1	—	17.70	6.00
8.00	0.04648	1504.8	0.32045	207.16	384.58	1.0258	1.6568	0.915	0.682	1.105	755.	127.	514.5	—	81.6	—	17.45	8.00
10.00	0.05057	1500.0	0.29622	209.00	385.79	1.0323	1.6567	0.924	0.686	1.105	747.	127.	502.0	—	81.0	—	17.21	10.00
12.00	0.05494	1495.2	0.27416	210.86	387.00	1.0389	1.6566	0.934	0.689	1.105	740.	127.	489.9	—	80.4	—	16.96	12.00
14.00	0.05961	1490.3	0.25405	212.74	388.22	1.0454	1.6565	0.943	0.693	1.106	733.	127.	478.3	—	79.8	—	16.72	14.00
16.00	0.06459	1485.5	0.23569	214.64	389.43	1.0520	1.6565	0.952	0.697	1.106	726.	128.	467.1	—	79.2	—	16.48	16.00
18.00	0.06990	1480.5	0.21890	216.55	390.65	1.0586	1.6565	0.961	0.701	1.106	719.	128.	456.3	—	78.7	—	16.24	18.00
20.00	0.07555	1475.6	0.20354	218.49	391.87	1.0652	1.6566	0.970	0.704	1.107	712.	128.	445.8	—	78.1	9.81	16.00	20.00
22.00	0.08157	1470.6	0.18946	220.44	393.09	1.0718	1.6568	0.978	0.708	1.107	705.	128.	435.7	—	77.5	9.95	15.76	22.00
24.00	0.08796	1465.7	0.17654	222.40	394.31	1.0784	1.6569	0.986	0.712	1.107	698.	128.	426.0	—	76.9	10.08	15.52	24.00
26.00	0.09473	1460.6	0.16467	224.39	395.54	1.0850	1.6572	0.994	0.716	1.108	692.	129.	416.5	—	76.3	10.22	15.28	26.00
27.84b	0.10133	1456.0	0.15460	226.22	396.66	1.0912	1.6574	1.001	0.719	1.108	685.	129.	408.1	—	75.8	10.35	15.06	27.84
28.00	0.10192	1455.6	0.15376	226.38	396.76	1.0917	1.6574	1.002	0.719	1.108	685.	129.	407.4	—	75.8	10.36	15.04	28.00
30.00	0.10952	1450.5	0.14371	228.40	397.98	1.0983	1.6577	1.009	0.723	1.109	678.	129.	398.5	—	75.2	10.49	14.80	30.00
32.00	0.11757	1445.4	0.13445	230.42	399.21	1.1050	1.6581	1.016	0.727	1.109	671.	129.	389.9	—	74.6	10.63	14.57	32.00
34.00	0.12607	1440.2	0.12590	232.46	400.43	1.1116	1.6585	1.023	0.731	1.110	664.	129.	381.6	—	74.0	10.77	14.33	34.00
36.00	0.13504	1435.1	0.11800	234.52	401.65	1.1183	1.6589	1.029	0.734	1.111	658.	129.	373.6	—	73.4	10.90	14.10	36.00
38.00	0.14451	1429.9	0.11070	236.59	402.88	1.1249	1.6594	1.035	0.738	1.111	651.	129.	365.7	—	72.9	11.04	13.86	38.00
40.00	0.15448	1424.6	0.10394	238.67	404.10	1.1316	1.6598	1.041	0.742	1.112	644.	129.	358.1	—	72.3	11.18	13.63	40.00
42.00	0.16498	1419.4	0.09768	240.76	405.32	1.1382	1.6604	1.047	0.745	1.113	637.	130.	350.7	—	71.7	11.32	13.39	42.00
44.00	0.17603	1414.0	0.09186	242.86	406.54	1.1448	1.6609	1.052	0.749	1.114	630.	130.	343.5	—	71.1	11.45	13.16	44.00
46.00	0.18764	1408.7	0.08647	244.97	407.76	1.1514	1.6615	1.058	0.753	1.115	623.	130.	336.5	—	70.5	11.59	12.93	46.00
48.00	0.19983	1403.3	0.08145	247.10	408.97	1.1580	1.6621	1.063	0.757	1.116	616.	130.	329.7	—	69.9	11.73	12.70	48.00
50.00	0.21261	1397.9	0.07678	249.23	410.19	1.1646	1.6627	1.067	0.760	1.117	609.	130.	323.0	11.72	69.4	11.86	12.47	50.00
52.00	0.22602	1392.4	0.07244	251.37	411.40	1.1712	1.6634	1.072	0.764	1.118	602.	130.	316.6	11.79	68.8	12.00	12.24	52.00
54.00	0.24007	1386.9	0.06839	253.53	412.61	1.1778	1.6641	1.076	0.768	1.119	595.	130.	310.2	11.86	68.2	12.14	12.01	54.00
56.00	0.25478	1381.4	0.06461	255.69	413.82	1.1843	1.6648	1.081	0.772	1.120	588.	130.	304.1	11.92	67.6	12.27	11.78	56.00
58.00	0.27016	1375.8	0.06108	257.85	415.02	1.1909	1.6655	1.084	0.775	1.122	581.	130.	298.0	11.99	67.0	12.41	11.55	58.00
60.00	0.28624	1370.2	0.05778	260.03	416.22	1.1974	1.6662	1.088	0.779	1.123	574.	130.	292.1	12.06	66.5	12.55	11.32	60.00
62.00	0.30304	1364.5	0.05469	262.21	417.41	1.2039	1.6670	1.092	0.783	1.125	566.	130.	286.4	12.12	65.9	12.68	11.10	62.00
64.00	0.32057	1358.8	0.05180	264.41	418.61	1.2104	1.6677	1.095	0.787	1.126	559.	129.	280.7	12.19	65.3	12.82	10.87	64.00
66.00	0.33887	1353.1	0.04910	266.60	419.79	1.2168	1.6685	1.099	0.791	1.128	552.	129.	275.2	12.26	64.7	12.96	10.65	66.00
68.00	0.35794	1347.3	0.04656	268.81	420.97	1.2233	1.6693	1.102	0.795	1.130	544.	129.	269.8	12.32	64.1	13.10	10.42	68.00
70.00	0.37782	1341.4	0.04418	271.02	422.15	1.2297	1.6701	1.105	0.798	1.132	537.	129.	264.5	12.39	63.6	13.23	10.20	70.00
72.00	0.39851	1335.5	0.04194	273.24	423.32	1.2361	1.6709	1.108	0.802	1.134	530.	129.	259.3	12.46	63.0	13.37	9.98	72.00
74.00	0.42005	1329.6	0.03983	275.46	424.49	1.2425	1.6717	1.111	0.807	1.136	522.	129.	254.2	12.52	62.4	13.51	9.76	74.00
76.00	9.44246	1323.6	0.03786	277.69	425.64	1.2488	1.6726	1.114	0.811	1.139	515.	129.	249.2	12.59	61.8	13.64	9.54	76.00
78.00	0.46575	1317.5	0.03599	279.92	426.80	1.2551	1.6734	1.117	0.815	1.141	507.	128.	244.3	12.66	61.2	13.78	9.32	78.00
80.00	0.48995	1311.4	0.03424	282.16	427.94	1.2614	1.6742	1.119	0.819	1.144	500.	128.	239.5	12.72	60.7	13.92	9.10	80.00
82.00	0.51508	1305.2	0.03259	284.40	429.08	1.2677	1.6751	1.122	0.823	1.146	492.	128.	—	12.79	60.1	14.05	8.88	82.00
84.00	0.54116	1299.0	0.03103	286.65	430.20	1.2740	1.6759	1.125	0.828	1.149	485.	128.	—	12.85	59.5	14.19	8.67	84.00
86.00	0.56822	1292.7	0.02955	288.91	431.32	1.2802	1.6768	1.127	0.832	1.153	477.	127.	—	12.92	58.9	14.33	8.45	86.00
88.00	0.59628	1286.4	0.02816	291.17	432.43	1.2864	1.6776	1.130	0.837	1.156	469.	127.	—	12.99	58.3	14.46	8.24	88.00
90.00	0.62537	1280.0	0.02685	293.43	433.54	1.2926	1.6784	1.133	0.842	1.159	462.	127.	—	13.05	57.8	14.60	8.02	90.00
92.00	0.65550	1273.5	0.02560	295.70	434.63	1.2988	1.6793	1.136	0.847	1.163	454.	127.	—	13.12	57.2	14.74	7.81	92.00
94.00	0.68670	1266.9	0.02443	297.97	435.71	1.3049	1.6801	1.138	0.852	1.167	447.	126.	—	13.18	56.6	—	7.60	94.00
96.00	0.71899	1260.3	0.02331	300.25	436.78	1.3111	1.6809	1.141	0.857	1.171	439.	126.	—	13.25	56.0	—	7.39	96.00
98.00	0.75240	1253.6	0.02225	302.54	437.84	1.3172	1.6817	1.144	0.862	1.176	432.	126.	—	13.31	55.4	—	7.18	98.00
100.00	0.78696	1246.8	0.02125	304.83	438.88	1.3232	1.6825	1.147	0.868	1.180	424.	125.	—	13.38	54.8	—	6.97	100.00
105.00	0.87851	1229.5	0.01896	310.58	441.44	1.3383	1.6844	1.156	0.883	1.194	405.	124.	—	13.54	—	—	6.45	105.00
110.00	0.97776	1211.6	0.01695	316.37	443.92	1.3533	1.6862	1.166	0.900	1.209	386.	123.	—	13.70	—	—	5.94	110.00
115.00	1.0851	1193.1	0.01517	322.20	446.29	1.3682	1.6879	1.177	0.918	1.227	367.	122.	—	13.87	—	—	5.44	115.00
120.00	1.2010	1173.9	0.01359	328.08	448.56	1.3830	1.6895	1.190	0.940	1.248	349.	120.	—	14.03	—	—	4.95	120.00
125.00	1.3258	1153.9	0.01219	334.02	450.71	1.3978	1.6909	1.207	0.965	1.274	330.	118.	—	14.19	—	—	4.47	125.00
130.00	1.4600	1133.0	0.01093	340.03	452.72	1.4125	1.6920	1.227	0.994	1.304	311.	117.	—	—	—	—	3.99	130.00
135.00	1.6042	1111.0	0.00980	346.13	454.58	1.4272	1.6929	1.252	1.029	1.342	292.	115.	—	—	—	—	3.53	135.00
140.00	1.7587	1087.7	0.00879	352.32	456.26	1.4419	1.6935	1.283	1.073	1.389	272.	112.	—	—	—	—	3.08	140.00
145.00	1.9241	1062.8	0.00787	358.64	457.72	1.4568	1.6937	1.323	1.129	1.449	253.	110.	—	—	—	—	2.64	145.00
150.00	2.1010	1036.0	0.00703	365.12	458.94	1.4718	1.6935	1.375	1.202	1.528	232.	107.	—	—	—	—	2.22	150.00
160.00	2.4921	974.2	0.00554	378.70	460.32	1.5026	1.6910	1.544	1.452	1.803	189.	100.	—	—	—	—	1.42	160.00
170.00	2.9390	893.3	0.00421	393.70	459.28	1.5357	1.6837	1.965	2.147	2.563	140.	93.	—	—	—	—	0.70	170.00
180.00	3.4545	756.2	0.00284	412.57	451.03	1.5764	1.6613	—	—	—	—	—	—	—	—	—	0.13	180.00
183.68c	3.6680	550.0	0.00182	431.77	431.77	1.6097	1.6097	∞	∞	∞	0.	0.	—	—	∞	∞	0.00	183.68

*temperatures are on the ITS-90 scale   b = boiling point   c = critical point

APPENDIX C

PROPOSED COMPOUND PARABOLIC COLLECTOR (CPC) TECHNICAL DRAWINGS